UNIVERSIDADE FEDERAL DO PARANÁ

RAFAEL FRANÇA DE MATTOS

CARACTERIZAÇÃO GEOQUÍMICA, FACIOLÓGICA E PERMO-POROSA DE CARBONATOS CONTINENTAIS DO JAPÃO

CURITIBA

2016

RAFAEL FRANÇA DE MATTOS

CARACTERIZAÇÃO GEOQUÍMICA, FACIOLÓGICA E PERMO-POROSA DE CARBONATOS CONTINENTAIS DO JAPÃO

Dissertação apresentada como requisito à obtenção do grau de Mestre em Geologia, no Programa de Pós-Graduação em Geologia, Setor de Ciências da Terra, Universidade Federal do Paraná.

Orientadora: Prof. Dr[a]. Anelize Manuela Bahniuk Rumbelsperger

CURITIBA

2016

M444c

Mattos, Rafael França de
Caracterização geoquímica, faciológica e permo-porosa de carbonatos continentais do Japão / Rafael França de Mattos. – Curitiba, 2016.
98 f. : il. color. ; 30 cm.

Dissertação - Universidade Federal do Paraná, Setor de Ciências da Terra, Programa de Pós-Graduação em Geologia, 2016.

Orientador: Anelize Manuela Bahniuk Rumbelsperger .
Bibliografia: p. .

1. Geoquímica. 2. Fáceis (Geologia). 3. Reservatórios Carbonáticos – Geologia. 4. Rochas Carbonáticas. I. Universidade Federal do Paraná. II.Rumbelsperger, Anelize Manuela Bahniuk. III. Título.

CDD: 551.9

TERMO DE APROVAÇÃO

RAFAEL FRANÇA DE MATTOS

"Caracterização geoquímica, faciológica e permo-porosa de carbonatos continentais modernos do Japão."

Dissertação de Mestrado aprovada como requisito parcial para obtenção do grau de Mestre no Programa de Pós-Graduação em Geologia, área de concentração em Geologia Exploratória, da Universidade Federal do Paraná. Comissão formada por:

Dr. Crisógono Vasconcelos - ETHZ

Prof. Dr. Luiz Alberto Fernandes - UFPR

Profª. Drª. Anelize Manuela Bahniuk Rumbelsperger – UFPR
Presidente

Curitiba, 10 de agosto de 2016.

Apresentação

Nome do Candidato
Rafael França de Mattos

Orientador
Prof. Drª. Anelize Manuela Bahniuk Rumbelsperger

Co-orientadores
Prof. Dr. Almério Barros França
Prof. Dr. Leonardo Fadel Cury

Área de Concentração
Geologia Exploratória

Linha de Pesquisa
Análises de Bacias

Nível
Mestrado

Curitiba, Agosto / 2016

Dedico este trabalho ao Prof. Dr. José Manoel dos Reis Neto *In memoriam.*

AGRADECIMENTOS

O período de mestrado foi um dos momentos mais marcantes da minha vida. Palavras não são capazes de expressar o sentimento de gratidão e felicidades que sinto.

Agradeço a Deus por me mostrar o caminho certo através de inúmeras linhas tortas. Tantas pedras apareceram no caminho e hoje consigo entender a razão de cada uma delas.

A toda a minha família, a qual amo muito, que mesmo lá do Rio de Janeiro, sempre esteve ao meu lado nos melhores e nos piores momentos. Jamais esquecerei do carinho e amor que me deram e me fizeram voltar a vida novamente. Tudo que conquistei devo aos meus pais Ana e Jorge e minhas irmãs Eduarda e Fernanda. Digo a vocês que a distância nunca vai mudar o sentimento que temos. Nem indo para o Japão consegui esquecer de vocês! Essa conquista é nossa!

A realização desse trabalho não seria possível sem a força de vontade e colaboração de uma equipe incrível com que tive o prazer de trabalhar.

Agradeço a Frade Petróleo Ltda. pelo financiamento do Projeto Geobiocal, o qual fomentou minha bolsa e os trabalhos de campo, bem como o intercâmbio no Japão, agradeço em especial o geólogo Jiro Asada. Foi uma experiência científica e cultural sensacional!

Dedico um agradecimento especial a Profª Drª. Anelize Bahniuk Rumbelsperger a quem aceitou de prontidão me orientar. Agradeço de verdade por me mostrar que a ciência vai muito além da sala de aula. As experiências de campo foram fantásticas e sua vontade de fazer ciência é contagiante! Você mostra que é possível trabalhar e fazer o que gosta ao mesmo tempo! Tenho muito orgulho de ser seu primeiro orientado! Melhor “desorientadora” não há! “Rafa, cadê o Gustavo?”, “Rafa que ano que o Gustavo nasceu?”, “Rafael, vem aqui!”, “É só chegar no Farol que eu sei”. Dá-lhe Operário!

Agradeço ao Prof. Dr. Almério Barros França por todo o conhecimento adquirido, por sua interminável paciência, prontidão e cultura musical. Uma verdadeira enciclopédia humana! Conversar com você é sempre um prazer!

Agradeço ao Prof. Dr. Leonardo Fadel Cury que me acompanhou desde a graduação e teve um papel fundamental na minha escolha profissional e na minha orientação.

Sou grato a toda equipe do LAMIR, em especial ao Secchi, Fran, Keiji, Thiago, Elisiane, Úrsula, Ivan, Roberto e Rodrigo. Vocês foram fundamentais nesse trabalho. Trabalhar com vocês sempre foi muito prazeroso. O profissionalismo de vocês é demais!

Agradeço aos meus fiéis parceiros de trabalho, Renato T. e Larissa C., que me acompanharam praticamente desde o começo. Os dias de trabalho não seriam completos sem a paçoca, o cachorro quente e a Coca-Cola do Renato, além dos cinco minutinhos pra fumar da Larissa. Não poderia esquecer dos amigos Coxinha, Thammy, Amanda, Letícia, Isis, João, Grávida e Fontanela.

Ao Nilo Matzuda e Prof. Dr. Luiz Alberto Fernandes, pela correção e orientação na qualificação que foi um divisor de águas para a confecção da minha dissertação.

Aos professores e colegas da graduação e pós-graduação da Universidade Federal do Paraná.

Aos Prof. Dr. Fumito Shiraishi e todos os alunos da Universidade de Hiroshima que me receberam de braços abertos no Japão.

Não posso de esquecer aos Hospitais Marcelino Champagnat e São Lucas e toda equipe a equipe técnica, inclusive o enfermeiro “Carla” de Resende, por todas as vezes que fui medicado com enxaquecas, cálculos, gastrites etc.

A todas as pessoas que, direta ou indiretamente, contribuíram para a realização desse sonho chamado “Dissertação de Mestrado”. Espero sempre contar com vocês!

“Castelos nascem de um sonho
pra no real achar seu lugar”

Oswaldo Montenegro

RESUMO

O objetivo deste trabalho foi uma detalhada investigação sedimentológica e geoquímica em rochas carbonáticas continentais modernas, entre elas microbialitos, no Japão. O termo "microbialito" é usado para descrever depósitos organosedimentares com ação direta e / ou indireta de bactérias, tais como estromatólitos, tufa e travertino. Apesar da idêntica composição química e mineralógica, tufas e travertinos diferem em algumas características ambientais, deposicionais e isotópicas. Este grupo específico de rochas carbonáticas tornou-se alvo de estudos, devido as recentes descobertas de petróleo em microbialitos. A ilha do Japão é um dos ambientes modernos, onde ocorre a formação de rochas carbonáticas, do tipo tufa e travertino. A área de estudo está localizada nas ilhas de Kyushu, Honshu e Hokkaido. Dez fontes hidrotermais foram amostras nas três ilhas, a fim de comparar diferentes condições ambientais e geológicas regionais, com base na química da água, e padrões físico-químicos e geoquímicos. Com base em dados macro e microscópicos, quatro fácies foram descritas: estromatólito, shrub, bubble e root. Os dados mostram que a química da água (temperatura, Potencial Hidrogeniônico, Oxigênio Dissolvido.) interferem diretamente na precipitação e, consequentemente, em diferentes fácies. Além disso, o relevo do substrato e a distância do *vent*, também contribuem para a formação de diferentes fácies. Os resultados mineralógicos mostram que a ilha de Kyushu, fontes hidrotermais (NAG, SHIO e MYO), são compostas principalmente por aragonita e as ilhas de Honshu, fontes hidrotermais (YAMA, NIIMI e KIBE) e Hokkaido, fontes hidrotermais (FURU, OKU, OHF e FUTA) são compostas majoritariamente por calcita. Os resultados químicos mostraram elevados teores de CaO e subordinadamente a ocorrência de Fe_2O_3 e SiO_2. Teores de arsênio também foram observados e sua origem ainda está em debate. Os sinais isotópicos mostram que as amostras majoritariamente seguem o *trend* isotópico nacional de água meteórica com valores depletados de $\delta^{18}O$. Os valores de $\delta^{13}C$ foram agrupados em 3 grupos principais: (a) valores próximos a 0‰ que representam pouca ou nenhuma influencia biológica na precipitação, (b) depletados, possivelmente biologicamente induzidos e (c) enriquecidos, possivelmente biologicamente influenciados. Portanto, estes carbonatos continentais foram interpretados como precipitados a partir de água meteórica em superfície devido a desgaseificação de CO_2, por vezes com contaminação de vulcanismo ativo, com pouca ou baixa precipitação biológica. As imagens de Microscopia Eletrônica de Varredura (MEV) permitiram observações em micro escala e mostraram fósseis relacionados com Substância Poliméricas Extracelulares (EPS) que caracterizam possível influência biológica durante a precipitação na fácies estromatólito. As observações de microtomografia computadorizada (micro-CT) permitiram uma análise detalhada dos poros de todas as fácies, mostrando que a fácies bubble é a mais porosa, seguida das fácies *shrub, root* e estromatólito. Esta rara sequência de carbonatos continentais encontrada no Japão permite inferir um entendimento preciso de sinais geoquímicos de rochas carbonáticas continentais e microbialitos associados às condições ambientais, assim como caracterizar o sistema permo poroso dessas rochas.

Palavras-chave: Microbialitos, Geoquímica, Fácies, Porosidade, Japão.

ABSTRACT

This research focused on a sedimentological and geochemical comprehensive research in modern continental carbonate rocks, including microbialites, in Japan. The term "microbialite" is used to describe organosedimentares deposits formed with direct and / or indirect action bacteria, such as stromatolites, tufa and travertine. Despite the identical chemical and mineralogical composition, tufa and travertine differ in some environmental, depositional and isotopic characteristics. The recent discoveries of oil reservoir rocks comprising continental carbonate rocks including microbialites, has issued the interest of studies in this particular group of deposits. The archipelago of Japan is one of modern environments, with precipitation of continental carbonate rocks and microbialites; tufa, travertine and stromatolite type. The study area is located in Kyushu, Honshu and Hokkaido Islands. Ten hot springs were sampled in the three islands in order to compare different regional environmental and geological conditions such as water chemistry, physico-chemical and geochemical patterns. Based on macro and microscopic data, four lithofacies have been described: stromatolite, shrub, bubble and root. The data show that the water chemistry (temperature, potential of Hydrogen, dissolved oxygen) directly interfere in the precipitation and consequently in different facies. Furthermore, the morphology of the substrate which carbonates grow, as well as the distance of the vent, also contribute to the formation of different facies. Mineralogical results show that the hot springs from the Kyushu island (NAG, SHIO and MYO) are composed of aragonite and the hot springs of Honshu (YAMA, NIIMI and KIBE) and Hokkaido islands, (FURU, OKU, OHF and FUTA) are composed mainly of calcite. The chemical results show high contents of CaO and subordinately contents of Fe_2O_3 and SiO_2 in all samples. Arsenic contents ranging from 1 to 17% are also observed and its origin is still under debate. The isotopic signals reveal that the majority of the samples follow the water national $\delta^{18}O$ trend, with depleted values in all samples. The $\delta^{13}C$ values were grouped in three main categories: (a) values near 0 ‰, indicate few or absence of biological influence on precipitation, (b) depleted values, indicating possible biologically induced carbonates and, (c) enriched values, indicating possible biologically influenced carbonates. Therefore, these carbonates are interpreted as precipitated from meteoric surface water, sometimes contaminated by volcanism, due to the CO_2 degassing, with little or insignificant biological precipitation. The scanning electron microscopy (SEM) observations allowed micro scale and reveal fossils related to Extracellular Polymeric Substance (EPS) characterizing possible biological influence during precipitation in stromatolite facies. The computed microtomography (micro-CT) observations allowed a detailed analysis of the pores in all facies, showing the highest volume of pores in bubble facies, followed by facies shrub, root, stromatolite facies. This particular sequence of modern continental carbonates in Japan allows the possibility of inferring a precise understanding of geochemical signs of continental carbonate rocks and microbialites associated with environmental conditions, and to evaluate the perm-pore system of these rocks.

Keywords: Microbialites, Geochemistry, Facies, Porosity, Japan.

SUMÁRIO

CAPÍTULO 1

1 Introdução

1.1 Prólogo

Depósitos de rochas carbonáticas sedimentares são importantes reservatórios de hidrocarbonetos nas recentes descobertas feitas nas bacias da costa sudeste brasileira. O entendimento dos processos responsáveis pela formação desses depósitos é primordial na caracterização de fácies sedimentares, forma e aspectos permo-porosos de reservatórios carbonáticos sedimentares. A compreensão destes parâmetros é fundamental na diminuição do risco exploratório e no avanço das pesquisas científicas em rochas sedimentares carbonáticas.

Microbialitos são definidos como depósitos organossedimentares acrescidos pela ação de comunidades microbiais que trapeiam e aglutinam os sedimentos detríticos e/ou precipitação mineral *in loco* (Burne e Moore, 1987 pp. 241–242) A caracterização geoquímica e permo-porosa de microbialitos recentes teve como objetivo a compreensão dos processos bióticos e abióticos atuantes na precipitação de carbonatos, bem como suas propriedades como rocha reservatório. A escassez de ambientes modernos com microbialitos torna essa pesquisa importante. As fontes hidrotermais do Japão, com formações modernas de travertinos e tufas, foram alvos principais do presente estudo. Os resultados deste trabalho podem ser uteis no entendimento dos processos geradores de porosidade dos carbonatos dos reservatórios de hidrocarbonetos.

A área de estudo está localizada em dez fontes hidrotermais ativas no Japão. Três das principais ilhas desse país foram analisadas, desde o Sul até o Norte, com o objetivo de entender o ambiente deposicional de carbonatos sedimentares continentais modernos, a partir de dados parâmetros de regiões com características distintas. A pesquisa teve início no Sul, região de Kyushu, nas fontes termais de Nagayu, Shiohitashi e Myoken, seguindo para fontes termais a Oeste, região de Kinki-Chugoku, nas fontes hidrotermais de Shionoha, Shimokuraida e Kibedani e finalizou-se nas fontes termais ao norte, na região de Aomori e Hokkaido nas fontes hidrotermais de Furutobe, Oku-Okuhachikuro, Ohfuna e Futamata (Figura 1).

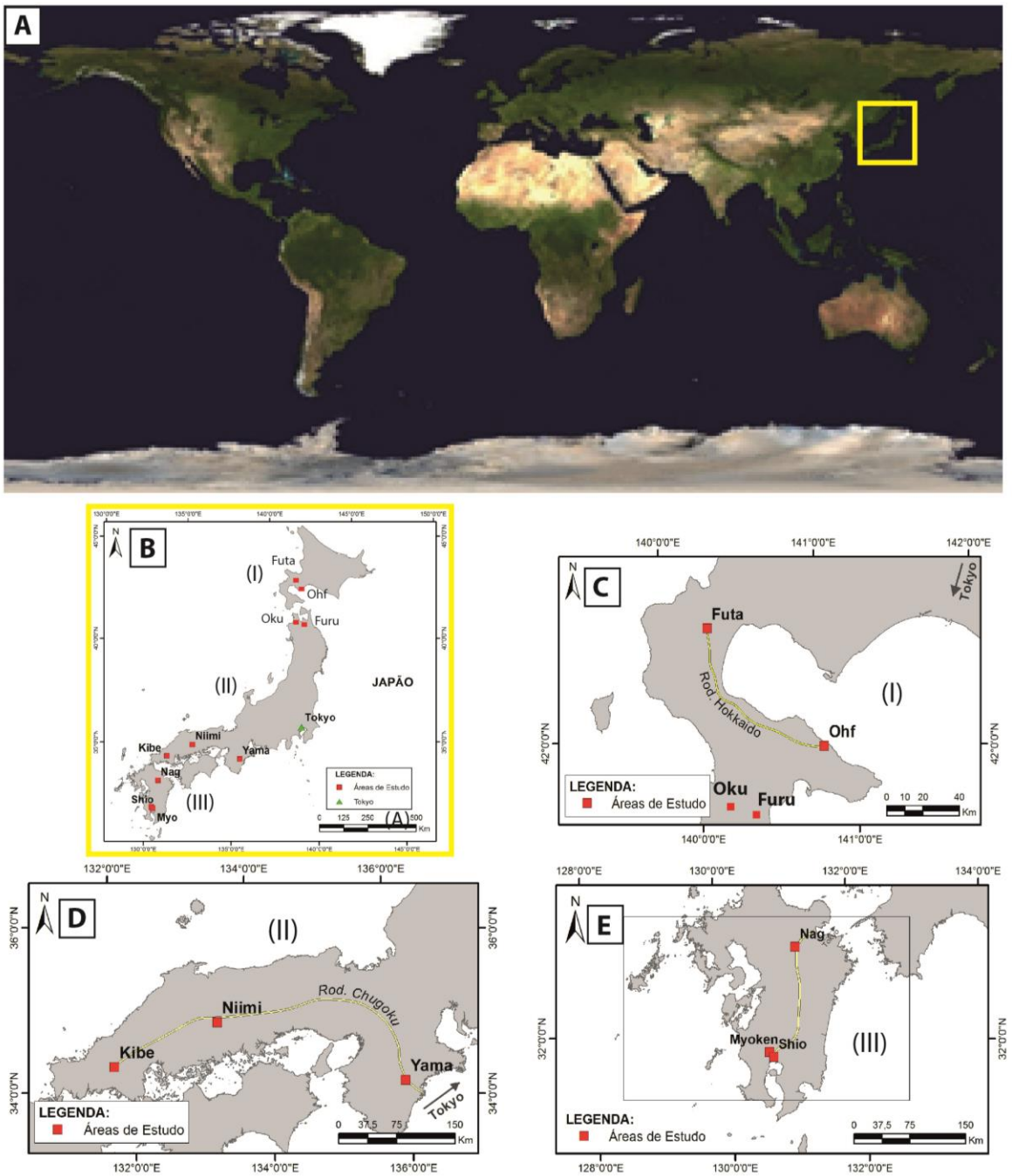

Figura 1: (A) Mapa *mundi*, com destaque para a área de estudo no Arquipélago do Japão. (B) Mapa de localização do Japão com destaque em vermelho para as fontes hidrotermais analisadas nas três principais ilhas do país. (C) Região de Aomori e Hokkaido, Norte do Japão. Destaque para as fontes hidrotermais de FURU, OKU, OHF e FUTA. (D) Ilha de Honshu, Centro Oeste do Japão. Destaque para as fontes hidrotermais de KIBE, NIIMI e YAMA. (E) Ilha de Kyushu, Sul do Japão. Destaque para as fontes hidrotermais de NAG, MYO e SHIO. (Fonte: simplificado de www.gsj.jp).

Essa pesquisa foi dividida em duas partes principais:

(I) *Environmental conditions playing important role in modern continental carbonate facies formation in Japan: geochemistry and facies patterns*.

Estudo de ambientes modernos e ativos no Japão onde ocorre a formação carbonatos sedimentares continentais modernos, sendo o enfoque principal o entendimento do ambiente geoquímico e a consequente geração de diferentes fácies. Além disso, compreender a influência biológica durante a precipitação de carbonatos. Os carbonatos observados em campo foram analisados para se obter dados geoquímicos e mineralógicos além de dados de isótopos estáveis de C^{13} e O^{18} visando a obtenção de informações sobre a origem do fluido envolvido na precipitação. Os objetivos deste trabalho de pesquisa são compreensão dos processos bióticos a abióticos atuantes durante a precipitação dos carbonatos continentais sedimentares modernos e a caracterização de fácies correlacionadas ao ambiente deposicional.

(II) *Perm-porosity characterization of modern continental sedimentary carbonate rocks: implication in reservoir quality*.

Caracterização permo-porosa de microbialitos do Japão e de suas propriedades como rocha reservatório. O estudo detalhado das microfácies observadas nos carbonatos continentais foi realizada a partir de análises de microscopia eletrônica de varredura (MEV) e microtomografia computadorizada (micro CT). A visualização e obtenção de dados quantitativos e qualitativos do o sistema permo-poroso permite classificar a fácies de acordo com a porosidade e permeabilidade. Esse estudo permite a caracterização de rochas de acordo com o volume de poros e sua conectividade, sendo aplicada ao estudo de reservatórios carbonáticos.

1.2 Microbialito – uma visão geral

Microbialitos são estruturas organossedimentares formadas pela atividade direta e / ou indireta de microrganismos associados (Gerard. 2013). O termo “microrganismos” significa eucariota unicelular ou multicelular, ou procariota de domínios Archea, Bactérias e Eucariotos (Fairchild, et al. 2015). No entanto, cianobactérias filamentosas e cocóides seriam responsáveis como produtores primários e construtores para ambos os microbialitos modernos e fósseis, especialmente estromatólitos (Knoll et al. 2013). O termo “tapete microbial” foi introduzido por Doemel e Brock (1974). No início foram utilizados os três termos "tapete de algas", "tapete de bactérias" e "tapete microbial”

simultaneamente e nem sempre discriminativamente (Gorbushina e Krumbein, 2000). Embora o termo é da década de 70, a sua discussão teve início a partir da descoberta de reservatório de óleo nesta rocha. Atualmente, o termo microbialito pode ser considerado como consolidado na literatura. No entanto, a consolidação de fato aconteceu após muita confusão, uma vez que a sua definição, como já foi apresentada, é quase idêntica à sugerida por Awramik e Margulis (1974) para "estromatólito", o mais comum dos microbialitos: Segundo esses autores, estromatólitos são "estruturas organosedimentares megascópicas" produzidas pelo aprisionamento, colagem e / ou precipitação de sedimentos, como resultado do crescimento e da atividade metabólica dos organismos, especialmente cianobactérias. Riding (1999) propôs uma solução simples e didática a esta questão, enfatizando que na definição de Burne e Moore (1987), todos microbialitos são depósitos microbiais bentônicos, litificados ou não (Fairchild, et al. 2015). Portanto, o termo pode ser aplicado tanto para depósitos de rocha, como calcário, (ex. Fm. Sete Lagoas, Neoproterozóico; Fm. Capiru, Neoproterozóico? e Grupo Bambuí, Brasil), para esteiras microbianas e estromatólitos modernos, (ex. sistema lagunar Fluminense, nordeste do Rio de Janeiro, Brasil, e fontes termais modernas, Japão).

Microbialitos desenvolvem-se ao longo de uma gama de salinidade, alcalinidade e temperatura, em água salobra, marinha, hipersalina, hiperalcalina, hidrotermais ou meteóricas ou ainda sob uma grande variedade de ambiente em condições secas como: sublitoral, abaixo do nível de base das ondas de tempo bom, bacia epicratônica, ambiente lacustre, fluvial e terrestre (Fairchild et al. 2015). Tais estruturas podem fornecer informações paleoambientais e paleogeográficas importantes, como por exemplo, em relação à profundidade, grau de agitação e a clareza de água, e a direção da linha de costa. Como corpos geológicos, (ex. recifes), microbialitos podem constituir barreiras, com propriedades estruturais e porosas próprias, entre paleoambientes sedimentares calmos ou agitados, rasos ou profundos e marinhos aberto ou fechado. Sendo assim, isso pode ter implicações muito importantes, especialmente com respeito à migração de óleo, bem como a localização de reservatórios de hidrocarbonetos, ou mineralizações de fosfato, Zn, Pb, Cu, L, etc. (Mendelsohn, 1976).

O papel dos microorganismos na formação microbialitos continua em discussão: eles induzem a precipitação mineral (micróbios primeiro) ou eles colonizam e / ou aprisionam minerais abióticos (minerais primeiro)? Será que esse papel varia de uma espécie para outra? E qual é o impacto da precipitação mineral sobre a ecologia microbial? (Gerard,. 2013). Parece, no entanto, que as condições ambientais definem o cenário para vários tipos de precipitação nas esteiras, em particular, controlando o impacto potencial do metabolismo microbial em produtos minerais (Dupraz et al. 2009). A atividade metabólica cria microambientes que promovem ou inibem a produção mineral (Dupraz et al. 2009). A composição e atividade da comunidade microbial também impactam na composição mineral e cristalografia. Segundo Bahniuk, 2013, microbialitos podem ser compostos por associações minerais distintas, sendo o carbonato o componente de formação mais comum.

Processos de precipitação (abióticos *versus* bióticos) e metabolismo podem influenciar diretamente na assinatura isotópica de carbono e oxigênio (Sumner, 2001). Microbialitos modernos podem ser usados como análogos dos estromatólitos fósseis mais antigos, do início do Arqueano 3,5 bilhões de anos (Awramik & Sprinkle, 1999). Riding (2006) compara mudanças ao longo do tempo geológico, nos últimos 3 milhões de anos, que incluem um pico de abundância 1,250 milhões atrás, relativa queda no final do Proterozóico, ressurgimento no Cambriano, e declínio flutuante durante o restante do Fanerozóico.

1.3 Outros termos importantes

Embora os termos tapete microbial e biofilmes sejam usados para descrever as comunidades microbianas, esses são diferentes em alguns aspectos.

Tapetes microbiais foram chamados tapetes de algas, esteiras de cianobactérias e potenciais estromatólitos por causa da predominância de espécies de espécies de cianobactéria e devido ao seu papel na formação de estruturas sedimentares laminadas (Krumbein, 1983). Tapetes microbiais são ainda caracterizados por variações químicas, abundância de microrganismos fototróficos e a estratificação das populações microbiais em camadas distintas

(Stolz 1991, 1999). Nessas estruturas organossedimentares ocorre a nucleação e precipitação em um sistema biogeoquímico extremamente complexo. Estes micro ecossistemas têm sido bem estudados no meio marinho, porém em ambientes continentais são sempre associados com depósitos ativos de tufa e permanecem desconhecidos (Pedley e Rogerson, 2010). Além disso, tapetes microbiais também têm sido estudados como ecossistemas modelo, bem como análogos para as comunidades microbianas antigas (Awramik, 1983).

Os biofilmes foram descritos como um conjunto de micro-organismos e seus produtos extracelulares ligado a uma superfície sólida (Marshall, 1992). Assim, ao contrário de tapetes microbianos, biofilmes se formam em substratos sólidos, tais como rochas, vidro, plástico (ex., cateteres), aço (ex., tubos) e madeira. A colonização bacteriana das superfícies é dependente da formação de Substâncias Poliméricas Extracelulares (EPS) (Marshall et al. 1971; Corstenton et al. 1978, 1981), nesse sentido muito semelhantes aos tapetes microbiais. As espécies, no entanto, podem variar drasticamente, de comunidades com uma única espécie até comunidades complexas compostas de diferentes espécies. Os tapetes microbiais, portanto, podem ser considerados como biofilmes complexos (Stolz, 1991).

1.4 Substâncias Exopoliméricas (EPS)

A colonização de bactérias em superfícies é dependente da formação de Substâncias Poliméricas Extracelulares (EPS) (Marshall et al. 1971; Costernton et al. 1981). O EPS é constituído de uma mistura de carboidratos, proteínas e ácidos nucleicos, excretados em diferentes proporções, e são conhecidos por terem um papel positivo ou negativo na formação de carbonato, em função da sua capacidade de ligação com cátion divalente, tornando Ca^{2+} ou Mg^{2+}, disponíveis ou não, para a precipitação (Dupraz et al. 2009). O EPS pode aprisionar componentes inorgânicos e abióticos (Characklis e Marshall, 1990), bem como represar água (Krumbein, 1994). A matriz de EPS do biofilme assegura a fixação de células à superfície de um sedimento. Sendo assim, as secreções exopoliméricas atuam como uma "cola" coesa para ligar partículas de sedimentos.

O EPS típico exibe texturas, suaves, às vezes fibrilar ou alveolar (*honeycomb*). Uma esteira filamentosa é posteriormente transformada em um muco orgânico, dentro do qual as estruturas são mal definidas (Bahniuk, 2013). Além disso, a atividade microbial pode levar à formação de determinadas estruturas mineralógicas, as quais, quando associadas com os restos de células ou de polímeros orgânicos, podem ser utilizadas como bioassinaturas da vida passada na Terra e / ou, eventualmente, outros planetas (Benzerara e Menguy, 2009; Dupraz et al. 2009).

O EPS está diretamente relacionado à mineralização intermediada por microorganismos. Esse tipo de mineralização pode ser classificada como biomineralização e ainda organomineralização, que pode ser subdividida em influenciada e induzida (Dupraz et al. 2009).

O termo 'biomineral' tem uma gama de definições. Em termos gerais, refere-se a um mineral que é produzido por organismos vivos, consistindo de tanto minerais como componentes orgânicos (Weiner e Dove, 2003; Skinner e Jahren, 2003). Em comparação com minerais inorganicamente produzidos, biominerais muitas vezes têm suas propriedades específicas de forma, tamanho, cristalinidade, além de composições isotópicas e de elementos traço (Weiner e Dove, 2003).

O termo "organomineral" foi proposto por Perry et al. (2007) para qualquer mineral precipitado pela interação com organopolímeros, componentes bioorgânicos, e / ou compostos orgânicos não biológicos, sem evidência de controle biológico direto, esquelético, intracelular ou extracelular. Organominerais são, portanto, uma evidência indireta de vida (Perry et al. 2007). Os principais componentes da organomineralização *sensu lato* são a "alcalinidade motora" (metabolismo microbial e condições ambientais afetando o índice de saturação de carbonato de cálcio) e uma matriz orgânica composta de EPS, que pode servir para a nucleação carbonato (Dupraz, et al. 2009).

A organomineralização induzida resulta da interação entre a atividade biológica e o ambiente, onde o micro-organismo exerce importante papel na precipitação mineral (Dupraz, et al. 2009). Já a organomineralização influenciada é definida como a mineralização passiva de matéria orgânica (origem biótica ou abiótica), cujas propriedades influenciam na forma e composição do cristal (Dupraz et al. 2009). Nesse caso, condições físico-

químicas (ex. estado de saturação da água) prevalecem sobre a influência de microorganismos no processo de precipitação, onde a presença ou ausência dos mesmos não interfere na precipitação. Ambos os termos são também classificados como organomineralização *sensu lato*.

1.5 Revisão das principais categorias de microbialitos

Os depósitos minerais resultantes da organomineralização *s.l.* (organomineralização induzida e influenciada) são chamados microbialitos (Burne e Moore, 1987). Estes microbialitos são classificados em estromatólitos, trombolítico e leiólitos de acordo com a sua forma.

1.5.1 Estromatólitos

Estromatólitos são definidos estruturas organossedimentares produzidos por aprisionamento e colagem e / ou precipitação mineral resultante das atividades metabólicas de microorganismos (Awramik et al. 1976). Kalkowsky (1908) já propôs uma definição que inclui a atividade microbial na gênese dessas estruturas. Hofmann (1969) definiu estromatólito como um registro sedimentar cumulativo das atividades de tapetes microbiais ao longo do tempo. Estromatólitos podem ser rastreados até o Arqueano, 3,5 bilhões de anos atrás (Awramik e Sprinkle, 1999).

A estrutura mais saliente de um estromatólito é a sua laminação interna. Laminações sempre registram algum tipo de oscilação temporal, sejam atividades microbiais ou sedimentares (Riding e Awramik, 2000). A distinção entre as lâminas depende do grau de qualquer forma de descontinuidade no processo da sua formação (Riding e Awramik, 2000).

Pelóides, esferulitos e micriticas, presentes em estromatólitos modernos e antigos foram descritos por diversos geólogos (Folk e Chafetz, 2000; Buczynski e Chafetz (1991); Chafetz e Buczynski, 1992). Os processos físicos, químicos e biológicos que controlam o crescimento de estromatólitos modernos ainda não foram totalmente compreendidos. Alguns autores consideram a formação de estromatólito como um processo estritamente biótico. Buczynski e Chafetz (1991) demonstraram que as bactérias são capazes de induzir a

precipitação de grãos de aragonita, que são essencialmente idênticos aos pelóides, esferulitos, micritas, que litificam os estromatólitos. O papel específico de microrganismos na formação de estromatólitos permanece elusivo, isto é, se eles têm um papel direto, promovendo a precipitação de carbonato, ou um papel indireto, pela colonização de minerais abioticamente precipitados e, eventualmente, aprisionando minerais abióticos. Atividades metabólicas, tais como a fotossíntese e sulfatorredução, são conhecidas por promover a precipitação de carbonato por alcalinização local (ou seja, aumento de pH), enquanto outras, tais como heterotrofia aeróbica ou fermentação, promovem a dissolução do carbonato por acidificação (Dupraz et al. 2009). Sabe-se que os organismos vivos colonizam a parte superior (1-10 mm) de um estromatólito em formação, na interface sedimento-água. Chafetz e Buczynski (1992) demonstraram que as bactérias preferencialmente induzem a precipitação de carbonato de cálcio em torno de filamentos de cianobactérias mortas, em comparação com filamentos de cianobactérias vivas, e, assim, formaram estromatólitos litificados, idênticos aos de ambiente natural. O precipitado que litifica a esteira de cianobactérias em estromatólitos forma-se ao redor de colônias de bactérias, semelhante ao processo de formação de pelóides em recifes (Folk e Chafetz, 2000).

A formação de estromatólitos continentais modernos ocorre em ambientes restritos e específicos, como observado no Japão (Figura 2).

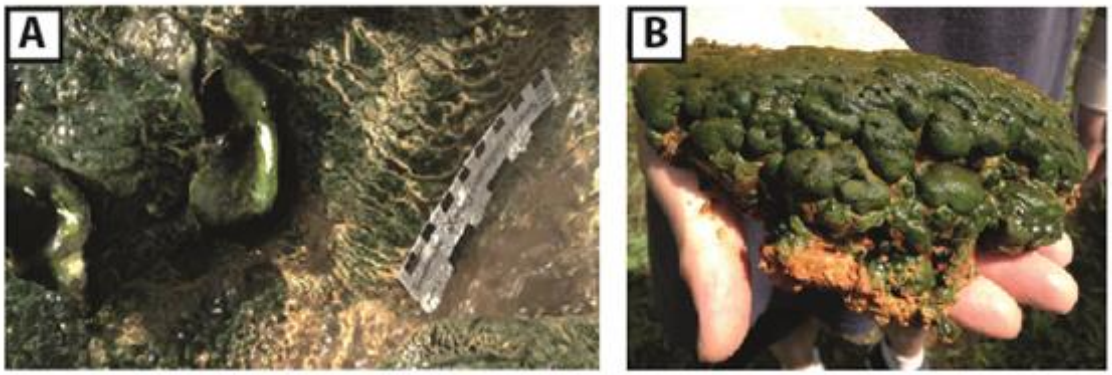

Figura 2: (A) Estromatólitos modernos coletados em cascata na Fonte Hidrotermal de Shiohitashi, Sul do Japão. Formação de estromatólito em cascata. A baixa velocidade do fluxo de água permite o crescimento dessas estruturas sem que ocorra erosão. Observa-se tendência de migração lateral dessa fácies, ocorrendo assim o recobrimento das camadas mais antigas (Fonte: cortesia de Bahniuk). (B) Aspecto de campo dos estromatólitos amostrados para análise na Fonte Hidrotemal de Kibedani, Oeste do Japão. Amostra coletada ao redor do gêiser, recoberta por um biofilme de cor verde escura recobrindo camadas subparalelas de cor vermelho (Fonte: cortesia de Bahniuk).

1.5.2 Trombólitos

Trombólitos distinguem-se dos demais microbialitos pela ausência de lâminas e / ou camadas bem desenvolvidas, por tramas irregulares ou coagulados macroscópicos, normalmente milimétricos a centimétricos, em matriz de cor clara (Aitken, 1967). Peloides, filamentos coagulados, tramas micríticas e microesparíticas ocorrem em trombólitos, bem como nos estromatólitos.

Os primeiros trombólitos relatados são da Formação Rocknest, de 1,9 Ga, e foram interpretados como formados através da incrustação inorgânica de comunidades microbianas prováveis por cimentos marinhos (Kah e Grotzinger, 1992). Aitken e Narbonne (1989) sugeriram que trombólitos foram importantes e diversificados durante o Proterozóico. Posteriormente, Riding (2008) relatou a falta de registro de trombólitos no Mesoproterozóico, mas existem diversos relatórios do Neoproterozóico. Trombólitos também ocorrem no Neoproterozóico de Omã e Namíbia (Grotzinger e James, 2000).

A abundância de trombólitos de trama filamentosa no Neoproterozóico refletem a visão de calcificação microbial (Kennard e James, 1986).

1.5.3 Dendrólitos

Dendrólitos constituem depósitos microbiais bentônicos não laminados ou fracamente laminados, com petrotramas dendriticas macroscópicas produzidas pela calcificação de micróbios, comumente filamentosos. (Riding, 1991). Esse tipo específico de microbialito tende a formar domos e colunas com camadas grossas, exibindo trama dendrítica do tipo arborescente vertical ou incompletas (Riding, 1991). A rápida calcificação e cimentação entre os fósseis arborescentes resultam na formação de uma estrutura que fornece um substrato rígido para a fixação de metazoans (ex. *archaecyaths, stromatoporoids*).

Dendrólitos foram observados em larga escala durante o início do Cambriano e do Ordoviciano, final do Devoniano e início do Carbonífero.

Estruturas arborescentes de dentrólitos contribuem significativamente para a formação de carbonatos não marinhos como os travertinos.

1.5.4 Leiólitos

Leiólitos são microbialitos praticamente afaníticos, sem laminação e sem petrotrama trombolítica ou dendrítica (Fairchild et al. 1995). Esse tipo específico de depósito microbial é constituído por micrítica sem arranjo preferencial e geralmente apresenta estrutura maciça ou mal definida com coágulos ou trama dendrítica. A formação de leiólitos está relacionada ao suprimento constante e variado de sedimentos em uma superfície colonizada por uma comunidade uniforme de micróbios (Fairchild et al. 1995).

1.6 Depósitos de tufa e travertino

Os termos tufa e travertino são frequentemente usados alternadamente na literatura (Dupraz et al. 2009). A distinção entre estes foi descrita por Ford e Pedley (1996), que categorizaram tufa para os depósitos sedimentares de água de temperatura próxima ao ambiente e travertino para depósitos hidrotermais continentais.

1.6.1 Travertino

Os travertinos constituem o principal grupo de carbonatos continentais, distribuídos por quase todo o mundo (Pentecost, 1995) (Figura 3). Pentecost (2005) revisou o termo travertino e o classificou como depósitos de carbonato continentais precipitados em decorrência de variações químicas que formam ao longo dos córregos e lagos.

A mineralogia é composta de aragonita ou calcita com baixa porosidade média intracristalina, porém com elevada porosidade estrutural e módica. A precipitação de $CaCO_3$ está principalmente relacionada com a desgaseificação de CO_2 a partir do sistema, o que resulta na supersaturação do carbonato de cálcio. A nucleação e crescimento de cristais geralmente ocorrem na interface ar-água (Dupraz et al. 2009). Micróbios termofílicos sido são relacionados à formação de travertino e sílica sínter (Renaut e Jones, 2000).

Travertinos precipitados em gêiseres hipertemais (> 75 ° C) geralmente são abióticos e comumente exibem morfologias cristalinas em desequilíbrio. A

precipitação de sílica em gêiseres hipertemais resulta principalmente do rápido resfriamento e evaporação. Micróbios, no entanto, podem desempenhar um papel importante, servindo de locais para nucleação de sílica e controlando o desenvolvimento de tramas de sínter e geyserita (Renaut e Jones, 2000).

De acordo com Pentecost (2005), travertinos podem ser classificados em dois tipos principais, de acordo com a fonte do CO_2. Os travertinos meteogenênicos capturam CO_2 da atmosfera e aparentemente apresentam forte relação com fatores climáticos, uma vez que o dióxido de carbono é proveniente principalmente do solo. Por outro lado, os travertinos termogênicos capturam CO_2 a partir de fontes hidrotermais e não apresentam relação direta com clima. No entanto, o fluxo de águas subterrâneas pode se tornar restrito e não interagir com a atmosfera sob períodos de glaciação ou na tundra (Pentecost, 1995). Esses depósitos são majoritariamente associados com fontes de água quente (Pentecost, 1995).

Viles e Pentecost (1994) também classificaram travertinos de acordo com os processos deposicionais e criaram uma subdivisão principal em depósitos autóctones e alóctones. Os travertinos autóctones foram subdivididos em: *spring mounds, fissure ridges,* cascatas*,* represas*,* crostas fluviais, crostas lacustres*, paludal deposits* e *surface-cemented.*

No entanto, alguns travertinos são rapidamente erodidos, formando depósitos alóctones, muitas vezes de elevado valor económico. Pedley (1990) subdividiram estes depósitos em cinco grupos: fácies *phytoclast*, oncóides, intraclastos, microdetritais e pelóides.

O Interesse em travertino tem aumentado, porque seus fósseis e informações isotópicas fornecem informações valiosas sobre condições climáticas passadas (Pentecost, 1995).

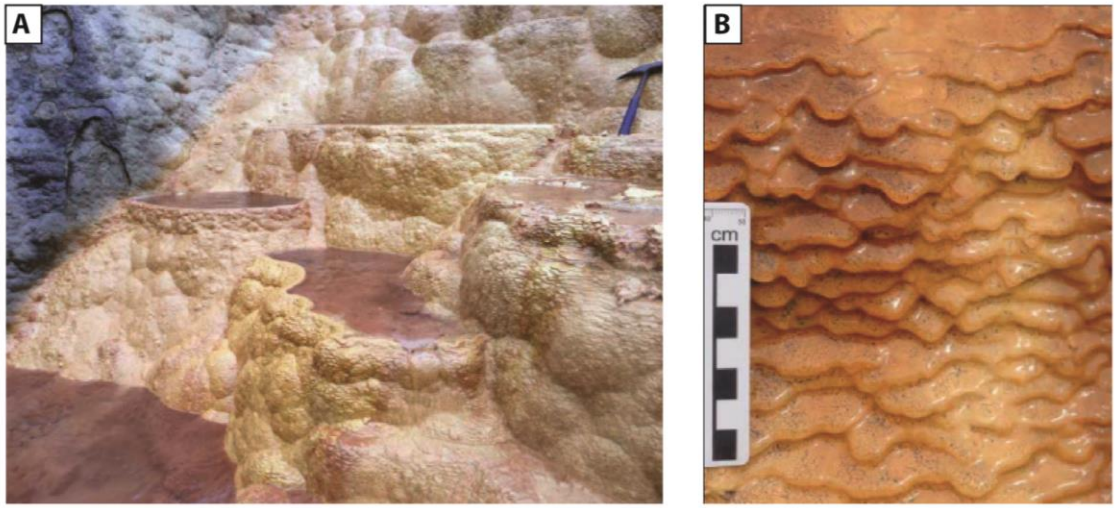

Figura 3: (A) Formação de piscinas na Fonte Hidrotermal de Futamata, Hokkaido, Norte do Japão. (Fonte: cortesia de Jiro Asada). (B) Formação de piscina em sistema de travertino, na Fonte Hidrotermal de Oku-okuhachikuro, Aomori, Norte do Japão. A formação dessas piscinas está diretamente relacionada com a forma do relevo, assim como a velocidade do fluxo de água. (Fonte: o Autor).

1.5.2 Tufa

Tufa como um nome geral abrange uma ampla variedade de depósitos de água doce calcárias que são particularmente comuns no final do Quaternário e sucessões recentes (Ford e Pedley, 1996). Tufa é um depósito de carbonato de cálcio que se forma em ambientes de água doce em condições de temperatura ambiente (Pedley, 1990). Diversos mecanismos de precipitação mineral têm sido propostos para explicar a formação do tufa, e estes variam de puramente abiótico para uma explicação puramente biótica (Manzo, et al. 2012). O principal controle físico abiótico na precipitação mineral é a desgaseificação de CO_2 a partir de água, levado precipitação passiva de substratos orgânicos e inorgânicos (Kano et al. 2003).

Tufas desenvolvem-se sob a influência de água doce corrente, em sistemas com tendência agradacional em vez de progradacionais. Os travertinos tendem a migrar lateralmente para tufas em áreas onde a água resfria-se a temperaturas próximas ao ambiente (Ford e Pedley, 1996). Tufas são geralmente distinguíveis de travertinos, mesmo em depósitos antigos, pela elevada diversidade de plantas, incluindo macrófitas e animais.

As razões e os mecanismos precisos que ocorrem na bio precipitação de carbonato ainda são incertas, mas são discutidos por Krumbein (1979) e Riding

(1991). No entanto, sabe-se que a micrita é subproduto acidental dos processos metabólicos de cianobactérias e bactérias heterotróficas.

Baker e Orr (1986) e Pedley (1992) sugeriram que os gradientes de diminuição das concentrações de CO_2 são desenvolvidos nas imediações das superfícies do biofilme. Consequentemente, em áreas com fluxo lento, a depleção local do CO_2 por micróbios pode ser o principal gatilho para a precipitação de carbonato (Pedley, 1990). A micrita, microesparita e esparíta, são os constituintes dominantes de tufa. Sua interpretação em termos de gênese ainda está sendo debatida; e o fator estritamente biológico tem sido interpretado como responsável pelo estágio inicial de precipitação da micrita (Pedley e Rogerson, 2010). A micrita precipitada parece crescer em *sites* de nucleação como pelóides, cristais embrionários que revestem bainhas de cianobactérias e partículas detríticas (Pedley, 1990). No entanto, a calcita esparítica na tufa é comumente considerada como cimento de produto inorgânico, embora comumente ocorra em finas camadas alternadas, diretamente associada com a micrita biótica (Pedley e Rogerson, 2010).

Espeleotemas podem ser considerados como o componente do extremo oposto inorgânico de um processo contínuo que, no outro extremo é representado por tufa precipitada por processos biológicos (Pedley, 1990). O termo tufa deve ser adotado para todas as variedades de depósitos calcários não hidrotermais e fluviais relacionados com depósitos de água doce calcários que contêm bactérias, plantas e animais, independentemente do grau de cristalinidade ou idade (Pedley, 1990) (Figura 4).

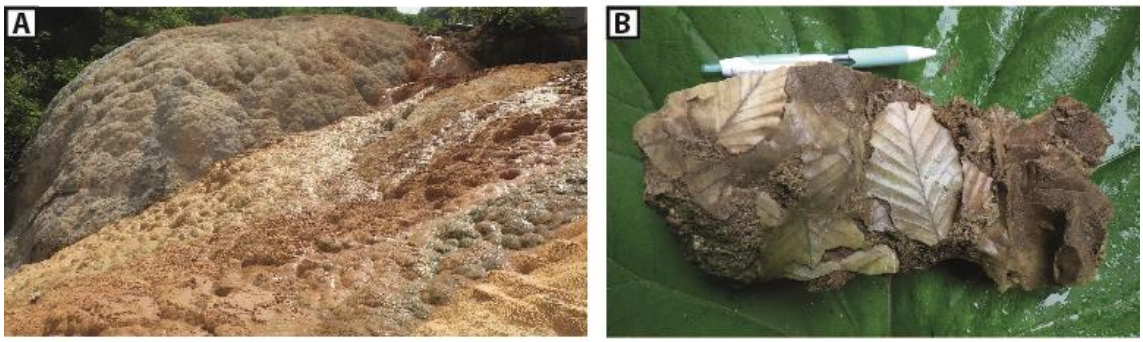

Figura 4: (A) Fonte Hidrotermal de Futamata, Hokkaido, Norte do Japão. Considerado o sistema de precipitação mais ativo de rochas carbonáticas no Japão é também tombado como Patrimônio Mundial da UNESCO (Fonte: cortesia de Jiro Asada). (B) Tufa contendo fósseis de folhas e fragmentos vegetais observados em escala mão. A rápida taxa de precipitação, assim como a degradação da matéria orgânica permitem a formação dessas estruturas (Fonte: cortesia de Jiro Asada)

1.7 Vida intraterrestre *versus* vida extraterrestre

Microbialitos também se tornaram debate em lugares onde não há muito tempo pensou-se que a vida não poderia existir como a terra profunda e lugares extraterrestres. Estas formas primordiais de vida intraterrestre alimentam-se de ferro e colonizam alguns dos terrenos mais inóspitos da Terra como a crosta ígnea que chega a cerca de 500 metros abaixo do fundo do oceano (Mascarelli, 2009). Relatórios de micróbios em habitats extremos foram mostrados desde o final dos anos 1990. Esses micróbios foram encontrados a 3 km abaixo da superfície na África do Sul e 2,5 quilómetros abaixo da superfície com temperaturas superiores a 120 ° C em Dakota do Sul, EUA. Desde então, esta temperatura é considerada como sendo o limite de temperatura de vida. Apesar de sua pouca semelhança entre as comunidades profundas da biosfera (*Archea*) e as comunidades de bactérias da superfície (Escherichia coli), estudos comparativos entre as essas comunidades mostram que, enquanto as bactérias de superfície dividem-se a cada poucos minutos, os organismos da biosfera profunda reproduzem em uma escala secular. Alguns micróbios subsuperficiais podem reproduzir uma vez a cada 1.000 anos (Wanger et al. 2008).

A fim de obter energia necessária para a vida, estes micróbios que vivem abaixo do fundo do mar podem metabolizar os restos orgânicos que foram concentrados através da fotossíntese em plantas e algas, e que foram carreadas para níveis profundos (Mascarelli, 2009). Este processo é chamado de "ciclo de carbono profundo". D'Hont et al. (2004), também investigam se sub micróbios do fundo do mar podem obter energia do hidrogênio liberado durante o decaimento da radioativo do urânio, tório e potássio quando nesse processo, a molécula de água é dividida em hidrogênio e oxigênio. De acordo com D'Hont et al. (2004), este processo pode ter ocorrido ao longo da história da Terra e deve estar ocorrendo atualmente em Marte. Os micróbios encontrados a 3 km de profundidade na África do Sul possuem metabolismo semelhante, uma vez que sobrevivem a partir do sulfato e hidrogênio geologicamente produzidos, livre de qualquer dependência da energia derivada do Sol (Lin et al. 2006). A bactéria *Candidatus Desulforudis audaxviator* sobrevive na escuridão a 60 ° C,

cerca de 2,8 quilômetros abaixo da superfície da Terra (Inagaki et al. 2006). Estes micróbios reduzem o sulfato gerado indiretamente pelo decaimento radioativo do urânio a fim de obter a sua energia e também extrair o carbono e nitrogênio das rochas circundantes (Mascarelli, 2009). Este ecossistema único "aponta para um modo de vida que potencialmente ocorria na Terra primitiva", antes oxigenação da atmosfera (Chivian, 2008).

Micróbios que habitam a zona abaixo do assoalho oceânico também são responsáveis pelo fornecimento de nutrientes para o oceano. Segundo os cientistas estes organismos produzem dióxido de carbono e metano, liberando nitrogênio, enxofre e fósforo dos sedimentos. Fluidos que percolam a crosta também carregam micróbios que liberam ferro e outros elementos e, consequentemente, liberam esses nutrientes para o oceano. O clima da Terra também é afetado por esses micróbios. Processos microbiais seriam os principais responsáveis pela geração de hidrato de metano (Mascarelli, 2009). Este metano pode ter formado grandes depósitos que foram desestabilizados em vários momentos ao longo do tempo geológico, liberando metano o suficiente, muito mais potente do que o CO_2, para aquecer substancialmente o planeta (Mascarelli, 2009).

Estas recentes descobertas estão mudando a maneira que os cientistas pensam sobre biosfera profunda. Menos de duas décadas atrás, estes micróbios eram considerados como mera curiosidade e hoje em dia representam as últimas fronteiras de alta tecnologia na Terra. Atualmente, os cientistas passaram a observar o importante e crucial papel destes organismos em ciclos globais, ajudando a repor os minerais essenciais para dentro do oceano e até mesmo mediar o clima (Mascarelli, 2009). Os estudos de microorganismos, bem como suas atividades servem de análogo para as descobertas sobre as origens da vida na Terra e em outros planetas.

REFERÊNCIAS

AITKEN, J.D. Classification and environmental significance of cryptalgal limestones and dolomites, with illustrations from the Cambrian and Ordovician of SW Alberta. **J. Sed. Petrol**, v.37, p.1163-1178, 1967.

AITKEN, J.D; NARBONNE, G. M. Two ocurrences of Precambrian thrombolites from the Mackenzie Mountains, northwestern Canada. **Palaios**, v.4, p.384-388, 1989.

AWRAMIK S. M.; MARGULIS L., Barghoorn E. S., Evolutionary processes in the formation of stromatolites. *In:* WALTER, M. R. Stromatolites: developments in sedimentology. **Elsevier**, v.20, p.149-162, 1976.

AWRAMIK, S. M.; SCHOPF, J. W.; WALTER, M. R. Filamentous fossil bacteria from the Archean of Western Australia. **Precambrian Research**, v.20, p.357, 1983.

AWRAMIK, S.M.; SPRINKLE, J. Proterozoic stromatolites: the first marine evolutionary biota. **Historical Biology**, v.13, p.241-253, 1999.

BAHNIUK, A.M. Coupling organic and inorganic methods to study growth and diagenesis of modern microbial carbonates, Rio de Janeiro State, Brazil: implications for interpreting ancient microbialite facies development. PhD Thesis. **ETHZ**, Zurich, 169 pp, 2013.

BAKER, J.H.; ORR, D.R. Distribution of epithytic bacteria on freshwater plants. **Journal of Ecology**, v.74, p.155-165, 1986.

BENZERARA, L.; MENGUY, N. Looking for traces of life in minerals. **Comptes Rendus Palevol**, v.8, p.617-628, 2009.

BUCZYNSKI, C.; CHAFETZ, H. S. Habits of bacterially induced precipitation of calcium carbonate and the influence of medium viscosity on mineralogy. **J. Sedimentary Petrol.** V.61, p.226-233, 1991.

BURNE, R. V.; MOORE, L. Microbialites; organosedimentary deposits of benthic microbial communities. **Palaios**, v.2, p.241–254, 1987.

CHAFETZ, H.S.;BUCZYNSKI, C., Bacterially induced lithification of microbial mats: **Palaios**, v.7, p.277-293, 1992.

CHAFETZ, H. S; BUCZYNSKI, C. Habits of bacterially induced precipitation of calcium carbonate: examples from laboratory experiments and recent sediments *In:* RIDING, R.; AWRAMIK, S.M. Microbial Sediments. **Springer**, v.1, p.40, 2000.

CHARACKLIS, W.G.; MARSHALL, K.C. Biofilms, **New York: Wiley** p.93-130, 1990.

CHIVIAN, D., 2008 *In:* MASCARELLI, A. L. Low Life, **Nature**, v.459, p.770-773, 2009.

CORSTENTON, J. W.; GEESEY C. G.; CHENG, K. J. How bacterias dig **Science**, v.238, p.86-95, 1978.

CORSTENTON, J. W.; IRVIN T. R.; CHENG, K. J. O glicocálice bacteriana na natureza e da doença. **Ann. Rev. Microbiologia**, v. 35, p.299-324, 1981.

D'HONT, S.; JORGENSEN, B. B., MILLER, D. J.; BATZKE, A.; BLAKE R. Distribuição de atividades microbianas em sedimentos subsuperfície profundas. **Science**, 2004.

DOEMEL, W. N.; BROCK, T. D. Bacterial stromatolites. Origin of laminations. **Science**. v. 184. p. 1083-1085, 1974

DUPRAZ, C.; REID, P.R.; BRAISSANT, O.; DECHO, A.W.; NORMAN, R.S.; VISCHER, P.T. Processes of carbonate precipitation in modern microbial mats. **Earth Science Reviews**, v. 96, p. 141–162, 2009.

FAIRCHILD, T. R.; ROHN, R.; DIAS-BRETO, D. Microbialitos do Brasil do Pré-Cambriano ao Recente. Um atlas, **UNESPetro**, 2015.

FOLK, R. L.; CHAFETZ, H.S. Bacterially induced microscale and nanoscale carbonate precipitates *In:* RIDING, R.; AWRAMIK, S.M. Microbial Sediments. **Springer**, v.1, p.41-49, 2000.

FORD, T. D.; PEDLEY, H.M. A review of tufa and travertines deposits of the world. **Earth Science Review**, v.41, p.117-175, 1996.

GERARD, E. – Specific carbonate-microbe interactions in the modern microbialites of Lake Alchichica (Mexico), **The ISME Journal,** 2013.

GORBUSHINA, A. A., KRUMBEIN, W. E. Subaerial biofilms and theis effects on soil and rock. *In:* RIDING, R. E., AWRAMIK, S. M. Microbial Sediments. **Springer**, v.1, p.161-170, 2000.

GROTZINGER, J.P.; JAMES, N.P. Precambrian carbonates: evolution of understanding. **SEPM, Spec. Publ**., v.67, p.3-20, 2000.

HOFMAN, H.J. Stromatolites from the Proterozoic Ahimikie and Sibley groups, Ontario. **Geol. Survey Canada**. v.68-69, p.55, 1969.

INAGAKI, F.; MARCEL M. M.; TSUNOGAI, U. K.; ISHIBASHI, J.; NAKAMURA, K.; TREUDE, T.; OHKUBO, S.; NAKASEAMA, .M; GENA, K.; CHIBA, H.; HIRAYAMA, H.; NUNOURA, T.; TAKAI, K.; JORGENSEN, B.; HORIKOSHI, K.; BOETIUS, A.; KAH, L.S. Microbial community in a sediment-hosted CO_2 lake of

the southern Okinawa Trough hydrothermal system. **The National Academy of Sciences of the USA,** V.103 (38), 2006.

KAH, L. C.; GROTZINGER, J. P. Early Proterozoic (1.9 Ga) thrombolites of the Rocknest Formation, Northwest Territories. - **Palaios**, v.7, p.305-315, 1992.

KALKOWSKY, E. Oolith und Stromatolith im norddeutschen Buntsandstein. **Zeitschrift der Deutschen Geologischen Gesellschaft**, v.60, p.69-125, 1908.

KANO, A.; MATSUOKA, J.; KOKO, T.; FUJI, H. Origin of annual laminations in tufa deposits, Southwest Japan, **Paleogeography Paleoclimatology Paleoecology**, v.191(2), p.243-262, 2003.

KENNARD, J.M.; JAMES, N.P. Thrombolites and stromatolites: Two distinct types of microbial structures. **Palaios**, v.1/5, p.492-503, 1986.

KNOLL, A. H.; WORNDLE, S.; KAH, L.C. Covariance of microfossil assemblages and microbialite textures across an upper Mesoproterozoic carbonate platform. **Palaios**, v.28, p.453-470, 2013.

KRUMBEIN, W.E. Calcification by bacteria and algae. *In*: Trudinger, P.A.; Swaine, D.J. (eds.): Biochemical cycling of mineral-forming elements. - Studies in Environmental Science, v.3, p.47-68, **New York (Elsevier)**, 1979.

KRUMBEIN, W.E. Stromatolites: the challenge of a term in space and time. **Precambrian Research**, v.20, p.493-531, 1983.

KRUMBEIN, W.E. The year of the slime. *In:* KRUMBEIN, W.E.; PATTERSON, D.; STAL L.J. Biostabilization of sediments. **Bibl. Inform.Carl von Ossietzky Universitat, Oldenburg**, p.1-7, 1994.

LIN L. H.; WANG, P.L.; RUMBLE, D.; LIPPMANN-PIPKE, J.; BOICE, E.;, PRATT, L.M.; SHERWOOD L. B.; BRODIE, E.L.; HAZEN, T.C.; ANDERSEN, G.L.; DESANTIS, T.Z.; MOSER, D.P.; KERSHAW, D.; ONSTOTT, T.C. Long-term sustainability of a high-energy, low-diversity crustal biome. **Science** v.314, p.479–482, 2006.

MANZO, E.; PERRI, E.; TUCKER, M.E. Carbonate deposition in a fluvial tufa system: processes and products (Corvino Valley – Southern Italy). **Sedimentology**, v. 59, p. 553-577, 2012.

MARSHALL, K. C.; SOUTU, R.; MIRCHELL, R. Mechanisms of the initial events in sorption of marine bacteria to solid surfaces. **J. Gen. Microbiol.** v.68, p.337-348, 1971.

MARSHALL, K. Biofilms: an overview of bacterial adhesion, activity, and control at surfaces. **ASM News**, v.58, p.202-207, 1992.

MASCARELLI, A. L. Low Life, **Nature**, v.459, p.770-773, 2009.

MENDELSOHN F. Mineral deposits associated with stromatolites. *In:* WALTER, M. R. Stromatolite. **Sedimentology**, v.20 p.645-662, 1976.

MERZ-PREIB, M.; RIDING, R. Cyanobacterial tufa calcification in two freshwater streams: ambient environment, chemical thresholds and biological processes. **Sedimentary Geology**, v.126, p.103-124, 1999.

PEDLEY, H.M. Classification and environmental models of cool freshwater tufas. **Sedimentary Geology**, v.68, p.143-154, 1990.

PEDLEY, H. M. Freshwater (phytoherm) reefs: the role of biofilms and their bearing on marine reef cementation. - **Sed. Geol**., v.79, p.255-274, 1992.

PEDLEY, H. M. Tufas and travertines of the Mediterranean region: a testing ground for freshwater carbonate concepts and developments. **Sedimentology**, v.56, p.221-246, 2009.

PEDLEY, H. M.; ROGERSON, M. Tufas and speleothems: Unravelling the microbial and physical controls. **Geological Society, London**, v.336, p.211-224, 2010.

PENTECOST, A. Quaternary travertine deposits of Europe and Asia Minor**. Quat. Sci. Rev** v.14, p.1005–1028, 1995.

PENTECOST, A. Travertine. **Springer** v.455, 2005.

PERRY, R.S.; MCLOUGHLIN, N., LYNNE, B.Y., SEPHTON, M.A., OLIVER, J.D., PERRY, C.C.; CAMPBELL, K., ENGEL, M.H., FARMER, J.D., BRASIER, M.D. AND STALEY, J.T. Defining biominerals and organominerals: direct and indirect indicators of life.**Sedimentary Geology**, v.201, p.157-179, 2007.

RENAUT, R. W.; JONES, B. Microbial precipitates around continental hot springs and geysers *In:* RIDING, R.; AWRAMIK, S.M. Microbial Sediments. **Springer**, v.1, p.187-195, 2000.

RIDING, R. Classification of microbial carbonates. *In*: Calcareous Algae and Stromatolites (Ed. Riding, R.), p. 21-51, **Springer-Verlag, New York**, 1991.

RIDING, R. The term stromatolite: towards and essential definition. **Lethaia**, v.32, p.321-330, 1999.

RIDING, R. Microbial carbonate abundance compared with fluctuations in metazoan diversity over geological time. **Sedimentary Geology**, v.185, p.229-238, 2006.

RIDING, R. Abiogenic, microbial and hybrid authigenic carbonate crusts: components of Precambrian stromatolites. **Geologia Croatica**, v.61, p.73-103, 2008.

RIDING, R. Microbialites, stromatolites and thrombolites. *In*: J. Reitner and V. Thiel (eds), Encyclopedia of Geobiology, Encyclopedia of Earth Science Series, **Springer**, Heidelberg, pp. 635-654, 2011.

RIDING, R.; AWRAMIK, S.M. Microbial Sediments. **Springer**, v.1, p.40, 2000.

SKINNER, H.C.; JAHREN, A.H. Biomineralization. **Treatise on Geochemistry**. v.8, 2003.

STOLZ, J. F. Distribution of phototrophic microbes in the laminated microbial mat at Laguna Figueroa, Baja California, Mexico. **BioSystems**, v.23, p.345-347, 1999.

STOLZ, J.F. The ecology of phototrophic bacteria. *In:* STOLZ, J.F. Structure of phototrophic prokaryotes. **CRC Press**, p.105-123, 1991.

SUMNER, D.Y. Microbial influences on local carbon isotopic ratios and their preservation in carbonate. **Astrobiology**, v.1, p.57-70, 2001.

VILES, H.; PENTECOST, A. Review and reassessment of travertine classification. **Géographie Physique et Quaternaire**, p.305-314, v. 48, 1994.

WANGER, G., ONSTOTT, T.C. AND SOUTHAM, G. Stars of the terrestrial deep subsurface: A novel ‘star-shaped’ bacterial morphotype from a South African platinum mine. **Geobiology**, v.6, p.325–330, 2008.

WEINER, S.; DOVE, P. M. An overview of biomineralization processes and the problem of the vital effect. **Geochemistry Soc.** p.1-29, 2003.

CAPÍTULO 2

ENVIRONMENTAL CONDITIONS PLAYING IMPORTANT ROLE IN CONTINENTAL CARBONATE FACIES FORMATION IN JAPAN: GEOCHEMISTRY AND FACIES PATTERNS.

ABSTRACT

The present work is about a detailed sedimentological and geochemical investigation in modern carbonate deposits in nine hot springs and one tufa creek in Japan. The study area is located in Kyushu, Honshu, and Hokkaido islands. The islands were sampled in order to compare different geological background and environmental conditions, based on water chemistry, physical-chemical and geochemical parameters. The data shows that water physicochemistry (temperature, pH, and dissolved oxygen) directly influences on carbonate precipitation and consequently in facies types. Furthermore, the morphology of the substrate where the carbonates grow, likewise distance away from the vent, also contribute to different facies formation. Mineralogical results show that the Southern hot springs (Nagayu, Shiohitashi, and Myoken hot springs) are mainly composed of aragonite while the Western (Yamabato and Kibedani hotsprings and Shimokuraida tufa) and Northern (Furutobe, Oku-okuhachikuro, Ohfuna, and Futamata hot springs) hot springs and tufa creek are mostly composed of calcite. Chemical results show high contents of CaO and subordinated contents of Fe_2O_3 and SiO_2 in all of the samples. Subordinated, arsenic contents were also observed and its origin is stills in debate. Subordinately biogenic precipitation might control the biomineral formation and the mineralogy might change, as well, accordingly to the phylogenetic lineage involved. The isotopic signals reveal depleted values of $\delta^{18}O$ in all samples. The majority of $\delta^{13}C$ values were near 0‰,and few depleted and also enriched values.Therefore, these carbonates are interpreted as precipitated from meteoric surface water, sometimes contaminated by volcanism, due to the CO_2 degassing, with little or insignificant biological precipitation. The SEM images allow nano scale observations and show fossils related to EPS (extracellular polymeric substances) characterizing biological influence during precipitation in the stromatolite facies. The Micro-CT observations allow a detailed examination of pores from all facies, showing that the bubble facies is the most porous one, followed by shrub, root, and stromatolite. This unique faciological characterization of continental carbonates might potentially be an analogue for carbonate reservoirs, such as the Pre-Salt in Brazil.

Key-words: microbialites, facies, geochemistry

This chapter will be submitted to Sedimentology by França, R.M; França, A.B.; Cury, L.F; Jiro, A.; Shiraishi, F.; Bahniuk, A.M.

2. Introduction

Microbialites are defined as organo-sedimentary deposits that accrete by the action of benthic microbial communities, which trap and bind detrital sediment and/or form the locus of mineral precipitation (Burne & Moore, 1987; Riding, 1991). The term "microbialite" is used to describe authigenic accumulations such as carbonate stromatolites, some tufa and also travertine (Riding, 2011). Julia (1983) already discussed the terms tufa and travertines as being used indiscriminately or even as alternative names for the same material. Despite their identical chemical composition and similar characteristics, tufa and travertine, are different in their lithofacies and depositional environments; generally, they are found at karstic or hydrothermal springs, small rivers and swamps Pentecost (1993, 1995). Pentecost (1993, 1995) also describes depositional temperature of precipitation as the main manner of characterization.

The study area is located in active hot springs in the South, West and North of Japan. Carbonates precipitate from continental, Ca-rich spring waters which flow in epigean conditions, derived from groundwaters mostly of meteoric, but also from supposed magmatic origin. These waters acquire specific geochemical and physical properties, depending on the depth of circulation/recharge paths and connections with older carbonate bedrock origin, geothermal fluids and magmatic rocks (Pentecost, 2005, Gandin & Capezzuoli, 2014). Considering that there are only a few and specific modern environments under such conditions to precipitate continental carbonates, including tufa and travertines, Japan has recently become subject of this kind of studies.

The main objective of this study is to understand the depositional and environmental processes of modern sedimentar continental carbonates precipitating around active hot springs and karst creek in Japan through the lithofacies caracterization. According to Selley (1985) *In* Claess *et al.,* (2015), “A sedimentary facies or lithofacies is a mass of sedimentary rock which can be defined and distinguished from another by its geometry, lithology, sedimentary structures, paleocurrent, pattern and fossils. It reflects a depositional environment that is preserved in the stratigraphic record in the form of a facies”. Different approaches were applied to asset carbonate facies. The depositional environmental models are

mainly based on Ford & Pedley (1996), that propose a barrage model (barrage system) and perched springline (slope system).

The combination of field investigations (i.e. physio-chemical and environmental conditions), petrography (thin section, Scanning Electron Microscope - SEM), geochemistry (X ray fluorescence - XRF and X ray diffraction - XRD) and also micro tomography - micro-CT, analyses provided a detailed facies characterization.

2.1. Regional setting

The origin of the Japanese Island Arc System occurred mainly along the continental margin of Asia since the Permian, being a result of subduction of the ancient substrate of the Pacific Ocean. The formation of backarc basins in the Tertiary has shaped the present configuration. The neotectonic regime characterized by strong East-West compression began with the movement of the Amur plate toward the east in the Quaternary (Taira, 2001). The Japanese archipelago is characterized by sedimentary, igneous and metamorphic units of the Phanerozoic, in one of the best examples of current tectonic Island Arcs (Kitano, 1963, Muramatsu, 1984).

The Japanese Island Arc System is a well-studied example of arc trench system in the Western Pacific (Sugimura, 1972; Uyeda 1973). The arcs are segmented into four parts: Kuril, Honshu, Ryukyu and Izu-Bonin, (Taira, 2001), including four large islands; Shikoku Hokkaido, Honshu and Kyushu.

The study area (Table 1) comprises three distinct geographical regions: South in the island of Kyushu (NAG, SHIO and MYO sites); West in the island of Honshu (YAMA, NIIMI and KIBE sites); and North in the island of Hokkaido (FURU, OKU, OHF and FUTA) (Figure. 1).

Table 1: List of site identification, site name, prefecture, geographical coordinates and number of collected samples.

Island	Site ID	Site Name (Hot Spring)	Latitude	Longitude	N° Samples	Samp. Period
Kyushu	NAG	Nagayu	33° 4'1.01"N	131°22'25.06"L	26	Jan/2014
	MYO	Myoken	31°48'39.92"N	130°45'28.32"L	16	Jan/2014
	SHIO	Shiohitashi	31°50'4.60"N	130°44'38.90"L	8	Jan/2014
Honshu	YAMA	Shionoha	34°15'43.16"N	136° 2'26.43"L	24	July/2014
	NIIMI	Shimokuraida	34°57'20.48"N	133°30'18.96"L	7	July/2014
	KIBE	Kibedani	34°25'44.20"N	131°53'42.42"L	8	July/2014
Hokkaido	FURU	Furutobe	40°25'48.33"N	140°40'7.88"L	21	June/2015
	OKU	Oku-okuhachikuro	40°24'28.07"N	140°45'16.86"L	23	June/2015
	OHF	Ohfune	41°58'42.90"N	140°52'59.52"L	8	June/2015
	FUTA	Futamata	42°34'36.76"N	140°14'22.12"L	15	June/2015

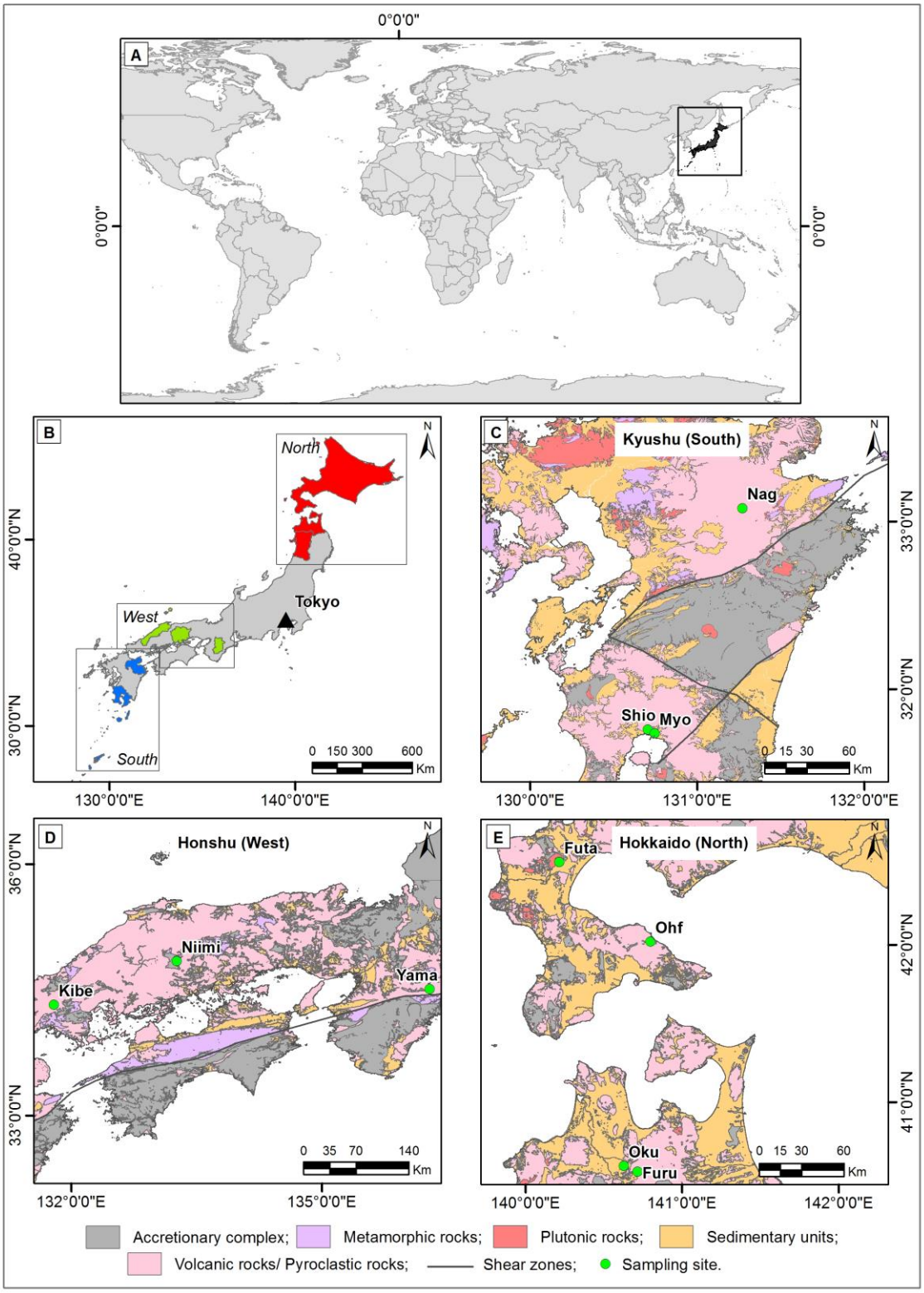

Figure 1: (A) World map, Japan highlighted. (B) Map of Japan and three main island in the north (Hokkaido), west (Honshu) and south (Kyushu). (C) Kyushu island, and the analyzed sites (NAG, SHIO and MYO; (D) Honshu island and the analyzed sites (KIBE, NIIMI and YAMA); (D) Honshu and Hokkaido island and, the analyzed sites (FURU, OKU, OHF and FUTA) (simplified from www.gsj.jp).

2.1.1 Geology of Kyushu Island

The Nagayu Hot Spring, samples called NAG, is located in the region of Oita, central area of Kyushu, in the eastern portion of the Beppu-Shimabara Graben. This Graben is located at the junction between the South-West Japan Arc and the Ryukyu Arc, developed with the subduction of the Philippine Plate under the Eurasian Plate (Aitchson, 1986). The Ohita-Kumamoto fault, which defines the Southern edge of the graben, concentrates several hydrothermal sources. The volcano Mt. Kuju, located approximately 10 km from the Nagayu Hot Spring is considered as a source of heat, CO_2, and calcium.

The Hot Springs of Myoken and Shiohitashi (Kagoshima Prefecture), defined as MYO and SHIO, respectively, are located in the Southern Kyushu region, in the Graben Kagoshima, characterized by intense volcanism. The Kagoshima Graben was formed three million years after the development of the back-arc basin (Okinawa Trough). There are several active volcanoes in the region, including Mt. Kirishima (0.3 million years). There is a compositional chemical zoning of spring water around the Mt. Kirishima, including a sulfur rich zone and high temperatures (~80°C) at the vicinity. The most distant water sources (approximately 15 km away from the Mt. Kirishima) have high ash content and moderate temperatures (~50°C) as sources of Myoken and Shiohitashi. These sources are located approximately 15 km away from the Mt. Kirishima. The water of the hydrothermal vents is enriched in CO_2 and calcium through water-rock interactions (Fujitimoto, 1961). Both hydrothermal vents are sourced in the Kokubu Group, middle Pleistocene, composed of lacustrine deposits and shallow marine noncarbonate rocks (Taira, 2001).

2.1.2 Geology of Honshu Island

According to Aitchison (1986) the province of Shionoha, defined as YAMA samples in this study, is a region with little volcanic influence, crossed by Median Japan Tectonics (LMTJ), from east to West. The region is located close to Interior Zone, where the North-South fault controls the landscape. The Shionoha fault separates the Chichibu east Terrain east of the Shimanto west Terrain West. These areas include *melange* alien blocks of chert, basalt and shales with deformed matrix.

The Shimanto Terrane was accreted to the Southeast portion of the Cretaceous to Miocene of Japan, as a result of subduction of the Kula plate.

The Shimokuraida region, called samples NIIMI, is geologically located on the plateau Limestone Atetsu, one of the largest occurrence of limestones in Japan. The deposition of the Limestone Atetsu occurred during the Permian on top of a basaltic submerse elevation. Similar to Shionoha, Ca^{2+} and CO_2 in Shimokuraida originate from water-rock interaction (Aitchison, 1986).

According to Aitchison (1986), the region of Shimane, more precisely Kibedani District, called samples KIBE, is geologically settled over granite, gabro, andesites, and rhyolites of Late Cretaceous and rhyolites and basalts of Pleistocene age. The bodies of rhyolites are prevalent in the area and occur continuously as a major NE intrusion.

Similarly to Shionoha and Shimokuraida, Ca^{2+} and CO_2 arise from the interaction of water with subsurface rocks. The percolation of meteoric water occurs through fractures and faults, returning to the surface through existing geysers in the area. Geological, hydrogeological and exploration of radioactive minerals suggest the existence of underground caves between conglomeratic and sandy levels in talus deposits.

2.1.3 Geology of the Honshu and Hokkaido Islands

The hot springs springs of Furutobe and Oku-okuhachicuro, samples defined as FURU and OKU, are located in the Akita region (Figure 1). This region is characterized by submarine volcanic rocks of Miocene age arranged in layers up to 350 m thick. These rocks overlie the Permian age basement consisting of phyllite, chert and marble (Fujimoto, 1961) and are covered by pumice flow deposits of the Towada Volcano.

The hot springs of Ohfuna and Futamata, samples called OHF FUTA, respectively, are located in the south of Hokkaido island. This region is mostly composed by intercalation of coal seams, sandstone, and conglomerates overlying thick layers of clay with localized levels of conglomerate. The clay layers are composed of pumice fragments, fragments of quartz, feldspar, hornblende and coal fragments that give a gray tint to rock.

There rocks were formed at the end of the Middle Miocene collision of the Kuril arc with Northeastern Japan arc in the central part of the island of Hokkaido.

2.2 Methods

The modern carbonate facies and correlated depositional environment in active hot springs in Japan were determined based on field observation and sample collections. The principal requirement for a successful classification is that sampling should be based on well-preserved, actively depositing environments or, at least, on diagenetically unmodified materials from relatively undismantled sites (Pedley, 2009). Geological maps were used for the bedrock interpretation and also for water underground circulation and contamination. The samples were carefully packed and mailed to Brazil to the Laboratory of minerals and rocks – LAMIR facilities at the Federal University of Paraná (UFPR) for geochemistry analyses.

2.2.1 Carbonate sampling

The sampling was programed to cover as much variations in physical-chemical conditions as possible, either in vertical, and horizontal profiles. The samples were described *in situ* to avoid chemical and bacteriological contamination.

The rocks and sediments were sampled along the main stream of hot springs with different physical-chemical conditions of precipitation. The first field work occurred in the South during winter time in cold and dry conditions, nevertheless snow is common in Nagayu region (January 2014). The second field work occurred in the West during summer time in hot and humid conditions (August, 2014); and, the third field work in the North, also during summer time, and, in hot and humid conditions (June, 2015). A total of ten hot springs were described in Japan and around 135 samples were collected (Table 1). The samples were minutely described and analyzed at LAMIR-UFPR.

2.3 Geochemistry

2.3.1 Petrography

The sedimentary carbonate facies, recognized and described macroscopically, were analyzed under digital lupe (Axios Cam MRc) and polarized microscopy (Zeiss Axios A.2M, LAMIR - UFPR). All samples were at least doubly embedded with blue or yellow epoxy, due to their fragility, to facilitate porosity comprehension.

The most representative samples of each facies were coated with palladium and gold (Denton Vacuum Desk V), prior to SEM analyses. The main subject of SEM analysis was to investigate presence of biotic precipitation such as EPS (extracellular polymeric substances) fossil remains and cyanobacteria filaments and/or characterize abiotic precipitation. The technique allowed high resolution observations achieving a resolution better than 1 nm (Nagatani et al.1987). The analyses were performed in a scanning electron microscope (JEOL JSM-6010LA), located at LAMIR-UFPR.

Similarly to the SEM analyses, the most representative samples of each facies were also analyzed in computerized micro tomography (micro-CT). These samples were cut into prisms (1,0cmx4,0cm) and analyzed in micro-CT to obtain qualitative and quantitative data on size, shape and pore connectivity. The total slices were 481. The pixel image size is 13mm voltage source 100 (KV) and current source 100 (uA) for all of them. The equipment used is a SkyScan X-ray 1172 micro tomography, equipped with a 10-megapixel camera (4000 x 2300) with 12-bit CCD coupled to fiber optic scintillator.

The programs used for process analysis and processing of data that the device offers are DataViewer, CTAN and CTVox. The calculation of total porosity was made in the AWC program and images with 3-axis were obtained with DataViewer.

2.3.2 Mineralogy composition

The mineralogy composition was determined by X-ray diffraction (XRD) at LAMIR using a Panalytical Difractometer model EMPERYAN with Cu (Cu Kα1= 1,5406 Å) the generator voltage and current adjusted to 40 kV and 40 mA, respectively. Scans were run from 3° a 70° 2θ angles. The interpretation of diffraction

patterns with semi-quantitative percentage of minerals was obtained by the method RIR (Reference Intensity Ratio), using the X'Pert High Score Plus Data Collector software with PDF-2 database at LAMIR. The semi-quantitative percentage obtained by software is then recalculated at 100%, obtaining an indirect result of the equivalent amount of the mineral in the sample, suitable for representing by graphs. The mineralogy analyses were performed at LAMIR-UFPR.

2.3.3 Chemistry composition

In order to obtain the chemical characterization, all the samples were analyzed under X-ray fluorescence (XRF). The XRF method consists of spraying about 30g of the sample in Tungsten mill in spray AMEF for 30 seconds for particle size reduction until they reach about 325 mesh. The resulting spray powder is then led to a 50°C oven temperature for 24 hours for drying. After drying the samples are weighed and mixed in the ratio of 7,000g ± 0.0003 0.0003 ± sample about 1,4000g of organic wax. After weighing the mixture is pressed for the manufacture of tablets. Each suitably dried mixture is then taken to PFAFF machine and pressed at a pressure of 20 ton / cm² with the rising time of 50s, 60s deconstruction time and fall time of 30 seconds, which is the standard use for carbonates.

The chemical analyzes were performed on PANalytical equipment, AXIOS MAX model from pressed samples. LAMIR developed a quantitative analytical program to carbonate rocks, called "Pressed Carbonate Rocks", where the 10 major oxides (CaO, MgO, SiO_2, Al_2O_3, Fe_2O_3, Na_2O, K_2O, TiO_2, MnO, P_2O_5) and 4 trace elements (S, Sr, Cl, Ba) were analyzed in pressed pellet. It also held the loss on ignition, or LOI-loss on ignition, complementary to chemical analysis (XRF), excepted for the samples with arsenic contents.

The Loss on Ignition tests were carried out in the Termogravimiter Mettler Toledo and Mulffle model Jung with 0.5g to 1100 ° C for a period of 2 hours. Samples with Arsenic are not subject to Loss on Ignition tests. The chemical analyses were performed at LAMIR-UFPR.

2.3.4 Oxygen and carbon isotopic composition

The isotopic variation in stable carbon and oxygen isotopic compositions ($\delta^{13}C$ and $\delta^{18}O$ values) of microbial carbonates have been used to estimate the biogeochemical processes of carbonate precipitation and interpret the origin of fluid responsible for the precipitation. The $\delta^{18}O$ of carbonates, changes according to the temperature of precipitation and the fluid where it grows, though some additional constraints are necessary to complete the interpretation. All samples were measured with mean values expressed in the conventional δ notation in parts per thousand (‰) on the Vienna Pee Dee Belemnite (VPBD) scale ($\delta^{13}C$, $\delta^{18}O$).

In order to precisely separate different microfacies, micro drilling was carried out in 120 carbonate samples. The Isotopic analyzes were performed on the GasBench II equipment and Mass spectrometer Thermo Delta V Advantage. The Internal reference samples are ISO and ISO-C1-D2:

- ISO_C1 + pure calcite: $\delta^{13}C$ = 6.28 ± 0.13 ‰ VPDB and $\delta^{18}O$ = -22.16 ± 0.14 ‰ and VPDB

- ISO _D2 Dolomite 95% pure: $\delta^{13}C$ = 0.58 ± 0.06 ‰ VPDB and $\delta^{18}O$ = -5.09 ± 0.11 ‰ VPDB.

The opening of the sample was performed with the weight (~ 400 ug) and packaging in glass tube in a dry bath at 72 ° C. The autosampler injected for eight minutes analytical helium gas inside the pipe to create an inert atmosphere and free of atmospheric CO_2. Next, the sampler injected approximately 0.5 ml of orthophosphoric acid (H_3PO_4) 100% within the sealed tube. The sample was then reacted with the acid for different times.

The isotopic ratio was performed after completion of the reaction time and subsequently the CO_2 gas produced was collected by the sampler with another needle. The gas was purified within the GasBench II and was injected into the Thermo Delta V Advantage spectrometer.

Statistical data were worked with 10 peaks evaluated in each analysis, and, the average and standard deviation are <0.1 ‰ VPDB. The linearity range set for the equipment was between 4000 and 6000mV.

The isotopic fractionation of the reference gas was tested daily through four analyzes (zero enrichment test) composed of 10 injections of the reference gas, with standard deviation <0.06 ‰ VPDB, as well as analysis of international standards and reference samples internal interspersed with samples.

2.4 Results

2.4.1 Lithofacies and depositional environment

Most of the tufas and travertines studies are based in regions where the system is no longer active. The simplest schemes of classification are based on colour and stratification (Pedley, 2009). Many of the early schemes were based on deposits in Southern Germany (Pedley, 2009) focussed on a detailed botanical approach, some schemes were based on general sedimentological or on geomorphological criteria (Pedley, 2009) whereas others schemes were process based (Julia, 1983).

The lithotypes were distinguished in 9 active hot springs and one tufa creeck, where modern carbonate rock precipitates, first by field observation and, subsequently, in macro and micro scales. Each lithotype was related to an environmental depositional system and its frequency of occurrence were also stablished.

Two depositional environment systems, cascade and pool, dominate the active hot springs and, stromatolite and bubble are their main lithofacies, respectively. Shrub and root facies are also observed in both systems. The lithofacies, macro and micro fabric features, depositional environment and predominance of facies are listed in Table 2.

2.4.2 Temperature and water chemistry

The ten different hot springs sampled in Japan were summarized in APPENDIX 1 including: Name of the Island, Region, Prefecture, Site identification, pH, Water temperature, Dissolved Oxygen and Climate sampling time and also the geomicrobiological and hydrogeochemical data.

2.4.3 Geochemistry

2.4.4 Mineralogy composition

The differences in the geological set ups, water chemistry and proximity to active volcanoes should influence on continental carbonate formation. The different sampling locations offer the opportunity to observe geochemistry variations throughout the islands of Kyushu, Honshu and Hokkaido (APPENDIX A2). Carbonate minerals, including calcite, aragonite and high-Mg calcite dominate the mineralogy. Few contents of quartz and amorphous Fe are also observed (Figure. 2).

The Ternary graphs show the predominance of aragonite and subordinated high Mg-calcite in South Hot Springs (NAG, MYO and SHIO), predominance of calcite and subordinated aragonite in the North Hot Springs (FURU, OKU, OHF and FUTA) and also West Hot Springs (YAMA, NIIMI and KIBE) is also observed. The distribution of mineralogical composition for each site and correlative trends is shown above (Figure2). The OHF samples also show subordinated contents of gypsum, cubanite and sophite.

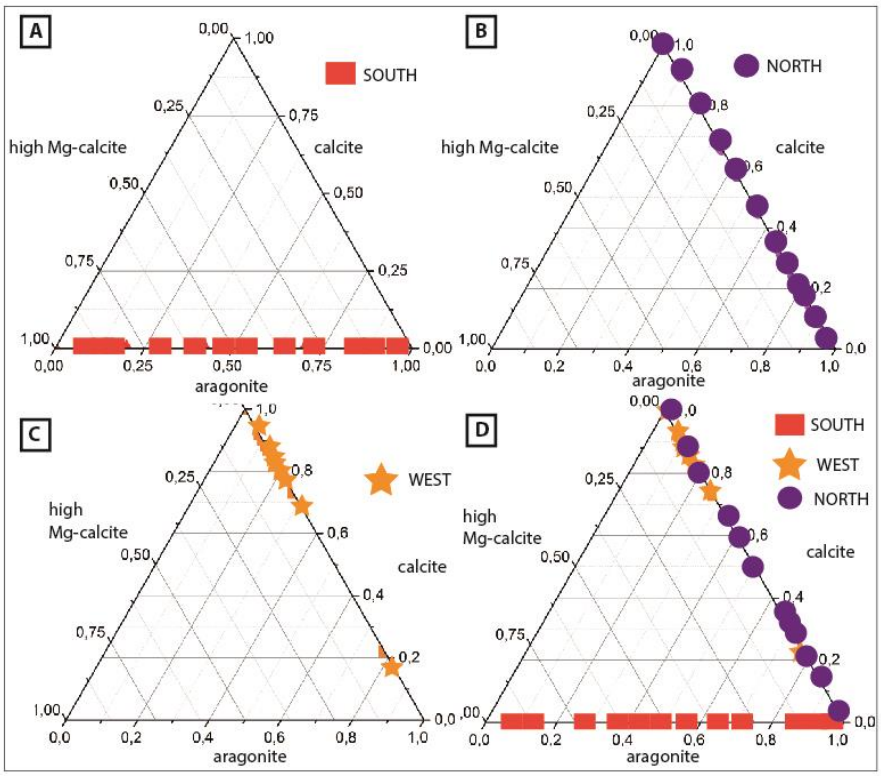

Figure 2: Ternary graphs showing mineralogical distribution in (A) South hot springs (NAG, MYO and SHIO); (B) North hot springs (FURU, OKU, OHF and FUTA); and (c) West hot springs (YAMA, NIIMI and KIBE); (D) Mineralogical of south, west and north plotted in the same ternary graph.

2.4.5 Chemistry composition

The Figure 3 comprises the chemistry composition of all samples. The chemical results from Kyushu Island show that NAG and MYO samples show high and homogeneous CaO, and low levels of other major oxides (MgO, SiO_2, Al2O3, Fe_2O_3, Na_2O, K_2O, TiO_2, MnO, P_2O_5). All the analyses show high levels of L.O.I., approximately 45%, consistent with the presence of carbonates. In contrast, the SHIO site, show variations in the levels of CaO, SiO_2 and Fe_2O_3 in all samples and no compositional trend was observed along the profile.

In the Honshu Island, the YAMA and NIIMI hot springs show high and homogeneous CaO, ranging between 47-57% and 49-53%, respectively. Subordinated contents of SiO_2 and Fe_2O_3 are observed in both hot springs. The analyses show high levels of loss on ignition – L.O.I., approximately 42%. The KIBE samples though, show high contents of CaO, Fe_2O_3 and As_2O_3, ranging from 0,1-17%, and also low levels of other major oxides (MgO, SiO_2, Al_2O_3, Na_2O, K_2O, TiO_2, MnO, P_2O_5). There was an increase in Fe_2O_3 and As_2O_3 content, from the vent until half of the main stream, where Fe_2O_3 and As_2O_3 content decrease, and CaO increases.

The Northern hot springs, in Honshu and Hokkaido Islands, show similarity to the Southern hot springs. The FURU, OKU, FUTA and OHF samples show high and homogeneous CaO content, excepted for OHF samples. They also show low levels of other major oxides (MgO, Fe_2O_3, SiO_2, Al_2O_3, Na_2O, K_2O, TiO_2, MnO, P_2O_5), excepted for the OHF samples that shows high levels of SiO_2.

Not all, but four of the ten hot springs from the three analyzed islands show arsenic contents ranging from 0,1% to 17,00% (Figure 4). High contents of arsenic are present mostly in stromatolite facies in SHIO and KIBE hot springs, whereas low level is present in stromatolites of FUTA. No LOI, was carried on these specific samples.

Figure 3: Results of the chemical analyses (XRF) of microbialites samples collected in 2014 and 2015 from hot springs in Japan, arranged according to geographic location, from south (left), west (middle) and north (right). Horizontal lines separate sample series from different hot springs. Chemical composition in the (a) South, (b) West and (c) North.

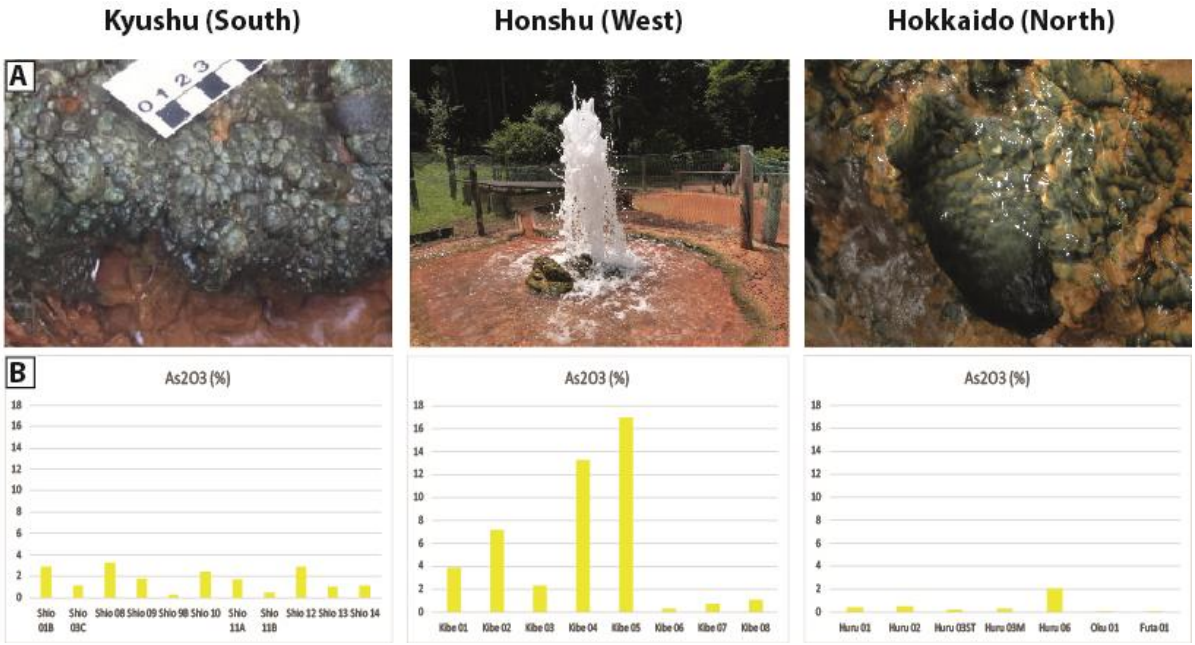

Figure. 4: (A) Stromatolite facies in the main stream with high as contents. (B) Graphs showing high contents of as ranging from 3-17%.

2.4.6 Oxygen and carbon isotopic composition ($\delta^{18}O$ and $\delta^{13}C$) of continental carbonates and possible precipitation scenario

A careful selection of samples avoiding cements and recrystallization spots, was made in order to obtain environmental information from stable-isotope composition. The samples selected for analyses correspond to carbonate rocks selected in different facies in the correlative depositional environment. The measurements of oxygen and carbon isotope values of all samples are listed in the Figure 5. Overall, the data illustrate that the samples tend to have more depleted $\delta^{18}O$ values, although two major groups are observed in $\delta^{13}C$ values.

The changes in isotopic composition in a single system seems to be controlled by physicochemical parameters such as CO_2 degassing, water temperature, water flow velocity, steepness and, also biological activities (e.g., photosynthesis respirations and sulphate reduction), (Sumner, 2001;. Kano *et al*., 2003). According to these authors, the fluctuation of ^{13}C in the tufa deposit mostly reflect the seasonal fluctuation of ^{13}C value in the water phase. However, the interpretation above is mainly based in the solid phase.

The southern samples show depleted values for $\delta^{18}O$ (-11 to-15‰) (VPBD) and also depleted values for $\delta^{13}C$ (0 to -4‰) (VPBD). Therefore, these samples are interpreted as precipitated from meteoric water with few or absent biological

precipitation. Among NAG, MYO and SHIO, the last one could be the most biologically influenced.

The Western samples show depleted values for $\delta^{18}O$ (-11 to -15‰) as well, but enriched values for $\delta^{13}C$ (0 to 3‰). Moreover, these samples are also interpreted as precipitated from meteoric water but in this case showing a light tendency for biological precipitation.

The Northern samples show the most different characteristics with enrichment values for $\delta^{13}C$ (1-7‰), but similar values for $\delta^{18}O$ (-11 to -15‰). The Northern samples are interpreted as the most biologically influenced, according to Dupraz *et al.* (2009) classification.

The isotopic measurements performed in hot springs and tufa creeks show variations in C and O isotopic values, corresponding to variations in physicochemical parameters, e.g. degassing, respiration and photosynthesis, and presence or absence of biological activity.

The $\delta^{18}O$ values isotopic values of the carbonate samples from Japan can be grouped in two major fields, despite the geographical situation. The majority compiled regional data in this work follow the range of the published data from previously works in Japan (Katsuyama, *et al.,* 2015), used as background. Also, mixture of available depth water can fraction the final isotope signal.

By using more specific regional backgrounds, the situation becomes quite different. As the majority samples from Hokkaido (FURU, OKU, OHF and FUTA) and Honshu (YAMA, NIIMI and KIBE) follow the background isotopic values, the carbonates from the Kyushu Island (NAG, MYO and SHIO) show rather different isotopic values. The difference observed in the YAMA samples is due to two main features: the large distance from the vent and slope topography in a short stream, which accelerate the CO_2 degassing. The difference observed from the background range (-6,4 to -8,6‰) and the isotopic values from the Kyushu samples (NAG, MYO and SHIO) (-11 to -15‰) is interpreted to be the result of a possible contamination from the Ohita-Kumamoto fault, that concentrates several hydrothermal sources, and also from the volcano Mt. Kuju, located nearby (Aitchson,1986).

The $\delta^{13}C$ values of the carbonate samples from Japan are grouped into two main categories, ranging from (0 to -10‰) and (0 to 6‰) despite the geographical situation.

Values of $\delta^{13}C$ near 0‰, indicate few or absence of biological influence on precipitation. The more enriched values of $\delta^{13}C$, up to 7‰ indicate a diversification of microorganisms in the system and according to Dupraz *et al*., (2009) a good indication of biologically influenced carbonates. The more depleted values of $\delta^{13}C$, down to -10‰, show the most biologically induced carbonates (Dupraz *et al.,*2009).

Notably, the values of $\delta^{13}C$, from NIIMI samples, close to -10‰, drastically differ from all the other hot springs due to its steep slope microenvironment and short stream. This tufa is the only one inside a forest, with thick soil, leaves remnants, and wood spread over the main water flux, leading to a meteogenic tufa interpretation where CO_2 originates in the soil (Pentecost, 2005). This microenvironment favour photosynthetic bacteria growth over and inside of microbial mat, leading to a deacreasing in Ca^{2+} concentration, and thus, photosynthesis induces the carbonate precipitation (Shiraishi *et al.,* 2010).

The YAMA hot spring shows a different trend, where values of $\delta^{13}C$ range from 0 to 3.7‰. This range in such a small path is interpreted as facies changes through the water stream and rapid CO_2 degassing. No preferential trend is observed along the water stream and despite the distance from the vent, flow path and freshwater influx, each facies shows different values of $\delta^{13}C$ as follow: (a) stromatolite 1,42‰, (b) cascade 1,70‰, (c) pool ,0,48‰, (d) bubble 3,00‰ and (e) shrub 0,65‰.

Remarkable environmental conditions (e.g. seasons, altitude, thaw, frozen period) and also fractionating may cause variations on isotopic analyses, depending on the period of sampling. This analysis is a valuable tool for studying the absence or presence of microbial processes during the carbonate deposition.

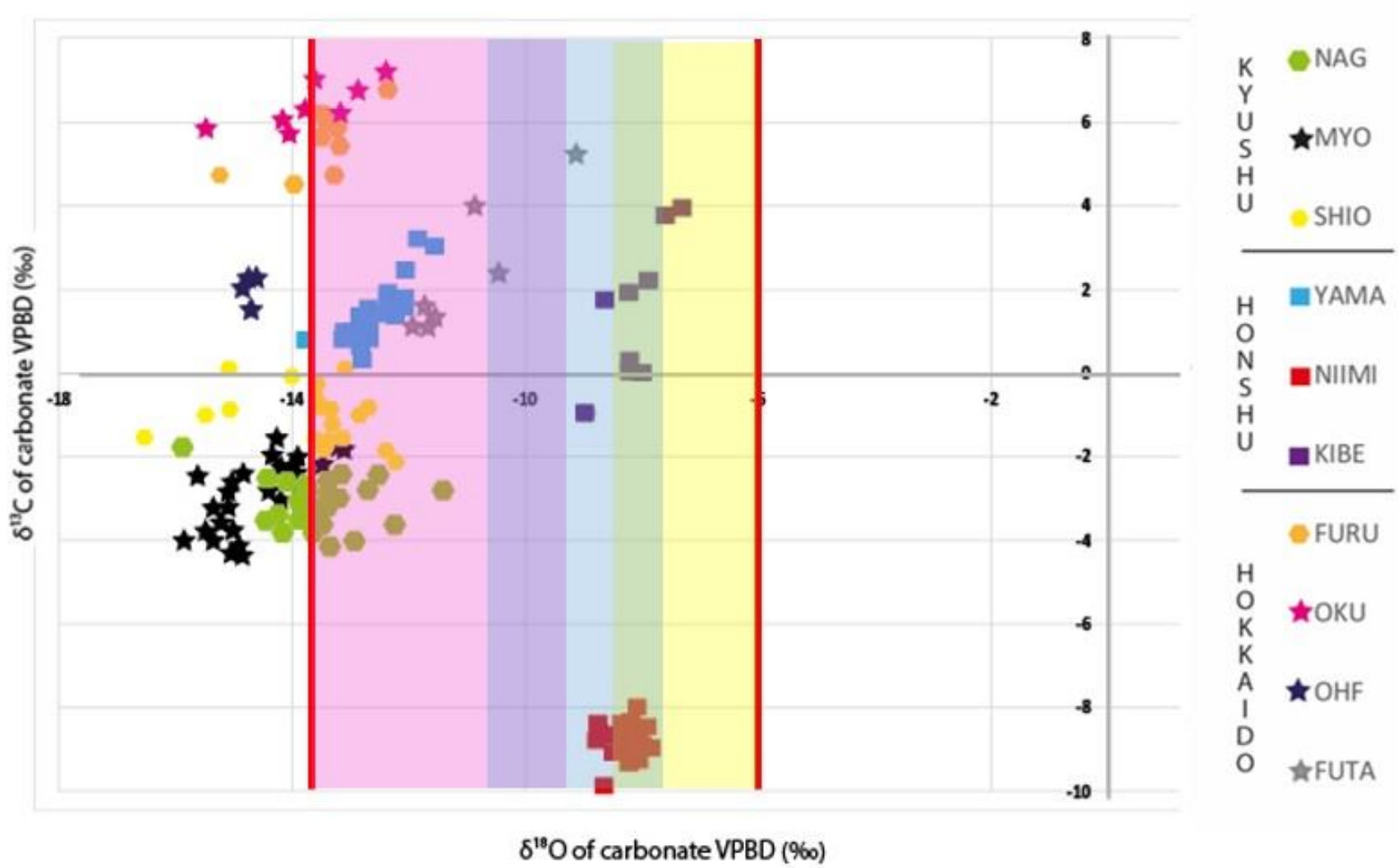

Figure 5: Cross plot of stable carbon and oxygen isotope data for all samples collected in Japan. Red lines represent water meteoric background of Japan, ranging from -5,9 to -13,7‰ (Katsuyama, 2015).

2.4.7 Facies characterization

2.4.7.1 Stromatolite facies

Description: The stromatolite facies occurs in SHIO/NAG (South), YAMA/NIIMI/KIBE (West) and FURU/OKU/FUTA (North) as a domal structure characterized by flat and laminated inner structure (Figure 6B). The stromatolites grow upon a gently slope in SHIO and FURU, and around the vent in KIBE**.** The lamination is characterized by milimetric and contiguous layers with low angle gently convex. The mineralogy and grain sizes are homogeneous along the sample. The SHIO and FURU stromatolites are mainly composed of aragonite whereas KIBE stromatolite is mainly composed of calcite. The water saturation state ranges from 0 to 8,9. The chemical results (XRF) show high and homogeneous contents of CaO, ranging between 64,1 - 74,40% in KIBE and FUTA stromatolites, whereas SHIO stromatolite shows only 2,90% content of CaO. All three stromatolites show high contents of Fe_2O_3 ranging between 13,20 and 54,30% and also high contents of As_2O_3 ranging from 0,1-17%. The petrographic analyses in thin sections from the KIBE samples show gently convex and contiguous layers with different thickness composed of calcite showing shrub structures. However, the layers are not vertically connected. Instead, the connectivity occurs horizontally along the contact surfaces, consequently reducing permeability. The NIIMI samples show subparallel, millimetric and contiguous flat layers composed of microesparite. The porosity occurs inside the micro-layers with a good horizontal connection though no vertical connection has been observed. The SEM observations on fresh surface of stromatolites from SHIO, KIBE and NIIMI show the presence of filamentous structures associated with EPS and only NIIMI shows calcite spherulite crystal. Computadorized microtomography shows good porosity and connection in horizontal layers but no vertical connectivity. The porosity is 26%.

Interpretation: The laminae thickness variation results from: (a) season oscillations in the amount of disposable water for precipitation, and (b) daily lamination (Takashima & Kano, 2008). The porosity observed inside the layers, among the feather like crystals, is interpreted as product of leaching of both, Fe and organic matter (Figure 6C and 6D). The porosity is preferably horizontally disposed, parallel to the growth substrate. The vertical permeability is due to secondary cracks and fractures (Figure 6E). The SEM images reveal that the spherical pipes (Figure 6F and 6G), probably

bacterial filaments, suiting as substrate for the growth of spherical crystal aggregates. The micro-CT images show horizontal permeability, related to environmental conditions as described above (Figure 6H).

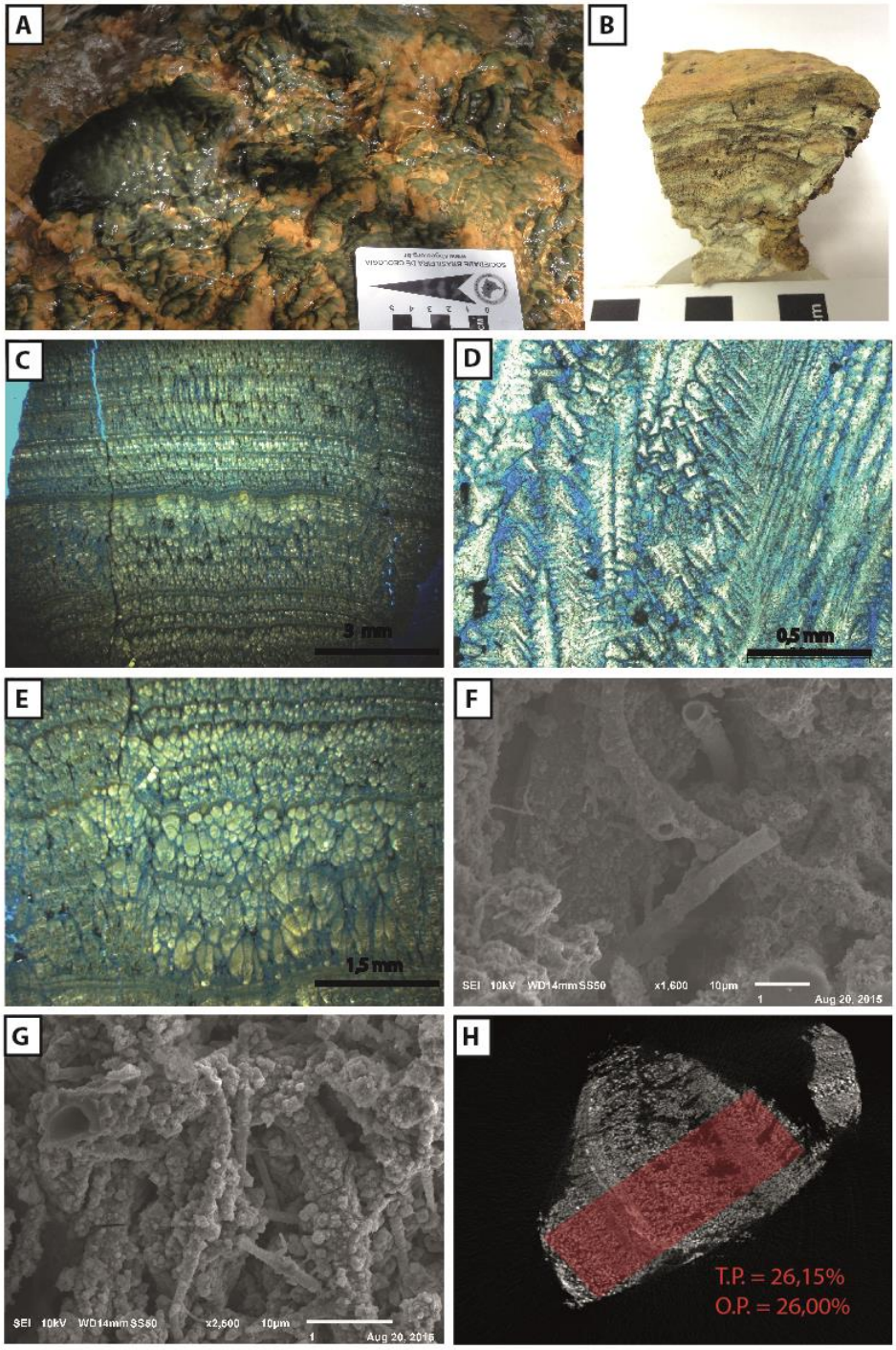

Figure. 6: (A) Stromatolite facies field photograph. (B) Stromatolite facies hand sample (C) (D) (E) Photomicropraphs (NX) showing subparallel layers composed of aragonite crystals exhibiting shrub morphology. The main porosity is horizontal and the only vertical connection is observed in secondary fractures. (F) (G) SEM image of aragonite crystals exhibiting spherulitic morphology growing around spherical tubes. (H) Micro-CT image showing 26,15% of volume of pores (T.P.)

2.4.7.2 Root facies

Description: The root facies was observed in South (MYO), West (YAMA) and North (FURU, OKU, OHF and FUTA). The root facies usually occurs associated with stromatolites and rarely with bubble facies. In outcrop, the root facies consists of brownish rocks with minerals randomly organized and hardness change throughout the sample, according to he presence of leaves and vegetal fragments (Figure 7A and 7B). Horizontal, discontinuous, and inhomogeneous layers composed of vegetal fossils interbeds with horizontal, discontinuous and homogeneous layers composed only of mineral assemblages. This trend observed in hand sample seems to directly interfere in the perm-porosity system. Layers with vegetal fossils contents show high porosity and high permeability without preferential orientation, whereas layers composed only of mineral assemblages apparently show no porosity (Figure 7C and 7D). The grain size ranges from less than 1 mm to milimetric in both layers, with or without vegetal fossils. The MYO and YAMA samples are composed of aragonite (100%) whereas FURU, OKU and FUTA samples are composed of aragonite and subordinated calcite. The water saturation state ranges from 1,20 to 10,00. The chemical results (XRF) show high and homogeneous contents of CaO, ranging between 56% in NAG and 91% in MYO, YAMA, FURU, OKU and FUTA. The four last hot spring show Arsenic content. The micro-CT observations show good porosity and good horizontal connectivity. No vertical connectivity has been observed. The total porosity is 30%.

Interpretation: The leaves and vegetals fragments suit as substrate for aragonite and calcite crystals growth and also as sediment traps. The interbedding of layers composed of vegetal fragments and layers composed of mineral assemblages is interpreted as seasonal variation. It might reflect the Autumn time, when the rate of leaves fall is higher than the other seasons. The pores and megapores are interpreted as primary syn-depositional features formed by the precipitation wrapping plants. The porosity observed inside the layers, mainly in the “vegetal fossil layers”, is interpreted as leaching of Fe and organic matter (Figure 7F). The vertical permeability is due to diagenetic processes, probably during burial. The SEM images show high porosity in layers composed of vegetal fragments (Figure 7G) that has worked as substrate for the growth of crystal needle aggregates that after decaying leads to moldic and framework porosities. Processes of dissolution and precipitation

is present in FUTA root facies, creating mega-moldic pores and stalactites precipitation. The micro-CT images show a higher volume of open pores along the contact surface of layers and no preferential orientation of porosity and permeability have been observed (Figure 7H). The root facies occur at the base of cascade and/or pool, and different descriptive patterns are observed. The vegetal fossil fragments in the pool seems to be better shaped and preserved when compared with the reworked fossils present in the base of cascade, which are more fragmented and smaller, being correlated to “phytoherm” and “phytoclast”, respectively (Pedley, 2009).

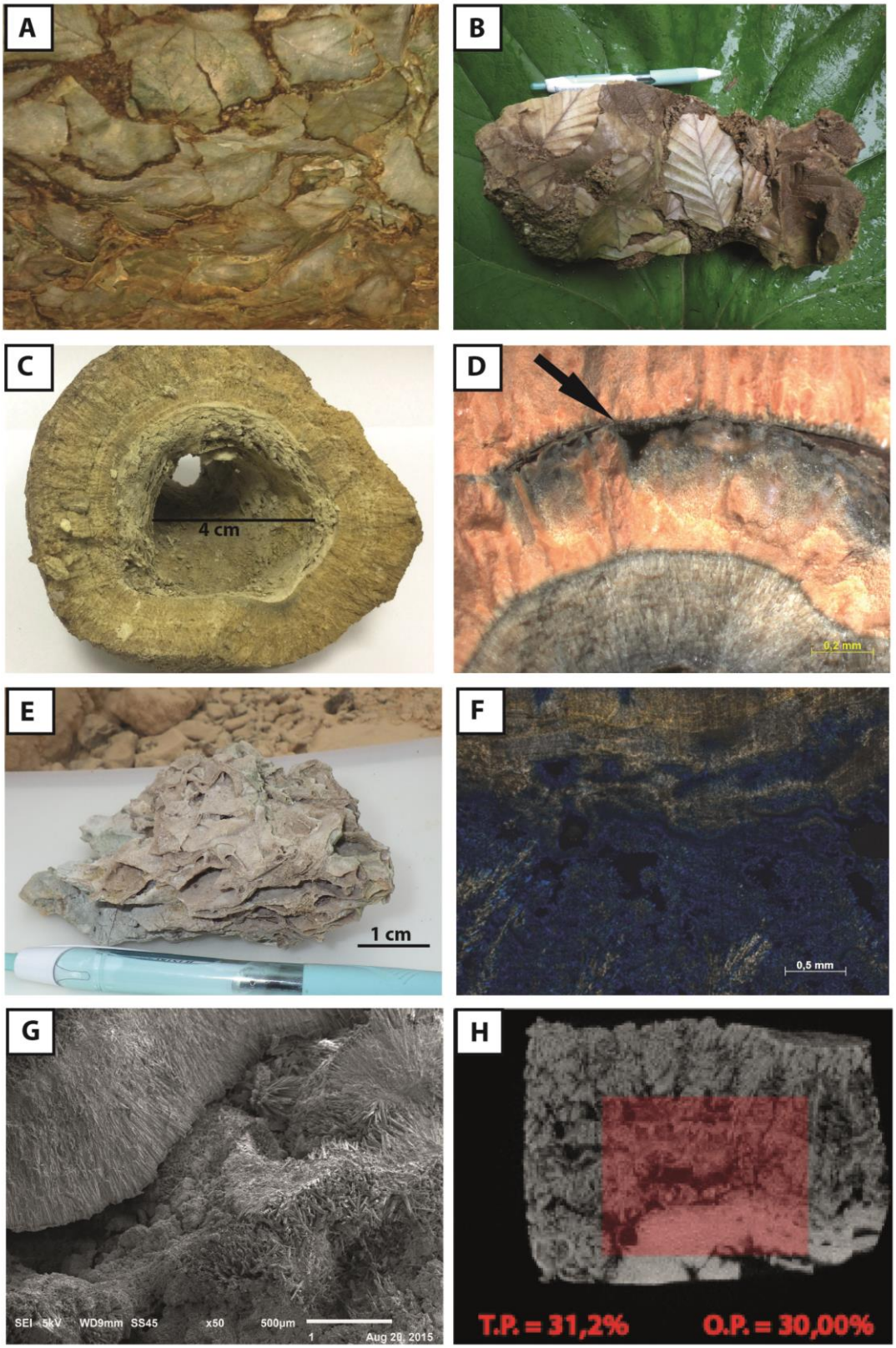

Figure 7: (A) (B) Root facies field photograph in FUTA hot spring. (C) Mega-primary pore, 4 cm diameter size (D) Lupe image. Dark arrow indicates moldic porosity. (E) Fossilized moulds of former plants entombed in carbonate rocks. Sub-horizontal layers of fossilized molds of plants. (F) Photomicrography (NX) showing aragonite crystals displayed in two different microfacies. (G) SEM images reveals aragonite crystals exhibiting shrub morphology. (H) Micro-CT image show porosity volume of 30% between two different microfacies.

2.4.7.3 Shrub facies

Description: The shrub-like morphology was observed in all the hot springs and is characterized by its morphological shrub like, fern-like or bush-like arborescent growths branching upwards to form colonies, resembling miniature forests. The shrub facies was observed in the KIBE stromatolites, growing from the substrate with laterally interfering bundles and tend to be less developed away from the substrate. The shrubs in YAMA and FUTA are bigger and well developed (Figure 8A). Subparallel, milimetric and contiguous flat layers composed of carbonates, display a straight pattern of porosity with good horizontal porosity and permeability though no vertical connectivity has been observed (Figure 8D and 8E). The petrographic analyses in thin sections show thick bundles of ray-crystal crusts formed in the hot spring with fair lateral continuity of shrubs and micrite aggregates. The water saturation state ranges from 0,00 to 13,10. The KIBE and FUTA samples are composed of calcite (100%). Chemical results (XRF) show high and homogeneous content of CaO, ranging between 64-96%. The KIBE samples show high contents of Fe_2O_3 ranging from 19-57%, Both hot springs contain low Arsenic contents. The micro-CT images show a higher volume of pores, 20,5%, on the right flank of the sample (Figure 8I).

Interpretation: The irregular form of shrubs observed, mainly in KIBE hot spring is attribute to biotic precipitation (bacterial shrubs) whereas regular geometric patterns observed in YAMA and FUTA are product of abiotic precipitation (crystal shrubs and ray-crystal crusts) (Chafetz & Guidry, 1999). The micropores observed in thin sections are associated with abiotic precipitation due to its regular shape (Chafetz & Guidry, 1999). The carbonate grew synchronously with multiple aggregates of shrubs intercalated with micritc bands. The SEM images show spherulitic and needle-like calcite crystals (Figure 8F, 8G and 8H). Thus, this features lead to a biotic precipitation nevertheless processes such as dissolution, can result in micron-sized spheres with shapes similar to bacteria colony (Claess *et. al.,* 2015). However, the occurrence of both spherulites and EPS, leads to a biotic influence.

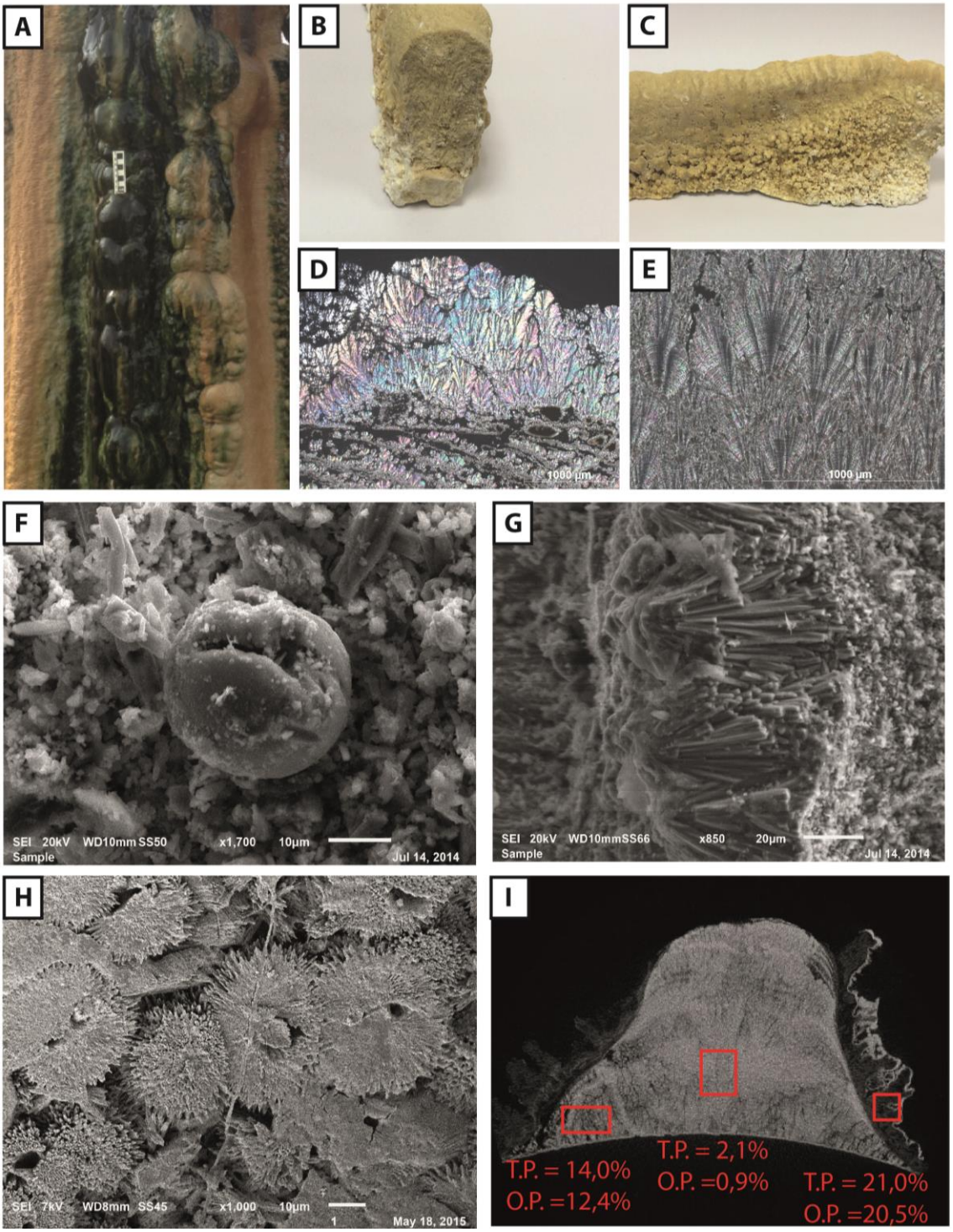

Figure 8: (A) Shrub facies in a cascade. (B) Photomicrography (NX) showing calcite shrub morphology, dark spots represent porosity. (C) Hand sample of shrub facies. (D) (E) Photomicrography (NX) zoom to shrub morphology growing over a flat substrate. Notice horizontal porosity and connectivity at the bottom and vertical porosity and connectivity inside shrub layers (F) SEM images spherulitic crystals. (G) SEM images reveals calcite crystals exhibiting shrub morphology. (H) Spherulites and Fossilized bacterial activity. (I) Micro CT image showing three different porosities along the sample. The best porosity around 20,50% (O.P.) is observed on the left site.

2.4.7.4 Bubble facies

Description: The bubble facies was observed in YAMA, FURU, OKU and FUTA Hot Springs (Figure 9). The bubble facies is characterized by randomly arranged open pore spaces coated by carbonate ranging from 0,.2 mm to 0,.7 mm. Paper thin rafts occur associated and bubbles are only observed in water mixing zone, right after fresh water input. The water saturation state ranges from 11,20 to 12,90. The mineralogical results in the YAMA samples show aragonite (100%). Samples from FUTA, FURU and OKU are composed of calcite and subordinated aragonite. The chemical results (XRF) in YAMA and FUTA show high and homogeneous contents of CaO, ranging between 56-96%. Quartz has also been observed in both hot springs as an accessory mineral. The FUTA sample shows low Arsenic contents. The micro CT shows a high volume of open pores arranged in a random way in all of the samples. Some micropores interconnect the largest pores both, horizontally and vertically. The total porosity is 75,62% (Figure 9).

Interpretation: The occurrence of bubbles depends on water temperature. Bubbles are present only at a certain distance from the hot spring, where water has cooled down. The bubbles are also coated in microbial mats, pools and on surface of carbonate rocks precipitated with low dip angle and slow water velocity. Sulfate reduction bacteria are thought to be related to precipitation in centimetric, contiguous gray layers at the bottom of the deposits. The process of bubble facies precipitation takes place in daily variation basis by physicochemical changes. It was concluded that at night (absence of light), specific bacteria start the processes of respiration, decreasing the pH values and consequently dissolving carbonates and precipitating amorphous silica. However, during the day (under light conditions), other bacteria start the photosynthesis absorbing CO_2 from the fluid. This process increases the environment pH leading to carbonate precipitation, and quartz dissolution. The silica bubbles produced at night are coated by the carbonate precipitation during daylight, although most of them escape into the atmosphere. The bubble formation is so high that while collecting samples many bubbles escaped during the precipitation. While ‘’escaping’’ from the sample, this bubbles build up a “path” and consequently increases the size of the pore. Accordingly, to the Kull equation (Kull, 1991), the shape of the pores changes due to the viscosity of the fluid (Figure 9H). Similar to bubble precipitation, rafts are formed by carbonate precipitation in static or slow

water velocity. The increasing weight of the rafts due to the continuous precipitation, or even the decrease of water volume causes the break of rafts that gently falls to the bottom of the deposit. Its accumulation may rise to several rafts cemented together or even interbedded with bubbles.

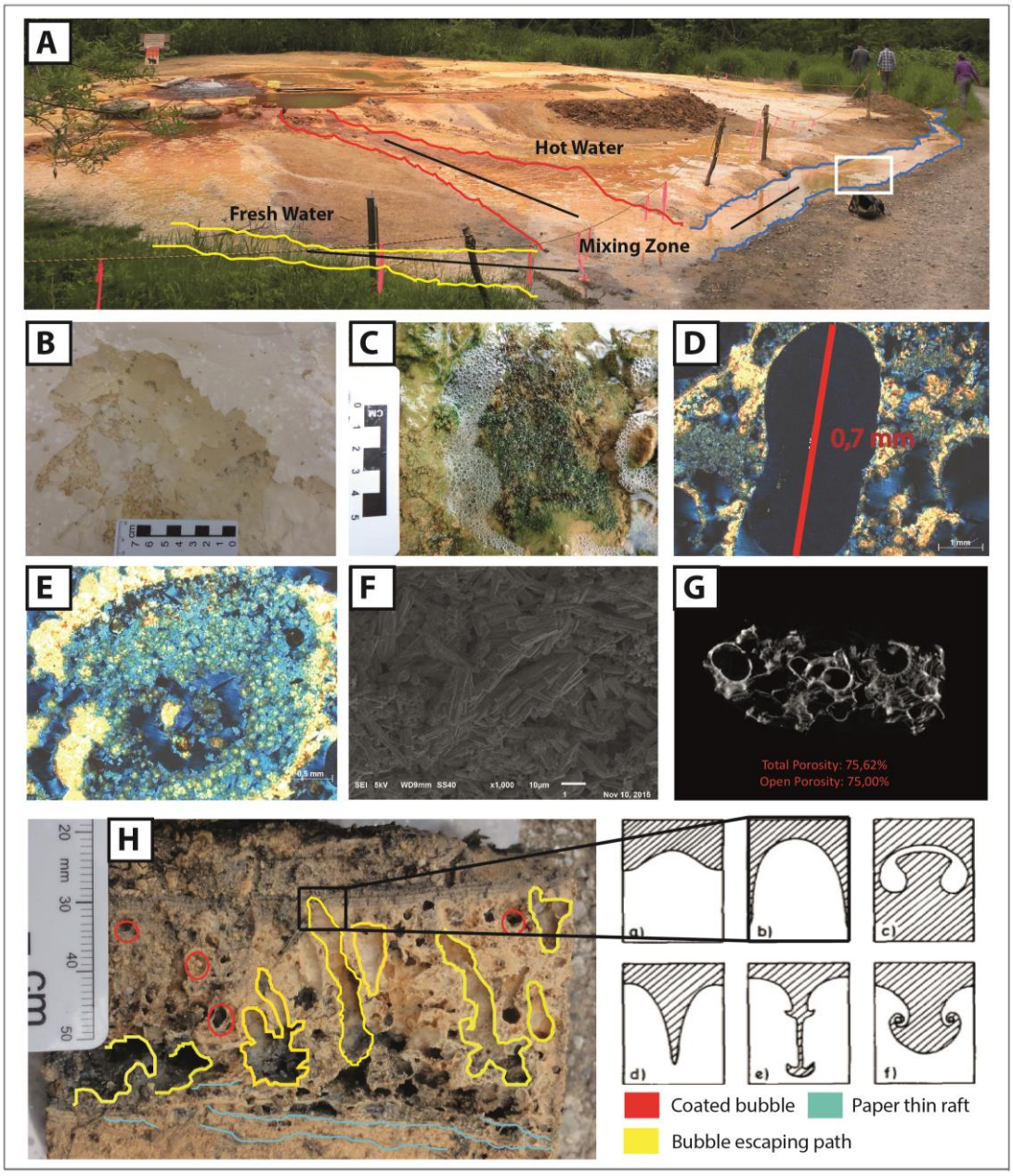

Figure 9: (A) Oku-okuhachicuro Hot Spring. The sampling occurred in a mix zone (white square) of fresh water and hot water. (B) Paper-thin raft growing on the top of water laminae and consequently covering bubbles. (C) Sampling site of Bubble facies. Note the bubbles escaping during their formation. (D) Photomicrography (NX) showing elongated bubble creating voids and consequently higher volume of Open Pores. (E)(F) Photomicrography (NX) showing Bubble composed of aragonite with secondary fill. (G) Three-dimensional (3-D) image obtained from Micro CT analyses scans porosity distributions of hole sample. The light gray is the nonporous area. The volume of Open Pores is 75,00%. (H) Different shapes of bubble observed in hand sample and classified according to Kull's classification. Classification of bubbles morphology. Coated round shaped bubble is the main pattern in hand sample. (modified from Kull, 1991)

2.5 Discussion and interpretation

2.5.1 Depositional environmental and lithofacies

The different lithofacies, stromatolite, shrub, root and bubble are associated to the corresponding depositional environment (Figure 10). The facies analyses carried out in active hot springs in Japan show the intimate association of lithofacies, microenvironments and environmental depositional systems. The carbonate depositional environment corresponds to a specific environment that can be delineated based on the description of physical (grain size, components, erosional features and bedding), chemical (inorganic, dissolution and precipitate) and biological (microbial) imprints. (Toker, *et al.,* 2015). This analysis resulted in a schematic depositional model consisting of cascade and pool environmental depositional systems and four related lithofacies (stromatolite, shrub, root and bubble/paper-thin raft) (APPENDIX B).

The carbonate precipitation observed around the active hot springs arises from two different genetic processes: (i) carbonate precipitation from flowing waters lithified during deposition as flowstones (abiotic crystalline and microbially mediated facies) in epigean conditions (subaerial thermal systems), and, (ii) carbonate precipitation in subaqueous settings, by suspension or transport of grains, lithified after deposition. The predominance of steep slope (>35°) and lack of contiguous flat horizontal terrains leads to a slight predominance of cascade over pool (Hammer *et al.,* 2007; Toker *et al.,* 2015).

The cascade environment occurs in steep depositional environment, leading to a fast crystal growth due to the rapid degasification and consequently an increase in pH. The cascade occurrence is also associated with pools and depending on the slope gradient, it can be partly ponded. In outcrops, sub horizontal bedding, sub parallel lamination and brownish color prevails. The stromatolite and shrub facies dominate the system and root facies subordinately occurs at the base of cascades.
Although contiguous, flat horizontal terrains are rare in the studied active hot springs, pools occur almost in the same frequency as cascade. The flat horizontal depositional environment is associated with root, and/or bubble facies and its size changes according to the slope gradient water, and flow velocity. The pools consist of light to dark brownish rocks, minerals randomly arranged and hardness ranging

from very soft to very hard. The occurrence of bubble/paper-thin raft is associated with the input of freshwater into the system, whereas root facies occurs regardless the hydrothermal or karst water source. Both bubbles and root facies increase the porosity in different ways. The bubble facies show randomly arranged open pores, whereas the root facies occurs in subparallel layers, formed by deposition of vegetal fragments at the bottom of the pool. The minimal pool model created by Hammer *et al.,* (2007), is applied in this study, and thus the formation and migration of pool are based on shallow-water flow and an empirical positive correlation between the flow velocity, precipitation rate, and microbial activity. The downstream migration of pools tends to be parallel to the main water flow. This temporal migration and development of pools is observed in cross sections in all of the hot springs. The high precipitation rate occurs due to accelerated CO_2 degassing caused by agitation, pressure drop and shallowing, since pools depth range from millimeters to a maximum of 4 centimeters. According to Hammer *et al.,* (2007), the pool growth rate is 0 to 1 mm/day.

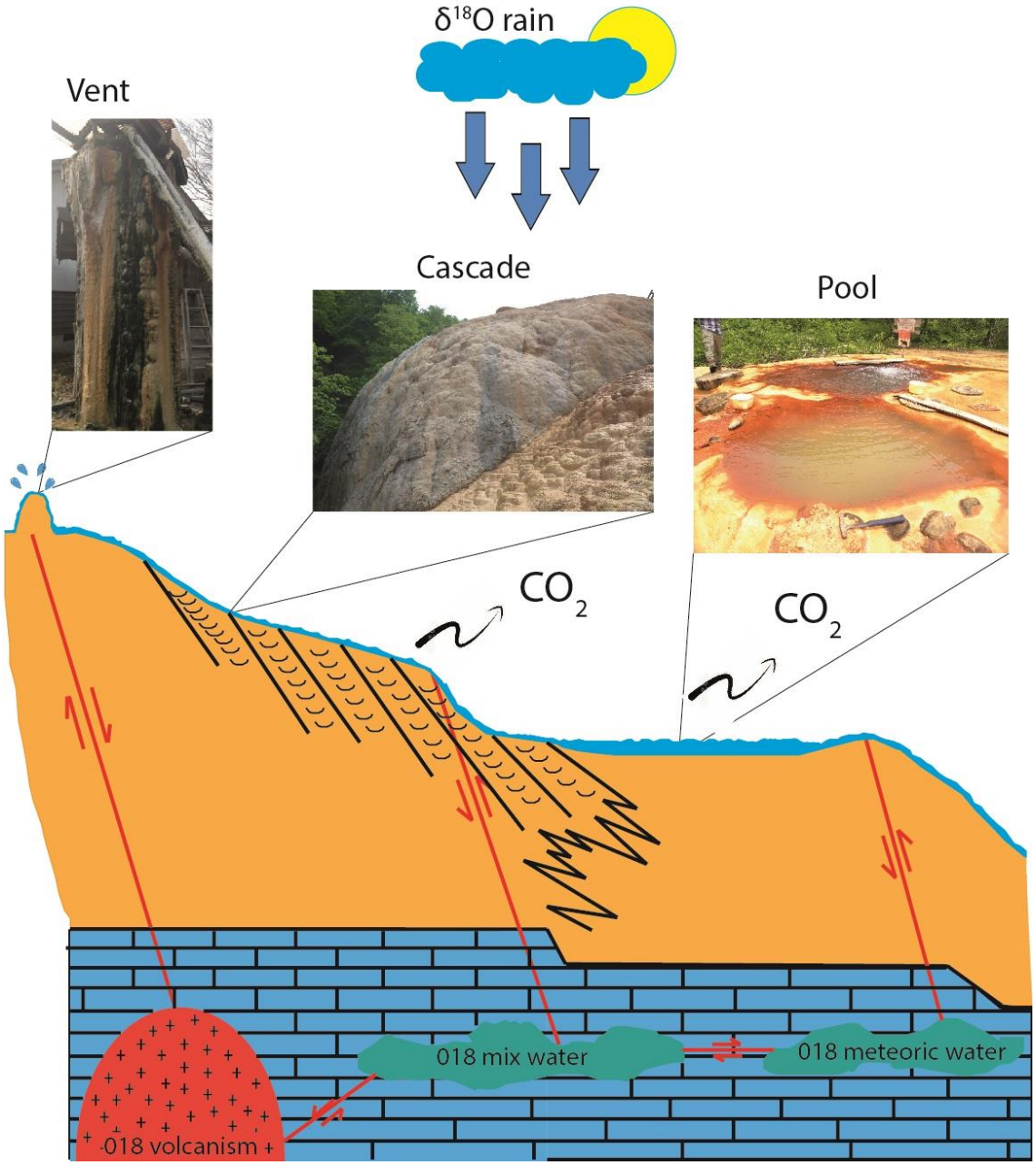

Figure 10: Simplified geological section illustrating the interaction between water, geological background and possible contamination by volcanism. Infiltration of rain and snow water occur along the faults, which cross underground carbonate rocks and migrate to the reservoir. The microbialites could thus have precipitated from meteoric water reservoir, magmatic water and also a mixture of both. Therefore, the microbialites $\delta^{13}c$ and $\delta^{18}o$ signatures reflect these specific trends.

2.5.2 Geochemistry

The carbonate deposition in a hot spring system investigated in this study is controlled by a geothermal/tectonic regime that provides a range of water temperature (18 to 78°C) and chemistry (pH range from 6,07 to 8,17). These

parameters are correlated to meteoric water flows in a deep or shallow hydrothermal circulation, contaminated by active volcanoes.

The rapid degassing of CO_2, mainly in cascade, causes the high saturation state of carbonate minerals in the water, and result in carbonate precipitation in all areas.

Changes in the chemical composition of hot springs waters is typical for travertine site, and the downstream CO_2 degassing increases the saturation state of $CaCO_3$ minerals. However, saturation state decreased at the end of flow path in some hot springs, due to rapid precipitation from the vent to the middle part.

The physicochemical parameters of hot spring waters interfere directly in the mineralogy composition of the NAG Hot Spring, characterized by high levels of alkalinity, Mg^2 ratio, SO_4^{2-} and carbonate saturation state.

The downstream degassing of CO_2 increases the saturation state carbonate in Myoken Hot Spring. Hydrodynamic conditions and temperatures around 50°C seem to control microbial activity. However, carbonate saturation is not high due to the relatively short flow path. Downstream, the alkalinity and Ca^2 ratio decrease due to carbonate precipitation and CO_2 degassing along the way and the temperature decreases due to heat loss to the environment.

The physicochemical parameters of SHIO are similar to MYO. In some sites the conditions such as calm flow and moderate temperature of water allow the development of a thick microbial mat with high microbial diversity. Basically, the rapid degassing of CO_2, the precipitation of carbonates, and rapid cooling water occur along a short path of water flow. The influence of photosynthesis on carbonate precipitation is relatively small.

The physicochemical parameters of YAMA and NIIMI are quite different when compared to all other microbialite sites. This is mostly because water in YAMA and NIIME is basically originated from meteoric water. The CO_2 addition from soil, dissolution of limestones and P_{CO2} atmosphere increased high values of Ca ratio and alkalinity.

The geyser at the KIBE Hot Spring has high values of P_{CO2} of 1000 atm because of its typical periodic discharge. Downstream to the geyser, the Ca ratio and alkalinity decrease due to the same factors: CO_2 degassing, carbonate precipitation and loss of temperature.

2.5.3 Mineralogy

The hot springs in Japan contains carbonate rocks dominated by calcite, aragonite and high Mg calcite. The precipitation of these minerals is mainly controlled by physicochemical parameters (e.g. salinity and Ph).

The aragonite domain in the Kyushu Island (NAG, MYO and SHIO) is due to physicochemical parameters characterized by high alkalinity values, Mg^{2+}, SO_4^{2} and carbonates saturation state. The High Mg^{2+} percentages are much higher than in Ca^{2+}, which ratio makes the conditions for the deposition of aragonite instead of calcite. The predominance of calcite and subordinated aragonite in the North Hot Springs (FURU, OKU, OHF and FUTA) and also West Hot Springs (YAMA, NIIMI and KIBE) is due to the Mg^{2+} percentages, much higher than Ca^{2+}, except for OHF, favoring the calcite precipitation. The occurrence of sophite in OHF is related to high water temperatures (80°C).

2.5.4 Arsenic ocurrence

The origin of arsenic in microbialites is an unresolved subject. Some authors have described specific bacteria able to use arsenic as bioenergetics substrate in either anaerobic arsenate respiration or chemolithotrophic growth of arsenite. The arsenic would be the electron donor, feeding bioenergetics chains in primordial life (Lebrun *et al.,* 2003). Oremland *et al.,* 2003 propose that arsenic seems to have been present at much higher concentrations in the ancient Earth's crust than it is today.

Ecological coupling of arsenic oxidation and reduction was already proposed where different bacteria perform either, arsenic oxidation under light conditions or anaerobic arsenic respiration in the dark (Hoeft *et al.,* 2009). Interestingly microbial mats with arsenic contents grow along the bottom of rocks during the winter when the water level is at a minimum, mineral concentrations are higher and dissolved oxygen is almost absent. Anaerobic respiration prevails in this set. On the other hand, during the summer time, the biofilms tend to disaggregate and bacteria adopt a free-living style. Some different metabolic strategies seem to be used and as oxygen is probably a limiting factor, respiratory processes sustain and maintain the biofilms (Hoeft *et al.,*2009). Some microbial mats form under extreme environmental

conditions such as high salinity, P_{CO2}, pH and also high arsenic concentration, like in Shiohitashi and Ofhuna hot springs, even inside a volcano crater (Rascovan *et al.,*2015). Moreover, the arsenic metabolism is proposed to be an ancient mechanism in microbial life in ancient microbialites (Mascarelli, 2009). The presence of arsenic has also been correlated to the presence of Fe.

2.5.6 Summary facies

The carbonate rocks sampled in the islands of Kyushu (South), Honshu (West) and Hokkaido (North) in Japan are characterized by four different facies (Stromatolite, Root, Shrub and Bubble) (Table 4).

At least three facies (stromatolite, shrub and root) are likely to be precipitated through biotic process, as described in SEM images. The EPS remnants observed lead to this conclusion. Although fossils related to bacteria were not observed in other facies, field descriptions of bubble facies have shown the possible presence of sulfate reducing bacteria. The precipitation of the other facies is mainly controlled by environmental physicochemical changes.

The petrography analyses reveal good porosity and good horizontal permeability in the stromatolite facies, though no vertical connectivity, was observed, excepted for fractures. The thickness variation observed in the stromatolite facies is interpreted as oscillations in water availability for precipitation due to fluctuations of wet/dry seasons. The thin discontinuity observed between the laminae, represented by void space or micrite lamina indicates the end of growing cycle. The porosity observed inside the layers is interpreted as product of organic matter leaching.

The Shrub facies is made up of milimetric to centimetric layers with inter crystal porosity among dendritic calcite crystals in a microesparite matrix.

The bubble facies is formed of void up 0,7mm in diameter coated by calcite. The intra crystal porosity predominates over inter crystal porosity and the connectivity of the pore system is poor. Under the SEM images, fossils of spherical milimetric sizes contiguous pipes were related to remnant of EPS, supporting the microbial-mediated origin of cascade, shrub and stromatolite facies.

Table4: Classification and description of carbonate facies type including macro and micro fabric, micro facies associated, description, depositional environment and predominance.

FACIES TYPE				**Depositional environment**	**Predominance**
MACRO-FABRIC		**MICRO-FABRIC**			
Name	**Description**	**Micro facies associated**	**Description**		
Stromatolite	Lamination is characterized by milimetric and contiguous layers with low angle gently convex curved	Shrub, bubble,	**XRD**: calcite **XRF**: CaO (64-74%), Fe_2O_3,(13-54%), As_2O_3(0,1-17%) **SEM**: EPS fossils **Micro CT**: Porosity (26%) **Diagenesis**:Fe leaching	Cascade	
Root	Horizontal, discontinuous and inhomogeneous layers composed of vegetal fossils are interbedded with horizontal, discontinuous and homogeneous layers composed only of mineral assemblages	Shrub, stromatolite	**XRD:** calcite or aragonite **XRF:** CaO (56-91%) **SEM:** abiotic precipitation **Micro CT:** Porosity (27%) **Diagenesis:**dissolution	Pool	
				Cascade	
Shrub	Subparallel, milimetric and contiguous flat layers composed of carbonate display a straight pattern of porosity	Root, stromatolite	**XRD:** calcite **XRF:** CaO (64-96%), Fe_2O_3, (19-57%), **SEM:** spherulites and calcite needles, and EPS fossils. **Micro** CT: Porosity (21%) **Diagenesis:** Fe leaching	Pool	
				Cascade	
Bubble	Porosity coated by carbonate rocks. Pore sizes ranging from 0,2-0,7mm, randomly organized.	Paper thin	**XRD:**aragonite or calcite and aragonite **XRF:**CaO (56-96%) **SEM:** abiotic precipitation **Micro CT:** Porosity (75%) **Diagenesis:** close pores	Pool	

2.6 Conclusion

1. Two depositional environment systems, cascade and pool, are observed in Japan. The precipitation process in cascade takes place on slopes in fast flowing water conditions. However, precipitation in pool occurs in slow-flowing to stagnant water flux. Based on macroscopic and microscopic analyses, four lithofacies have been defined: stromatolite, shrubs, bubble and root. The stromatolite and shrub facies are the main lithofacies. The occurrence of stromatolite is observed in cascade whereas bubble is observed only in a mixing zone of hot and meteoric water. Field observations on modern hot spring of Japan suggest a cyclicity in the upward and lateral evolution from cascade into the pool system.

2. Based on petrographic and SEM analyses, microbial communities probably have acted as nucleation sites. The presence of organic matter and fossils related to EPS within the microbialite suggests possible biological influence. The influenced organomineralization could be the main precipitation process in travertine and tufa in Japan as living and/or nonliving microorganisms are observed in almost all samples. However, in NIIMI, induced organomineralization may dominates the system. The fabrics occurring in low energy areas, low water flow velocity seem to be more biologically influenced than fabrics occurring in fast water flow velocity where abiotic processes of physical degassing prevail.

3. Mineralogy distribution: predominance of aragonite in Kyushu Island (South Japan), calcite in Honshu Island (West Japan) and aragonite and calcite in Hokkaido Island (North Japan).

4. The isotopic signals reveal depleted values of $\delta^{18}O$ in all samples. The majority of the compiled isotopic data in this work follow the range of the published meteoric isotopic data from previously works in Japan. Nevertheless, samples which do not follow this range are interpreted to be the result of a possible contamination from the Ohita-Kumamoto fault, that concentrates several hydrothermal sources, and also from the volcanoes nearby sampling sites. Also, mixture of available meteoric, magmatic and also mixed water may fraction the final isotope signature The $\delta^{13}C$ values were grouped in three main categories: (a) values near 0 ‰, indicate few or

absence of biological influence on precipitation, (b) depleted values, indicating possible biologically induced carbonates and, (c) enriched values, indicating possible biologically influenced carbonates. Therefore, these carbonates are interpreted as precipitated from meteoric surface water, sometimes contaminated by volcanism, due to the CO_2 degassing, with little or insignificant biological precipitation

5. The unique modern environment of Japan, with a range of physio-chemical conditions, where modern continental carbonate rocks, including microbialites, precipitate serve as analogue for carbonate reservoirs.

REFERENCES

AITCHISON, J.C. (1986) Stratigraphy, sedimentology and tectonic evolution of the Shimanto Terrane, South West Japan. Chikyu Kagaku. *Earth Science*, **40**,337-363.

BURNE, R.V.; Moore, L.S. (1987) Microbialites: organosedimentary deposits of benthic microbial communities. *Palaios*, **2**, 241-254.

CHAFETZ, H.S, GUIDRY, S., A. (1999) Bacterial shrubs, crystal shrubs, and ray-crystal shrubs: bacterial vs. abiotic precipitation. *Sedimentary Geology***, 126**, 57-74.

CLAESS, H., SOETE, J., VAN NOTEN, K., EL DESOUKY, H., ERTHAL, M. M., VANHAECKE. F., OZKUL. M., SWENNEN. R. (2015) Sedimentology, three-dimensional geobody reconstruction and carbon dioxide origin of Pleistocene travertine deposits in the Ballik area (south-west, Turkey). *Sedimentology*, **62**, 1408-1445.

DUPRAZ, C., REID, R.P., BRAISSANT, O., DECHO, A.W., NORMAN, R.S. AND VISSCHER, P.T. (2009) Processes of carbonate precipitation in modern microbial mats. *Earth-Science Reviews*, **96**, 141-162.

FORD T. D.; PEDLEY, H.M. (1996) A review of tufa and travertines deposits of the world. *Earth Science Review*, **41**, 117-175.

FUJIMOTO, H. (1961) Explanatory text of the geological map of Japan Tochigi 1:50000. *Geological Survey of Japan*, 62, 1961.

GANDIN , A., CAPEZZUOLI, E. (2014) Travertine: Distinctive depositional fabrics of carbonates from thermal spring systems. *Sedimentology*, **61**, 264-290.

HAMMER, O., DYSTHE, D. K., JAMTVEIT, B. (2007) The dynamics of travertine dams. *Elsevier***, 256**, 258-263.

HOEFT, S., E., KULP, T., R., ASAO, M., MADIGAN, M., T., HOLLIBAUGH, J., T., FISCHER, J., C. (2009) Arsenic fuels anoxygenic photsynthesis in hot spring biofilms from Mono Lake, California. *Nature***, 321**, 967-970.

JULIA, R. (1983) Travertines. In: Scholle. P. A., Bebeout, D.G. e Moore, C. H. (Eds) Carbonate Depositional Enviroments *AAPG Memoir*, **33**, 62-72.

KANO, A.; MATSUOKA, J.; KOKO, T.; FUJI, H. (2003) Origin of annual laminations in tufa deposits, Southwest Japan, Paleogeography Paleoclimatology Paleoecology,**191(2)**, 243-262.

KATSUYAMA, M., YOSHIOKA, T., KONOHIRA, E. (2015) Spatial distribution of oxygen-18 and deuterium in stream waters across the Japanese archipelago, *Hydrol. Earth Syst. Sci,***19**, 1577-1588.

KITANO, Y. (1963) Geochemistry of calcareous deposits found in hot springs. *J. Earth Sci. Nagoya University*. **1**, 68-100.

KULL H.J. (1991) Theory of the Rayleigh-Taylor instability, *Physics Reports***,** 206, 197-325.

LEBRUN, E.,BRUGNA, M. BAYAMANN, F. MULLER, D. LIEVREMONT, D. LETT, M.,C., NITSCHKE W. (2003) Arsenite oxidase, an ancient bioenergetics enzyme. *Mol Biol E,* 20, 686-693.

MASCARELLI, A. L (2009). Low life, *Nature*, **459**, 770-773.

MURAMATSU, T. (1984) On the Shimanto Group in the upper reaches of the Ooi River, Shizuoka prefecture. Coli. Abs. 91st meeting, *Geol. Soc.Japan*, 175.

NAGATANI, T.; SAITO S,; SATO, M.; YAMADA, M. (1987) Development of an ultra high resolution scanning electron microscope by means of a field emission source and in-lens system**.** *Scanning Microscopy*, 11, 901-909.

OREMLAND, R., S., STOLZ J. F. (2003) The ecology of arsenic. *Science**,*** **300**, 939-944.

PEDLEY, M. (2009) Tufas and travertines of the Mediterranean region: a testing ground for freshwater carbonate concepts and developments. *Sedimentology*, **56**, 221-246.

PENTECOST, A. (1993) British travertines: a review. *Proc. Geol. Assoc*., **104**, 23-39.

PENTECOST, A. (1995) Quaternary travertine deposits of Europe and Asia Minor**.** *Quat. Sci. Rev*, **14**, 1005-1028.

PENTECOST, A. (2005) Travertine. *Springer-Verlag, Berlin, Heidelberg*, 445.

RASCOVAN, N., MALDONADO, J., VAZQUEZ, M., P. (2015) Metagenomic stufy of red biofilms from Diamante Lake reveals ancient arsenic bioenergetics in haloarchae. *The ISME Journal*, 1-11.

RIDING, R. (1991) Classification of microbial carbonates. In: *Calcareous Algae and Stromatolites* (Ed. Riding, R.), *Springer-Verlag, New York*, 21-51.

RIDING, R. (2011) Microbialites, stromatolites and thrombolites. In: J. Reitner and V. Thiel (eds), Encyclopedia of Geobiology, Encyclopedia of Earth Science Series, *Springer*, Heidelberg, 635-654.

SELLEY, R. C. (1985) Sedimentary environments and facies in ancient sedimentary environments, Cornell Cniversity Press, Ithaca, **3**, 317.

SUGIMURA, A. (1972) Plate boundaries around Japan. *Kagaku*, **42**, 192-202.

SUMNER, D. Y. (2001) Microbial influences on local carbon isotopic ratios and their preservation in carbonate. *Astrobiology*, **1**, 57-70.

SHIRAISHI, F., OKUMURA, T., TAKAHASHI, Y., KANO, AKIHIRO. (2010) Influence of Microbial Photosynthesis on Tufa Stromatolite Formation and Ambient Water Chemistry SW Japan. *Geochimica et Cosmochimica Acta,* 74, 5289-5304.

TAIRA, A. (2001) Tectonic evolution of the Japanese island arc system. *Annual Rev. Earth* e *Planet Sci.***, 29**, 109-134.

TAKASHIMA, C., KANO, A. (2008) Microbial process forming daily lamination in stromatolitic travertine. *Sedment Geol*, **208**, 114-119.

TOKER, E., KAYSERI-ÖSER, M. S., OZKUL, M., KELE, S. (2015) Depositional system and paleoclimatic interpretations of Middle to Late Pleistocene travertines: Kobacas, Denizli, south-west Turkey,. *Sedimentology*, **62**, 1360-1383.

UIYEDA, S. (1973) Island arcs: Japan and its environs. *Elsevier*.

CAPÍTULO 3

PERM-POROSITY CHARACTERIZATION OF CONTINENTAL CARBONATE ROCKS: IMPLICATIONS IN RESERVOIR QUALITY

ABSTRACT

In the last decade, some of the largest oil discoveries in the world were in carbonate reservoirs, including the Pre-Salt oil fields in Brazil. The reservoir quality and facies heterogeneity are the main risk, early in the exploration stage. The present work shows the results of facies analysis and permoporosity characterization in continental carbonates from 10 different active hot springs in the islands of Kyushu (South), Honshu (West) and Hokkaido (North) in Japan. Four lithofacies have been recognized during field work: *stromatolite, root*, *shrub*, and *bubble*. Thin sections, SEM images and, computed microtomography (micro CT) providing 3D images, were used to obtain a realistic spatial image of the porosity system. Petrographic analyzes show that secondary porosity prevails over primary porosity, chiefly due to organic matter (OM) leaching. Nevertheless, bubble facies exhibit a great amount of open primary porosity. The primary porosity is often reduced by compaction but also is enhanced by dissolution. The mineralogy content does not interfere in the porosity volume. Experimentations done with micro-CT indicate a wide range in open pores, from 2% to 75% in shrub and bubble facies, respectively. At micro scale (lupe and thin section) and nano scale (SEM and micro CT), images and numerical modelling suggest that bubble facies is the most porous one (open pores), followed by shrub, root and stromatolite. Large differences in porosities, among different lithofacies, show that porosity losses result directly from secondary diagenetic processes, such as dissolution and compaction. Most of the carbonate features seen in the continental carbonates of Japan have also been seen in the Pre-Salt reservoirs. The results herein presented might be important in oil industry, for continental carbonates seem to play important role in the deposition of reservoirs in the Pre-Salt rocks.

Key-words: Continental carbonates, Reservoir, Porosity

This chapter will be submitted to Association of American Petroleum Geologists AAPG by França, R.M; França, A.B.; Cury, L.F; Jiro, A.; Gomes, T.; Bahniuk, A.M.

3 Introduction

The main subject of this research is to understand the porosity system of modern continental carbonate rocks in active hot springs of Japan. The hot springs deposits were studied using detailed facies analyses based on fieldwork data, petrography, SEM and micro CT analyses. The four different lithofacies, stromatolite, root, shrub and bubble, were characterized in modern carbonate deposits in active hot springs. The same carbonate facies described in Japan are observed in carbonate reservoirs, such as the Aptian Pre-Salt reservoirs, despite remarkable differences in the porosity system. According to Mello, 2009 the Pre-Salt carbonate reservoirs have porosities ranging from 8% to 20%, whereas continental carbonate samples from Japan present porosities ranging from 25% to 75%.

Statistic data have shown that sedimentary rocks cover 5% of upper crust and 75% of Earth's surface (Press and Sevier, 2001). Carbonate rocks represent 15%, including continental carbonate. Non-marine carbonates lack a clear understanding when compared with the vast information for the marine counterpart. The basic nature of the carbonate factories in these systems, whether microbial, macrophytic, skeletal or abiogenic, is not resolved (Wright, 2012). The availability of porosity–permeability data set for subsurface carbonates are in fact surprisingly rare (Ehrenberg *et al.,* 2006). Quantitative information about porosity and permeability in subsurface is important for understanding the processes of fluid displacement involved in diagenesis, petroleum migration and exploitation (Lucia, 1995; Moore, 2001). All the volumetric estimation is based on the premise that the same permoporosity distribution exists for all the stromatolites, coquinas, and clastic basal reservoirs (Mello *et al.,* 2009). Nevertheless, these features change vertically and horizontally within a few meters, as proposed in this research. The reservoir heterogeneity, at all scales, is a challenge to modelling, and it is not an easy task to make reliable predictions about their production performance (Shepherd, 2009).

It is estimated that more than 60% of the world's oil and 40% of the world's gas reserves are in carbonate reservoirs (Figure 1). In the Middle East, for example, around 70% of oil and 90% of gas reserves are in carbonate rocks. In the last decade four of the eight largest oil discoveries in the world are in carbonates in the deepwater Santos basin of Southern Brazil, including the Carioca-Sugar Loaf, Tupi, and Jupiter oil fields (Mello *et al.,* 2009).

Carbonates commonly bears multiple-porosity systems inflicting petrophysical heterogeneity to the reservoirs (Mazzullo and Chilingarian, 1992). The way that fluids flow through a porous system is an important phenomenon in nature (Bielecki *et al.,* 2013) and changes according to rock type. Therefore, different lithofacies has a significant impact on fluid flow. The differences in lithofacies have profound significance for diagenesis and reservoir quality, because carbonates are characterized by extensive early lithification and porosity modification (Ehrenberg and Nadeau, 2005). Mello *et al.,* (2009), stated that petrophysics of stromatolite reservoirs in Pre-Salt are unique preserving permoporosity in quite deep conditions (over 5000 meters). Large and systematic differences are observed in the permoporosity characterization of different continental carbonate facies. The volume of porosity widely ranges in 50% according to the lithofacies. Although the existence of different facies is widely accepted, their perm-pore characterization stills a complex subject.

The modern carbonate continental environment in hot springs of the islands of Kyushu, Honshu and Hokkaido in the archipelago of Japan could be a good analog for the excellent reservoirs of the Pre-Salt. The lack of a clear understanding over continental carbonate deposits and the difficult and expensive access to oil reservoirs, calls the attention to the modern carbonate sites of the islands of Kyushu, Honshu and Hokkaido (Figure 2).

3.1 Regional setting

Although Japan is not inserted in the world carbonate reservoir map (Figure 1), it comprises modern precipitation of continental carbonate rocks that could be good analogue for the unique microbialite reservoirs present in the Brazilian Pre-Salt and possible similar occurrences throughout the globe. The Japanese Island Arc System is a well-studied example of arc trench system in the Western Pacific (Sugimura, 1972). The arcs are segmented into four parts: Kuril, Honshu, Ryukyu and Izu-Bonin, (Taira, 2001), including four large islands; Shikoku Hokkaido, Honshu and Kyushu.

The study area (Table 1) comprises three distinct geographical regions: South in the island of Kyushu; West in the island of Honshu and North in the island of Hokkaido (Figure 2).

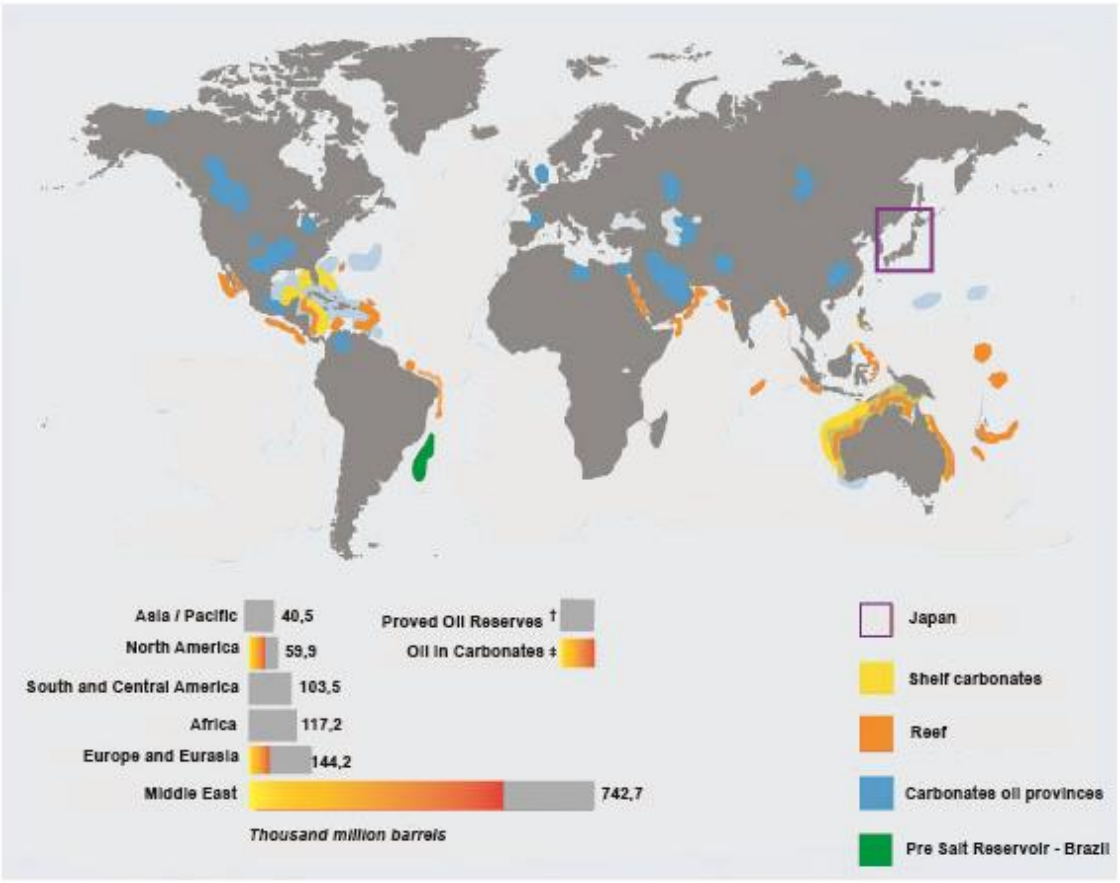

Figure 1: (A) World map and geographic distribution of petroleum reservoirs. Study area comprising modern precipitation of continental carbonates, Japan highlighted.

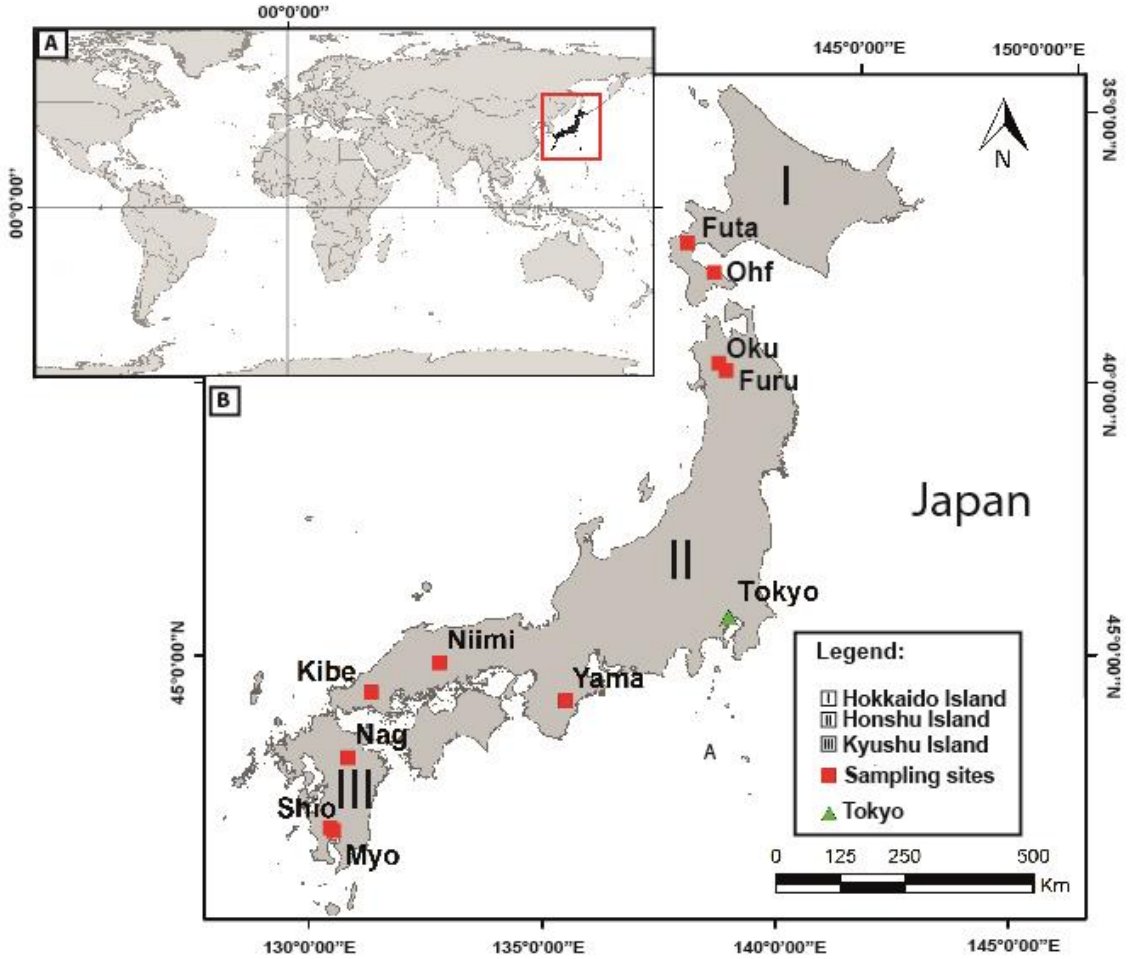

Figure 2: (A) Map of Japan and carbonate sampling sites in the north (Hokkaido Island), west (Honshu Island) and south (Kyushu Island). (Simplified from www.gsj.jp).

3.2 Methodology

A total of eight samples were collected from ten hot springs across the islands of Kyushu, Honshu, and Hokkaido in Japan. Four lithofacies, stromatolite, root, shrub and bubbles were defined based on field observation and macroscopic description. To study the porosity system, the first approach was thin section description followed by SEM analysis. In order to obtain 3D information, some samples were selected for micro CT analyzes including volume, shape, size, connectivity and distribution of pores.

The classical carbonate classification of Choquette and Pray (1970) is used in present work for the study of porosity. This descriptive and genetic system classified the carbonates rocks based on the timing of evolution into primary and secondary pores. The primary or depositional pores are inherent to newly deposited sediments and the particles that comprise them. Such pore types include interparticle pores in, for example, carbonate sands (but also in muddy carbonates), intraparticle pores (within particles such as foraminifera or gastropod shells), fenestral pores (formed by gas bubbles and sediment shrinkage in tidal-flat carbonates), and shelter and growth-framework pores (common in reef buildups) (Mazzullo, 2004). The secondary pores, are those that form as a result of later, generally post-depositional dissolution. Such pore types include all of those mentioned above, but only when it can be demonstrated that primary pores which subsequently were occluded by cement later had all or some of that cement dissolved (resulting in the generation of exhumed pores), as well as vugs (large pores that transect rock fabric, that is, dissolution was not fabric-selective) and dissolution-enlarged fractures (Mazzullo, 2004).

The porosity classification stablished in this paper was applied in different carbonate facies. According to Selley (1985) *in* Claes *et al.,* (2015, p.1412), “A sedimentary facies or lithofacies is a mass of sedimentary rock which can be defined and distinguished from another by its geometry, lithology, sedimentary structures, paleocurrent, pattern and fossils. It reflects a depositional environment that is preserved in the stratigraphic record in the form of a facies”.

3.3 Carbonate sampling

Table 1 shows data from the sampling sites and carbonate facies. Rocks and sediment were sampled along the main stream of active hot springs with different physical-chemical conditions in the South (January 2014), West (August 2015) and North (June 2015) of Japan.

Table 1: List of sample, facies, island, hot spring and geographical coordinates of the samples.

Facies	Island	Hot Spring	Latitute	Longitude
Stromatolite	Kyushu	Shiohitashi	31°50'.4.60"N	130°44'38.90"L
Stromatolite	Honshu	Kibedani	34°25'44.20"N	131°53'42.42"L
Root	Kyushu	Nagayu	33°41'01"N	131°22'25.06"L
Root	Kyushu	Myoken	31°48'.39.92"N	130°45'28.32"L
Shrub	Kyushu	Shiohitashi	31°50'4.60"N	130°44'38.90"L
Shrub	Honshu	Shionoha	34°15'43.16"N	136°2'26.43"L
Bubble	Honshu	Shionoha	34°15'43.16"N	136°2'26.43"L
Bubble	Honshu	Oku-okuhachikuro	40°24'28"N	140°45'16.86"L

3.4 Mineralogy

Thin section petrographic analyze was used to describe the composition, pore type, fabric and evidence of diagenesis. The thin section preparation started with the rocks cut in approximately 4 cm edge, followed by embeddedation. All the samples were impregnated with resin due to its fragility and stained with blue or yellow die in order to distinguish pores. Subsequently, they were taken to oven drying for 24 hours and then forwarded to the normal lamination procedure.

The hand samples and thin sections were described and defined using digital lupe (Axio Cam MRc) and microscopy in transmitted light ZeissAxios A.2M, at Laboratório de Análise de Minerais e Rochas at Federal University of Paraná, Brazil. The type of porosity was based in the porosity classification model on Choquette and Pray (1970). However, extremely small pores could not be described.

Therefore, the samples were coated with palladium and gold (Denton Vacuum Desk V), to be analyzed under the Scanning Electron Microscope (SEM). This technique allows observations better than 1 nm (Nagatani *et al.,* 1987) and was applied to investigate pore types and pore preservation. The analyses were performed in a scanning electron microscope (JEOL JSM-6010LA).

The same samples previously selected for thin sections and SEM analysis were cut in cubes (1,0 cm x 4,0 cm) for 3D high-resolution images by X-Ray

computer microtomography (SkyScan X-ray 1172). Also 3-D rendered high-resolution images of the samples were obtained by X-Ray micro computed tomography (µ-CT), in a Bruker SkyScan 1172 microtomograph. µ-CT technique complement the petrography and SEM observations due its efficiency to obtain both quantitative and qualitative data for: mineral phase separation in a three-dimensional volume, shape, size, connectivity and distribution of pores. The samples corresponded to the same selected for thin section and SEM analysis. Previously to the micro CT scan, the samples were cut into prismatic form (10 x 10 x 40 mm). The projection images were achieved using 12,8 µm of pixel size, 0.4 º as rotation step and an 8 bit CCD camera with resolution of 2000 x1336 pixels. The X ray source operated at 90 kV and 112µA as source potential and current respectively, and the total rotation of the support holder was 180º. After the acquisition of the projection images, the production of tomographic sections take place by use of Bruker NRecon software. A total of 480 µ-CT slices were achieved for each sample. The 3-D data processing and the 3D volume rendering were obtained by use the Bruker CTAnalyzer and CTVol software. The software Bruker CTVox was used to the samples internal visualization.

Pores phase and mineral phase was separated by segmentation process using the CTAnalyzer software. The segmentation process consists in convert a slice of tomographic section to a grey scale level. CTAnalyzer differs 256 shades of gray, and due the different contrast between the pores and mineral phase, it is possible separate the two phases into distinct range of the scale of grey. This process corresponds to the binarization of the phase. After this, 3D rendering and 3D volume of the phase can be available.

3.5 Geochemistry

The mineralogical composition was determined by X-ray diffraction (XRD) using a Panalytical Difractometer model EMPERYAN with Cu (Cu Kα1= 1,5406 Å) the generator voltage and current adjusted to 40 kV and 40 mA, respectively. Scans were run from 3° a 70° 2θ angles. The interpretation of diffraction patterns with semi-quantitative percentage of minerals was done by the method RIR (Reference Intensity Ratio), using the X'Pert High Score Plus DataCollector software with PDF-2 database at LAMIR-UFPR.

Fluorescence X-ray analyzes have determined the chemical characterization of the samples. The method consists of spraying about 30g sample Tungsten mill in spray AMEF for 30 seconds for particle size reduction until they reach size of 325 mesh. The resulting spray powder is then led to a 50 ° C oven temperature for 24 hours for drying. After drying the samples are weighed and mixed in the ratio of 7,000g ± 0.0003 0.0003 ± sample with 1,4000g of organic wax. After weighting the mixture, it is pressed for the manufacture of Tablets. Each mixture is then suitably dried taken to PFAFF machine and then pressed at a pressure of 20 ton/cm² with the rise time of 50s, 60s deconstruction time and fall time of 30 seconds, the standard used for carbonates. The chemical analyzes were performed at PANalytical equipment, AXIOS MAX model at LAMIR-UFPR.

3.6 Results and discussion

In order to understand the porosity system as well as permeability, the carbonate samples from Japan have been compared in terms of sedimentary texture, structure, diagenesis, microfacies classification (Dunham, 1962), pore structures, and the presence and distribution of fractures. (Figure 6). Unlike their marine counterparts, continental carbonates today seem able to develop under a wide range of salinities from fresh to hypersaline (Wright, 2012).

3.6.1 Facies versus porosity

3.6.2 Stromatolite. facies

The stromatolite facies (Figure 3) oftenly occurs as a domal structure growing upon gently slopes around vents. Although they occur in different settings, there are remarkable macroscopic similarities like laminated inner structure (Figure 3A) The samples are typical light brown or reddish colors. Millimetric and contiguous layers characterize the lamination with with low angle gently convex, following the substrate morphology. We also detect the presence of vertical and horizontal post depositional open fractures. It was not possible to measure the stromatolite thickness, but its lateral continuity is controlled by the extension of the depositional environment.

The petrographic analysis in thin sections show gently convex and contiguous millimetric layers with different thickness composed of spar and or microspar aragonite crystals, exhibiting arborescent structures (Figure 3B). The laminae thickness variation is interpreted as season oscillations controlling the amount of water for precipitation. The micro interparticles are vertically disposed among arborescent structures, parallel to the growth direction and inside the layers. Macro and also micro fenestral pores, are also horizontally disposed in the contact surface among the layers, comprising, at the same time, the end and the beginning of a new water cycle and consequently crystal growths. The origin of most of the pores in stromatolites is attributed organic matter leaching. Horizontal permeability, parallel to the layers, are not vertically connected excepted for secondary fractures. Although rare, the presence of open fractures enhances vertical permeability and hydraulic interconnectivity.

The SEM observations on fresh surface of stromatolites reveal micro porosity inside and among empty cylindrical pipes which seem to suit as substrate for the growth of spherical crystal aggregates (Figure 3D).

Computadorized microtomography shows high volume of porosity and permeability in horizontal layers with little or no vertical connectivity. The total porosity is 26% (Figure 3C).

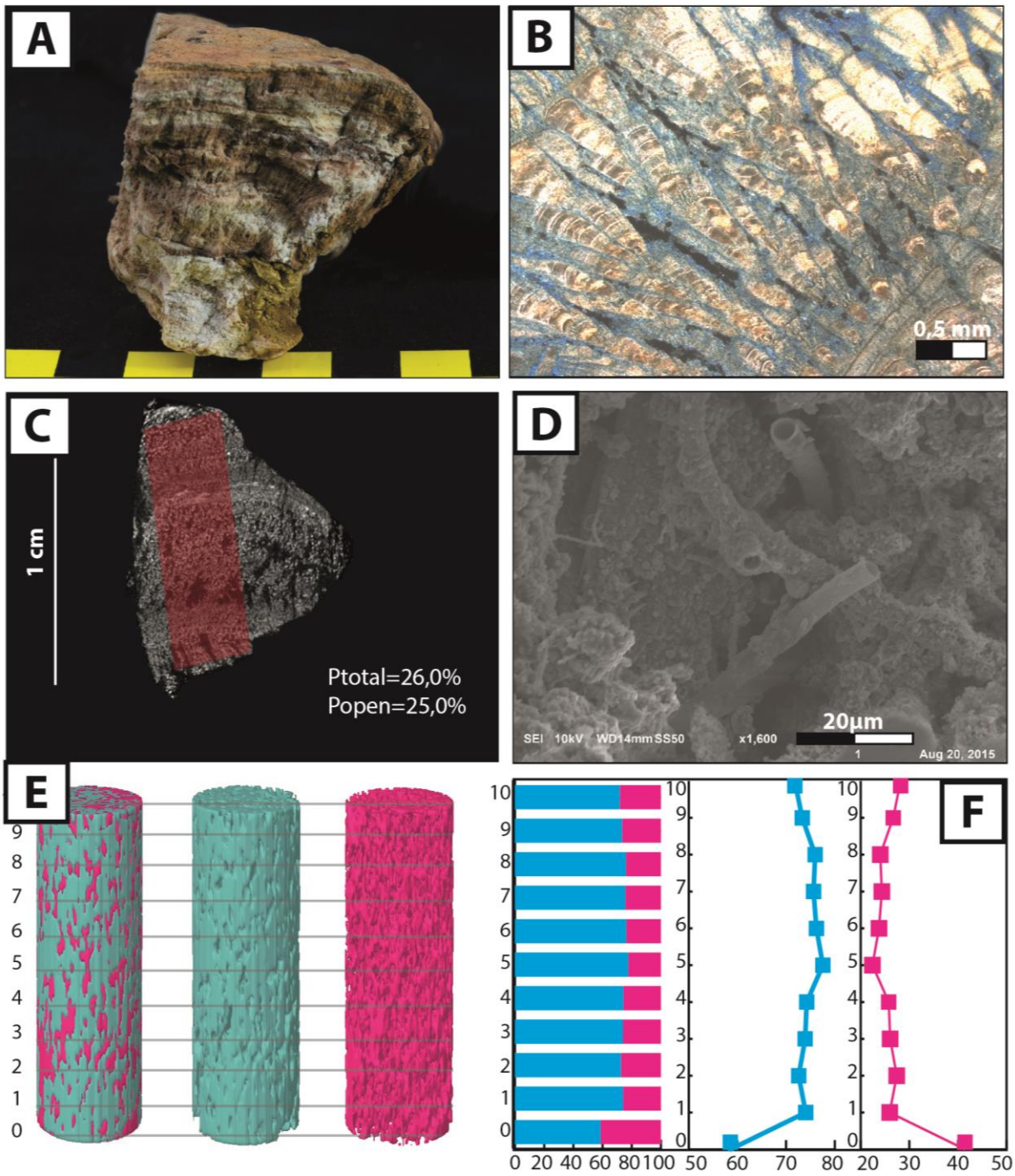

Figure 3: (A) Stromatolite facies. (B) Photomicrograph in cross polarized light. Gently convex and contiguous millimetric layers of microspar and spar calcite crystals, interleaved with porosity layers. Pore space appears in black. (C) Photomicrograph of micro-CT analyzes displays horizontal porosity and permeability and a total of 15% of open pores. The red rectangle represents the analyzed areas (D) SEM image of aragonite crystals exhibiting spherical morphology growing around empty cylindrical tubes. (E) Vertical 3D core samples sectioned in 10 slices from base to top obtained from micro-CT analyzes. From lefty to right: rock and porosity; rock; and porosity cores. (F) Graph showing the volume of rock and porosity. Left- volume of rock in blue and porosity in pink. The blue line displays the volume of rock along the 10 vertical slices. The pink line displays the volume of porosity.

3.6.3 Root facies

The root facies is the second prevailing lithofacies. In outcrop, they consist of brownish rocks occurring at the base of cascade and/or pool. In pools,the vegetal fossil fragments in pools seem to be better preserved when compared with the reworked fossils present in the base of cascades, that are smaller and more fragmented, being correlated to “phytoherm” and “phytoclast”, respectively (Buccino *et al.,*1978 *In* Padley, 2009). The hardness changes throughout the sample, according to distribution of leaves and vegetal fragments. The vegetal fragments work as substrate for aragonite and calcite crystal growth and also as sediment traps. The horizontal, discontinuous, and inhomogeneous layers composed of vegetal fossils interbeds with horizontal, discontinuous and homogeneous layers composed only of mineral assemblages. The porosity is concentrated in the highly fossiliferous intervals. Moldic and megapores are observed in all samples (Figure 4A).

The petrographic analyses in thin sections show the surface contact between the vegetal fossil layers composed of feather like aragonite with a microspar level (Figure 4B). The porosity is either, micro pores observed among feather like aragonite structures, probably due to leaching of organic matter, or macro moldic porosity up to 0,5 mm interpreted as molds of vegetal fragments. Both, micro and macro pores are interpreted as post depositional features. All the layers composed only of mineral assemblages apparently show no porosity and permeability. The aragonite (100%) grain size ranges from less than 1 mm to milimetric in both layers, with despite vegetal fossils contents.

The SEM images reveal mega pores and high horizontal permeability in the contact surface between distinctive layers. Under high magnifications it is possible to observe aragonite needle crystals growing from a single point. (Figure 4D). Dissolution and reprecipitation are also observed in the root facies, creating mega-moldic pores and stalactites.

The micro-CT analysis show high volume of porosity and permeability. Porosity and permeability are randomly organized, although a higher volume of porosity occurs along the contact surface of layers, following the vegetal fossil fragments. Vertical connectivity, however has not been observed. Vertical connectivity, however has not been observed. The total porosity is 30%(Figure 4C).

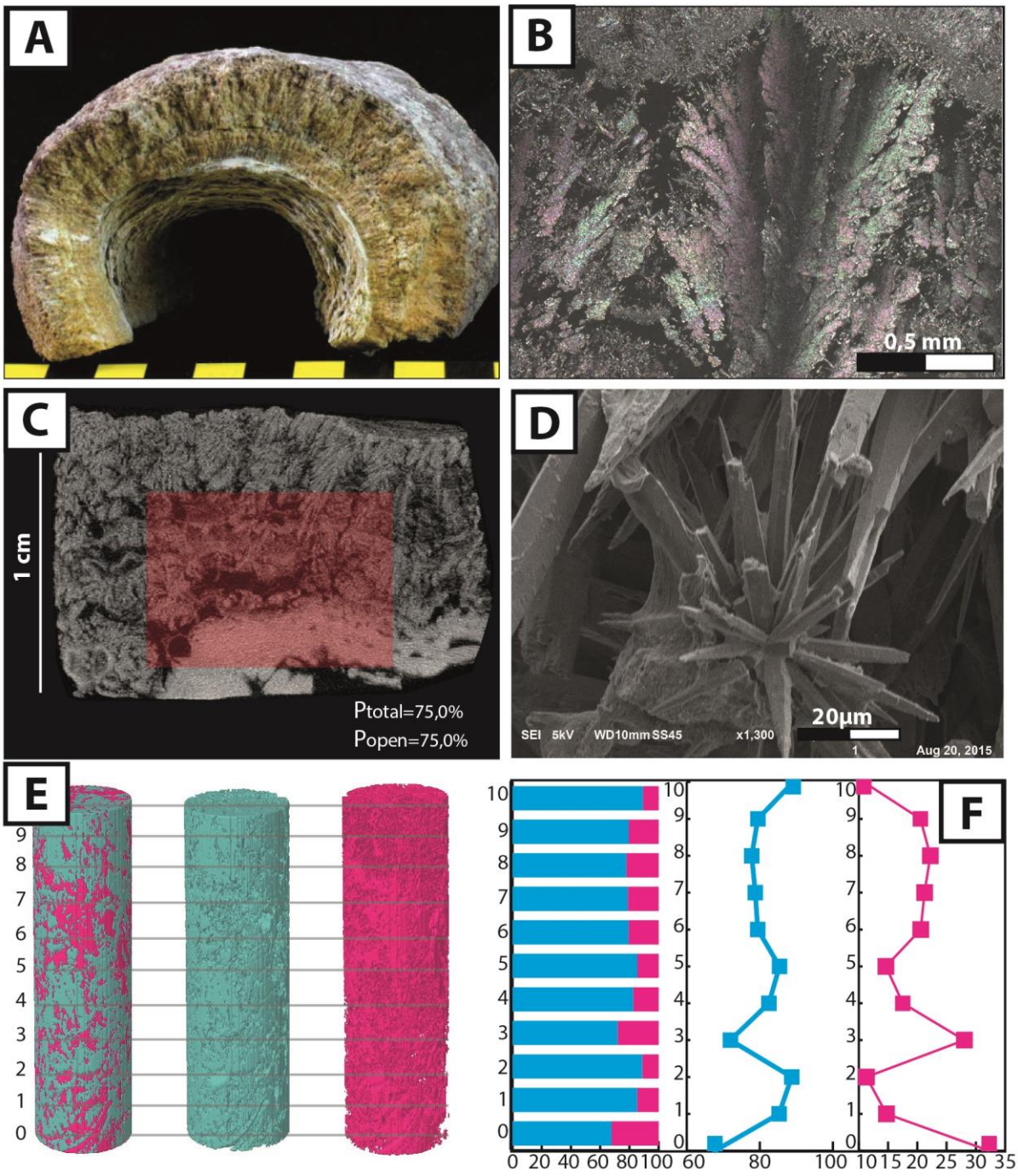

Figure 4: (A) Root facies exhibiting mega moldic pore. (B) Photomicrograph in cross polarized light showing feather like, aragonite crystals. Dark points represent porosity. (C) Photomicrograph of micro-CT analyzes displaying horizontal porosity and permeability - total of 30% of open pores. The red rectangle represents the analyzed area. The basal area has few pores due to the absence of vegetal fossil fragments. (D) SEM image of aragonite needle crystals exhibiting spherulitic morphology. Porosity is observed between contact surface. (E) Vertical 3d core samples sectioned in 10 slices from base to top obtained from micro-CT analyzes. From lefty to right: rock and porosity; rock; and porosity cores. (F) Graphs displaying the volume of rock and porosity. Left: volume of rock in blue and volume of porosity in pink. The blue line displays the volume of rock along the 10 vertical slices. The pink line displays the volume of porosity.

3.6.4 Shrub facies

The shrub-like morphology was observed in all the hot springs and is characterized by its morphological shrub like, fern-like or bush-like arborescent growths branching upwards to form colonies, resembling miniature forests (Figure 5). The shrub facies has been observed in inner stromatolites structures, growing from the substrate with laterally interfering bundles and tend to be less developed vertically away from the substrate. Micro porosity is observed among shrub crystals and parallel to horizontal laminae.

Macroscopically, the inner microfacies is light brown and composed of aragonite shrub crystals with low volume of pores observed among shrub crystals. Horizontal connectivity is displayed between the layers.

Petrographic analyzes of thin sections show subparallel, millimetric and contiguous flat layers composed of carbonate and a straight pattern of fenestral porosity. There is a relative high volume of horizontal porosity and permeability is observed despite the absence of vertical connectivity. Thick bundles of ray-crystal crusts grow over a slightly curved substrate with lateral continuity of shrubs and micrite aggregates. There is micro porosity among the shrub crystals and, macro pores between horizontal layers, due to organic matter leaching. The morphology of the porosity related to shrub is characterized by vertical voids, associated with growth directions as arborescent structures. Also, it is possible to observe a remarkable horizontal porosity, related to the substrate which grew synchronously with multiple aggregates of shrubs intercalated with micritic (Figure 5B).

Scanning electron microscopy (SEM) observations reveal two microfacies (Figure 5C). Similar to the thin section observations, SEM images show aragonite shrub crystals grow from a single point with little volume of pores among then. Organic matter leaching has promoted micropores with apparent low permeability.

Three points were selected for Micro CT analyses (Figure 5D), depicting the same permoporosity pattern seen in section and SEM. The 3D images allowed the observation of low volume of pores in the inner part (2%), good porosity in the left flank (20%) and in the right flank (24%). The morphology of the shrub is related to free space, that means available growing free space directly interfere in volume of porosity (Figure 5C).

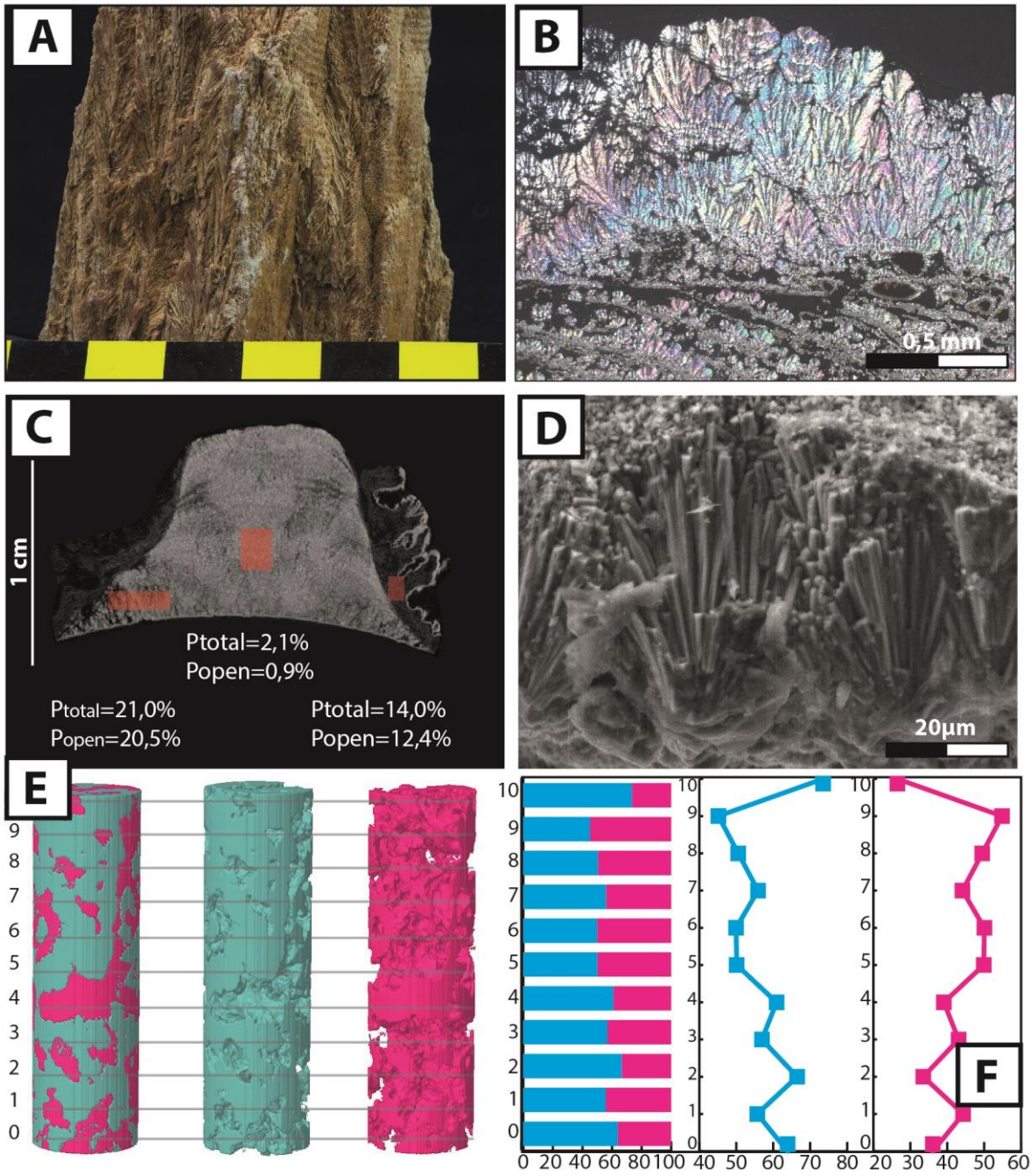

Figure 5: (A) Shrub facies exhibiting arborescent structure. (B) Photomicrograph in cross polarized light showing spar aragonite shrub crystals growing over a flat substrate. The horizontal porosity is observed at the bottom of the image and vertical porosity is observed between shrubs. The dark points represent porosity. (C) Photomicrograph of micro-CT analyzes shows three different porosity realms along the sample. The higher porosity, around 20,5%, is observed in the left side. The red areas represent the analyzed areas (D) SEM image of aragonite needle crystals. Porosity is observed between crystal needles. (E) Vertical 3d core samples sectioned in 10 slices from base to top obtained from micro-CT analyzes. From left to right: rock and porosity; rock; and porosity cores. (F) Graph showing the volume of rock and porosity. Left: volume of rock in blue and porosity in pink. The blue line shows the volume of rock along the 10 vertical slices. The pink line shows the volume of pore space.

3.6.5 Bubble facies

The bubble facies is characterized by open pore spaces coated by carbonate ranging from 0,2mm to 0,7mm, normally disposable in a random way (Figure 6A). The bubble facies precipitate when drastic changes occur in physicochemical parameters, with the inversion of pH leading to a fast precipitation of silica. The occurrence of bubbles is associated to zones of hydrothermal and meteoric mixing waters zone. Bubbles are present only at a certain distance from the hot spring, due to water cooling.

The bubbles are also coating microbial mats in pools and on surface of limestones precipitated with low dip angle and slow water velocity. The occurrence of this facies is associated with paper-thin rafts in water mixing zone, right after fresh water input.

Petrographic analyses of thin sections show a high volume of pores. Intracrystaline micropores and inter/moldic crystalline macropores (Figure 6A). Mega-moldic pores of 0,7mm are randomly arranged throughout the sample. The random permeability is mainly controlled by the intercrystalline porosity.

Scanning electron microscopy (SEM) allow the observation of the aragonite crystals randomly crystalized and a low volume of intercrystalline micropores and low permeability (Figure 6C).

Computadorized microtomography analyses show the highest volume of open pores. Moldic macropores were observed throughout the sample. The ‘’escaping path’’ left for bubbles during precipitation strongly increases the porosity and permeability of the sample. The total porosity was 75,5% and open porosity 75% (Figure 6D).

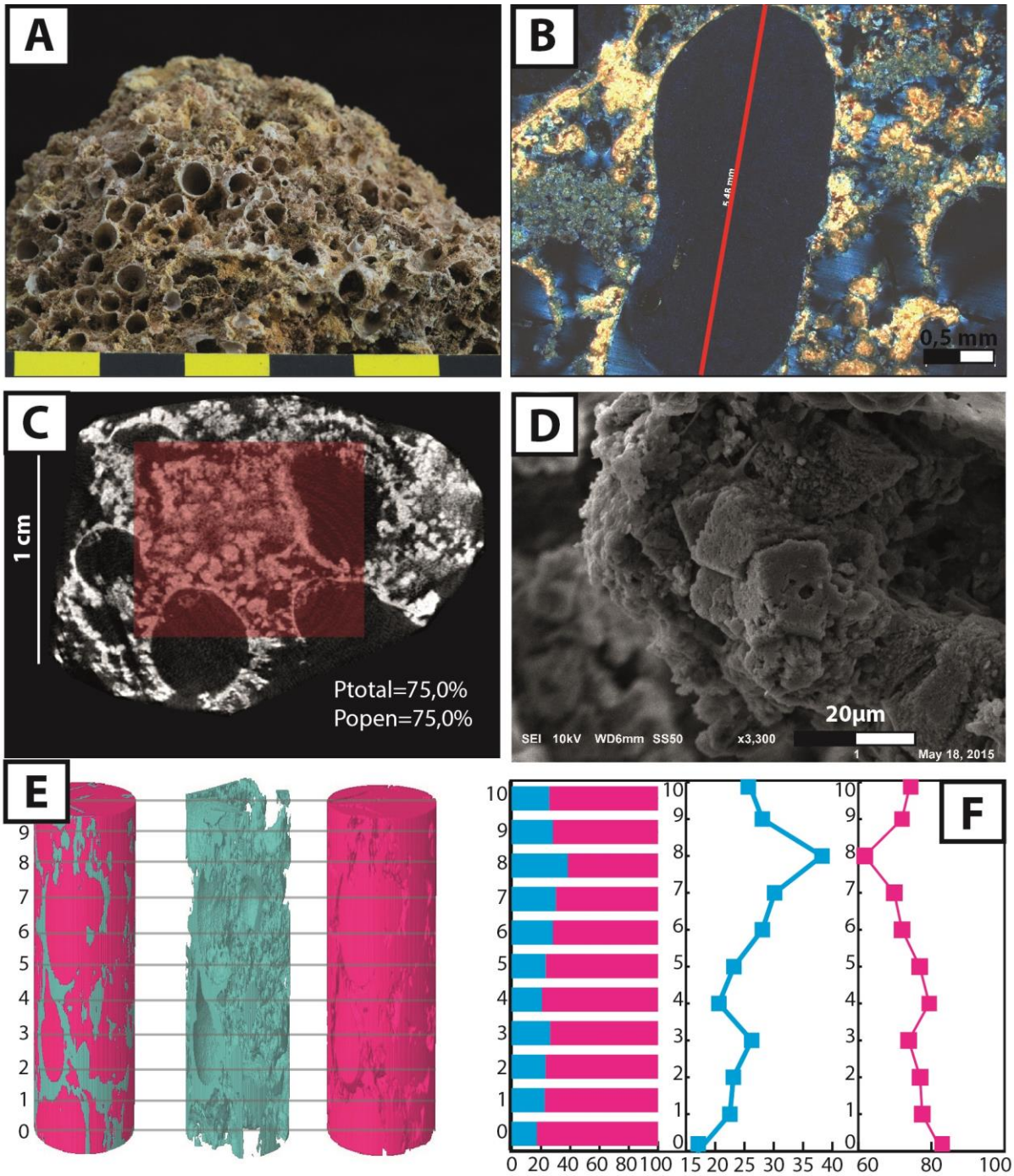

Figure 6: (A) Bubble facies exhibiting huge bubble pores. (B) Photomicrograph in cross polarized light showing macro pores and spar aragonite crystals. The pore space are either empty or partially filled with matrix. (C) Photomicrograph of micro-CT analyzes shows 75% of open pores. (D) SEM image of microporosity in calcite crystals. Porosity and permeability is observed between needle crystals. (E) Vertical 3d core samples sectioned in 10 slices from base to top obtained from micro-CT analyzes. From left to right: rock and porosity; rock; and porosity cores. (F) Graph displaying the volume of rock and porosity. Left: volume of rock in blue and porosity in pink. The blue line displays the volume of rock along the 10 vertical slices. The pink line displays the volume of porosity.

3.6.6. Porosity characterization

Modern carbonate sediments are deposited with large amounts of porosities; commonly they contain more pore space than grain volume. In contrast, ancient carbonate rocks usually retain a few percent porosity (Halley, 1981) except for some Pre-Salt reservoirs (Mello *et al.,* 2008). Most carbonate rocks are frequently characterized by multiple porosity systems that impart petrophysical heterogeneity to reservoir rocks (Mazzullo and Chilingarian, 1992). Consequently, the value of porosity, the porosity type, and porosity distribution often govern the production values and simulation characteristics of the gross carbonate reservoir interval (Wardlaw, 1996). In this study, the value of porosity, the type and origin of the pores and other petrophysical data are quantified and described according to the lithofacies.

The continental carbonate rocks from Japan have porosities ranging from (2,1% to 75%). The porosity system is quite heterogeneous, implying complexity into the reservoirs and exploitation. The distribution of porosity values is shown in Figure 7, grouped into the four different lithofacies (stromatolite, root, shrub and bubble) easily recognized in outcrops.

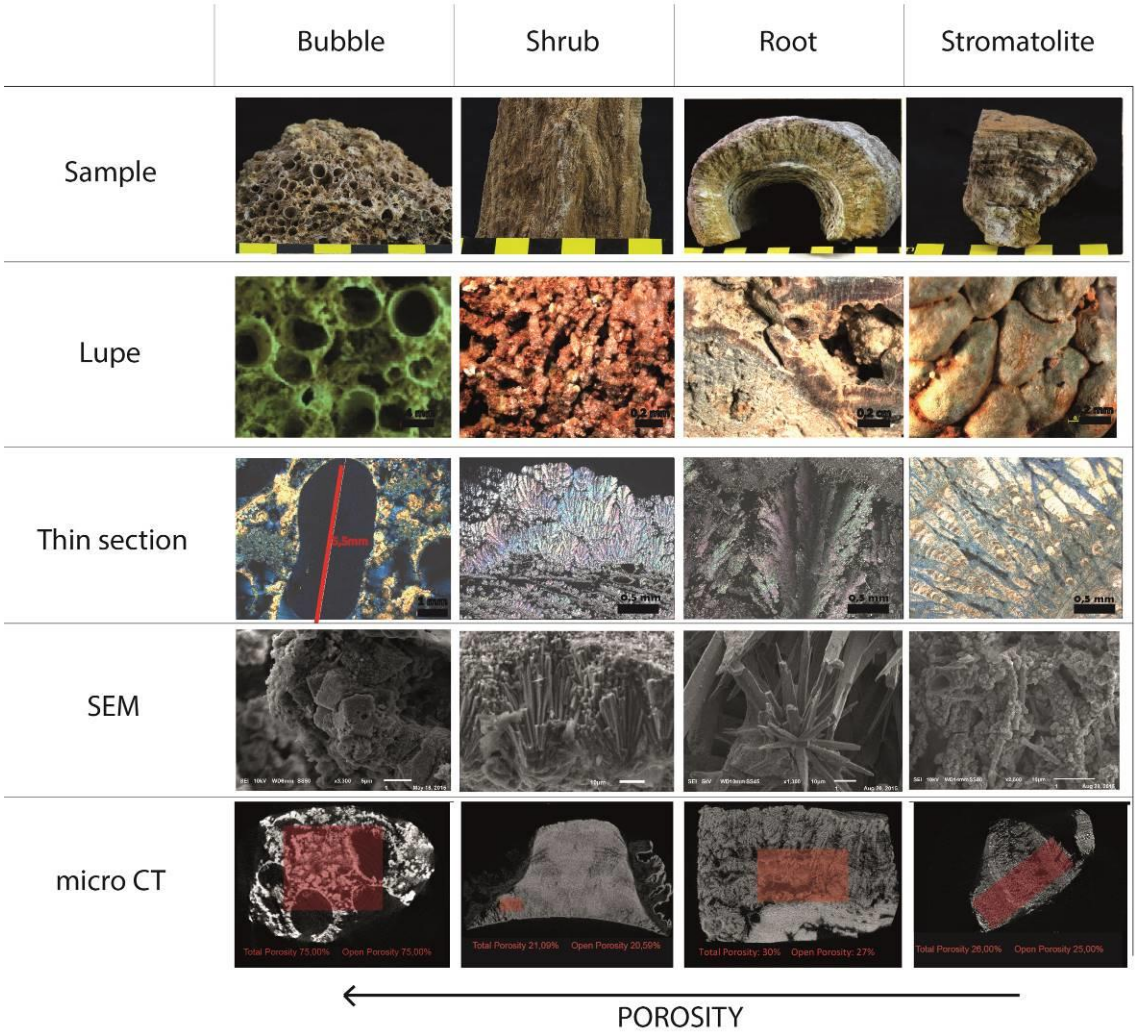

Figure 7: Summary of continental carbonate facies from Japan and their characterization.

3.7. Discussion

Porosity and permeability are the two most important factors determining reservoir quality. The porosity and permeability are controlled by the amount and type of porosity and how that porosity is interconnected. In carbonates, they are controlled by diagenetic processes including compaction, dissolution, precipitation and alteration (Rashid, *et al.,* 2015).

Although most of carbonate diagenesis knowledge is applied on marine environment, this study focused on continental carbonates. According to Guo and Riding (1994), and Pentecost, (2005) the phreatic and the vadose diagenesis is thought to be responsible for dominant transformations of the fabrics and associated porosity. Even though carbonates commonly increase in porosity by dissolution during deeper burial, these reservoirs have greater chemical reactivity, resulting lower resistance to chemical compaction and associated cementation (Ehrenberg and Nadeau, 2005). In the other hand, some authors as Bahniuk (2013) and Mello *et al.,* (2009) suggest that if no reaction fluid percolate the reservoir, the framework of the microbialites are well preserved, and the preservation of the primary porosity is higher than the second..Also, organic matter decay is considered an important part in diagenetic processes, creating moldic porosity. Various diagenetic processes have affected the continental carbonate rocks in Japan. In particular, cementation, dissolution and leaching.

The fenestral porosity observed in petrographic analyses in the stromatolite facies is interpreted as a product of organic matter leaching, due to vadose meteoric diagenesis and also to water-rock interaction, and contamination of infiltrating waters. The same principle is applied to porosity observed in shrub and root facies. The primary microspar is also observed in stromatolite facies. Cementation is more abundant in root facies and appears to have formed during post diagenesis process such as dissolution, and consequently reducing the porosity.

Dissolution takes place when pore fluids are under saturated with respect to the carbonate mineralogy (Tucker and Wright, 1990). Additionally, the dissolution products are observed in root facies represented by karstic features consisting of fissures, caves, and speleothems. This process may open pores or even partially or totally fill them. Although the mineralogy composition shows different contents of aragonite, high-Mg calcite and calcite, any polymorphism processes have been

observed in petrographic and SEM analyses. Nevertheless, changes in crystal size and shape, without a change in mineralogy was observed in stromatolite facies, being interpreted as neomorphism processes. In thin sections, the empty primary voids observed in stromatolite, shrub and root facies are interpreted as leaching of organic matter. In stromatolite facies, the voids are horizontally disposed and parallel to the growth substrate and transversal to the water flux. However, in shrub and root facies, these voids are displayed among the vertical growth of calcite and aragonite crystals. Subsequently, the leaching of organic matter persistently increases the volume of open pores in all facies.

The present data strongly suggest that bubble facies has the highest porosity (52-75%). Shrub, root and stromatolite facies also have good reservoir properties with pores volume of 42%, 27% and 25%, respectively. The lithification process of root, shrub and stromatolite are accomplished on the surface where the structures achieve as rock, which probably acquired and framework as consolidate rock. However, most likely during the burial process the bubble facies suffer compaction and may resemble bird eyes structures. Thus, the best primary porosity probably will be find in shrub, root and stromatolite facies.

3.8 Conclusion

The techniques of X-ray diffraction (XRD), X-ray fluorescence (XRF), and computed microtomography X-ray assisted with detailed petrographic description were applied on modern continental carbonates samples of possible microbial origin, in order to characterize the permo pore system, as well as conducting quantification of porosity. The samples were collected at modern active hot springs located in the South, West and North of Japan.

The analysis indicated that the root and bubble facies have a variation in their internal structure, presenting a heterogeneous typology, having pores of vugular and moldic types, respectively. However, shrub and stromatolite facies have homogeneous fenestral type internal structure.

The morphology of porosity in bubble facies was shown to be well rounded pores, although root, shrub and root facies shown varied elongated pores. Concerning the morphometry has pores from the micrometer scale to centimetric and effective porosity in stromatolite is relatively high.

Adequate porosity for commercial production is found in all continental carbonate facies from Japan as determined by examinations. The compiled data strongly suggest that bubble facies has optimum potentialities as a reservoir due to its 52-75% volume of open pores and also vertical and horizontal connectivity. Nevertheless, such facies is not found in carbonate reservoirs because is easily destroyed with diagenesis and compaction. Shrub, root and stromatolite facies also have reservoir properties potentialities, with pores volume of 42%, 27% and 25%, respectively. Contiguous horizontal connectivity despite the absence of vertical connectivity prevails in these facies. However, natural or anthropic faults and cracks in this reservoir could increase the permeability, and the optimum reservoir quality would be reached.

In conclusion, the carbonate perm pore characterization allows a better understanding of the development of porosity in continental carbonates from Japan, and yield a more trustworthy method of envisaging porosity trends. Such research may be useful in the oil industry, for both explorer geologists and producer's' engineers, in order to reduce risks of exploitation.

REFERENCES

BAHNIUK, A.M., 2013, Coupling organic and inorganic methods to study growth and diagenesis of modern microbial carbonates, Rio de Janeiro State, Brazil: implications for interpreting ancient microbialite facies development: PhD Thesis. ETHZ, Zurich, p. 1-169.

BIELECKI, J.; JARZYNA, J.; BO.ZEK, S., and W. M. KWIATEK. 2013, Computed microtomography and numerical study of porous rock samples: Radiation Physics and Chemistry, n. 93.

BUCCINO,G.; D'ARGENIO,B.; FERRERI,V.; BRANCACCIO,I.; FERRERI,M.; PANICHI,C., and D. STAZIONE, 1978, I travertine della basse valle del tanagro (Campania) .Studio geomorfologia, sedimentologia e geochimico: Boll. Soc. Geol. Ital. v.98: p.617-646.

CHAFETZ, H.S., and S. A. GUIDRY, 1999, Bacterial shrubs, crystal shrubs, and ray-crystal shrubs: bacterial vs. abiotic precipitation: Sedimentary Geology, v.126, p.57-74.

CHOQUETTE, P. W., and L. C., PRAY, 1970, Geologic nomenclature and classification of porosity in sedimentary carbonates: American Association of Petroleum Geologists Bulletin, v. 54, p. 207 – 250.

CLAESS, H., SOETE, J., VAN NOTEN, K., EL DESOUKY, H., ERTHAL, M. M., VANHAECKE. F., OZKUL. M., and R. SWENNEN, 2015, Sedimentology, three-dimensional geobody reconstruction and carbon dioxide origin of Pleistocene travertine deposits in the Ballik area (south-west, Turkey): Sedimentology, v.62, p.1408-1445.

DUNHAM, R. J., 1962, Classification of carbonate rocks according to depositional texture, *in* W. E. Ham, ed., Classification of carbonate rocks: AAPG Memoir v.1, p. 108–121.

EHRENBERG, S. N., and P. H. NADEAU, 2005, Sandstone vs. carbonate petroleum reservoirs: A global perspective on porosity-depth and porosity-permeability relationships: AAPG Bulletin, v. 89, no. 4, p. 435–445.

EHRENBERG, S. N.; EBERLI, G.P., and G. BAECHLE., 2006, Porosity–permeability relationships in Miocene carbonate platforms and slopes seaward of the Great Barrier Reef, Australia (ODP Leg 194, Marion Plateau): Sedimentology, v.53, p. 1289-1318.

GUO, L., and R. RIDING, 1994, Origin and diagenesis of Quaternary travertine shrub fabrics, Rapolano Terme, central Italy: Sedimentology, v.41, p.499–520.

HALLEY, R. B., 1981, Evolution of Carbonate Porosity During Burial--Bahamas, Florida, and Gulf Coast: Holocene to Jurassic: AAPG Bull., v.65, p.2466-2467.

LUCIA, F.J., 1995, Rock-fabric/petrophysical classification of carbonate pore space for reservoir characterization: AAPG Bull., v.79, p.1275–1300.

MAZZULLO, S.J., and G. V. CHILINGARIAN, 1992, Diagenesis and origin of porosity,*in* Chilingarian G.V.; Mazzullo, S.J., and H.H. Rieke, Carbonate Reservoir Characterization: A Geologic-Engineering Analysis, Part I: Elsevier Publ. Co., Amsterdam, Developments in Petroleum Science v.30, p. 199-270.

MAZZULLO, S.J., 2004, Overview of Porosity Evolution in Carbonate Reservoirs: Kansas Geological Society Bulletin, v. 79, nos. 1 and 2.

MELLO, M. R., AZAMBUJA FILHO, N.C., BENDER, A., BRUNO. P.S., DE MIO, E., CATTO, A. J., SCHMIT, P., and C.L. JESUS, 2009, The super-Giant Discoveries in the Pre-salt Hydrocarbon Province of Santos Basin: Submitted to AAPG bulletin.

MOORE, C.H., 2001, Carbonate Reservoirs Porosity Evolution and Diagenesis in a Sequence Stratigraphic Framework: Elsevier, Amsterdam, p.444.

NAGATANI, T.; SAITO S.; SATO, M., and M. YAMADA, 1987, Development of an ultra high resolution scanning electron microscope by means of a field emission source and in-lens system: Scanning Microscopy. v.11, p.901-909.

PEDLEY, H. M., 2009, Tufas and travertines of the Mediterranean region: a testing ground for freshwater carbonate concepts and developments: Sedimentology, v.56, p.221-246.

PENTECOST, A., 2005, Travertine: Springer, v.455.

PRESS, F., and R. SIEVER., 2001, Understanding Earth,:Wiley InterScience, v.3.

RASHID, M. H.; KREHHENBRINK, M., and M. S. AKHTAR., 2015, Nitrogen-fizing plant-microbe symbioses *in* LICHTFOUSE, E. (ed) Sustainable agriculture reviews:. Springer International Publishing, Switzerland, v. 15, p.193-234.

SELLEY, R. C., 1985, Sedimentary environments and facies in Ancient Sedimentary Environments: Cornell University Press, Ithaca, ed.3, p.317.

SHEPHERD, M., 2009, Oil field production geology: AAPG Memoir, v.91, p.301-309.

SUGIMURA, A., 2001, Plate boundaries around Japan: Kagaku, v.42, p.192-202.

TAIRA, A., 2001, Tectonic evolution of the Japanese island arc system: Annual Rev. Earth e Planet Sci., v.29, p.109-134.

TUCKER, M.E., and V. P. WRIGHT, 1990, Carbonate Sedimentology: Blackwell Scientific Publications, Oxford, v.482.

WARDLAW, N. C., 1996, Factors affecting oil recovery from carbonate reservoirs and prediction of recovery, carbonate reservoir characterization: a geologic engineering analysis part II. Elsevier Publ. Co, v.30,pp. 867-903.

WRIGHT, V.P., 2012, Lacustrine carbonates in rift settings: the interaction of volcanic and microbial processes on carbonate deposition: Geological Society, London, Special Publications.

CAPÍTULO 4

4.1 Conclusões

O objeto de estudo deste trabalho foram rochas carbonáticas continentais modernas coletadas em 10 fontes termais no Japão

Os principais objetivos foram: (a) compreender as litofácies encontradas em carbonatos continentais modernos e relacioná-las ao ambiente deposicional, e (b) compreender suas propriedades petrofísicas como rocha reservatório em diferentes escalas. A compreensão da importância das variáveis responsáveis na formação de diferentes fácies como geradoras de diferentes texturas sedimentares em rochas carbonáticas permite descrever novas estruturas e feições de porosidade com implicação direta em modelos de reservatórios carbonáticos.

Esta pesquisa desenvolveu uma abordagem sistemática para estudar carbonatos continentais modernos em seu ambiente de formação com o objetivo de interpretar sinais geoquímicos e sedimentares. Esses sinais permitem interpretar o papel relativo dos processos físico-químicos, bioquímicos e influências ambientais na formação destas rochas e depósitos. Além disso, a relação entre as fácies sedimentares e o ambiente deposicional, observadas em depósitos modernos, fornece uma oportunidade para explorar um modelo análogo a reservatórios carbonáticos antigos.

Esta dissertação foi subdividida em três capítulos principais, além das conclusões e perspectivas.

O capítulo 1 apresenta uma revisão sobre carbonatos continentais com um enfoque em microbialitos e terminologias relacionadas ao assunto.

O capítulo 2 "*Environmental conditions playing important role in modern continental carbonate facies formation in Japan: geochemistry and facies patterns*" compara diferentes condições ambientais, com base na química da água, padrões físico-químicos e geoquímicos atuando na precipitação de carbonatos modernos. Com base em dados macro e microscópicos, quatro fácies foram descritas: estromatólito, *shrub, bubble* e *root*. Os dados mostram que a química da água (temperatura, pH, O.D.) interferem diretamente na precipitação e,

consequentemente, em diferentes fácies. Além disso, a forma do substrato a partir do qual estes carbonatos crescem, assim como a distância do *vent*, também contribuem para a formação de diferentes fácies. Os resultados mineralógicos mostram a predominância de calcita ou aragonita. Os resultados químicos mostraram elevados teores de CaO e subordinadamente Fe_2O_3 e SiO_2 em todas as amostras. Teores de arsênio também foram observados e sua origem ainda está em debate. Os sinais isotópicos mostram que as amostras majoritariamente seguem o *trend* isotópico nacional de água meteórica com valores depletados de $\delta^{18}O$. Os valores de $\delta^{13}C$ foram agrupados em 3 grupos principais: (a) valores próximos a 0‰ que representam pouca ou nenhuma influencia biológica na precipitação, (b) depletados, possivelmente biologicamente induzidos e (c) enriquecidos, possivelmente biologicamente influenciados. Portanto, estes carbonatos continentais foram interpretados como precipitados a partir de água meteórica em superfície devido a desgaseificação de CO_2, por vezes com contaminação de vulcanismo ativo, com pouca ou baixa precipitação biológica.. As imagens de MEV mostram fósseis relacionados com EPS, caracterizando possível influência biológica durante a precipitação na fácies estromatólito. As observações de micro-CT permitiram uma análise detalhada dos poros de todas as fácies, mostrando que as fácies *bubble* é a mais porosa, seguida das fácies *shrub, root*, estromatólito.

No Capítulo 3, "*Perm-porosity characterization of modern continental sedimentary carbonate rocks: implication in reservoir quality*", a microtomografia computadorizada (micro-CT), foi utilizada na caracterização permo-porosa de carbonatos continentais modernos do Japão. Essa técnica permitiu observar a porosidade e permeabilidade em diferentes fácies. As imagens em 3D foram reconstruídas e permitiram a caracterização em micro escala da permeabilidade. Correlações sistemáticas obtidas a partir de petrografia, MEV e micro-CT permitiram uma detalhada caracterização permo-porosa de quatro diferentes fácies. Os experimentos realizados em macro e microescalas indicaram grande variedade no volume de poros abertos dessas fácies. Na micro (lupa e petrografia) e nano escalas (MEV e micro CT),as imagens e modelagens numéricas mostram que a fácies *bubble* é a mais porosa, seguida pelas fácies *shrub, root* e estromatólito. As fácies *shrub* e estromatólito são constituídas por níveis contínuos, sub milimétricos e subparalelos, por vezes curvados, de cristais de carbonato, com boa porosidade e

permeabilidade horizontal. Permeabilidade vertical só foi observada em fraturas. As fácies *bubble* e *root* não apresentam arranjo preferencial de poros, os quais parecem seguir o escape de bolhas durante a precipitação e moldes de fragmentos vegetais. Observa-se boa permeabilidade horizontal e vertical em ambas as fácies. No entanto, processos diagenéticos não permitem a preservação da fácies *bubble*, razão

O capítulo 4 apresenta de forma sucinta as principais conclusões do trabalho assim como as perspectivas.

4.2 Perspectivas

- Análise isotópica da água das fontes termais do Japão é fundamental para complementar os resultados isotópicos obtidos nos carbonatos continentais modernos.
- Mais estudos sobre a continuidade lateral das litofácies observadas. Essa informação é de suma importância na caracterização de reservatórios carbonáticos, uma vez que as características permo porosas dessas fácies poderiam ser extrapoladas lateralmente e verticalmente.
- Mais estudos sobre processos diagenéticos, incluindo compactação, atuantes não apenas logo após a litificação, mas também em elevadas profundidades.
- Além disso, composição isotópica da água, análise de microscopia Confocal e análises de microelétrodos somadas as análises das fases sólidas propiciarão uma interpretação mais precisa.

APÊNDICE A

Tabelas de química da água e temperatura de parâmetros físico químicos

APÊNDICE 1: Tabela de química da água e temperatura de acordo com a ilha, região, *hot* spring e *site* de amostragem.

Island	Region	Hot Spring	Prefecture	Site	pH	Water temp.°C	DO (mg/mol))	Climate at Sampling time
Kyushu	South	NAG	Oita	Nag 1	7,94	34,6	9,00	Winter
				Nag 2	7,87	37,7	8,11	
				Nag 3	7,93	37,4	8,40	
				Nag 4	8,13	13,8	11,54	
		MYO	Kagoshima	Myo 1	6,85	55,6	4,05	
				Myo 2	6,85	54,8	5,87	
				Myo 3	7,69	52,5	5,83	
				Myo 4	7,05	50,4	5,25	
				Myo 5	7,39	52,3	6,18	
				Myo 6	7,44	52,2	6,12	
		SHIO	Kagoshima	Shio 1	6,17	50,2	0,56	
				Shio 2	6,27	49,2	1,35	
				Shio 3	6,86	48,5	4,31	
				Shio 4	7,21	45,7	5,50	
				Shio 5	7,35	45,0	5,76	
				Shio 6	7,48	46,0	5,48	
				Shio 7	7,58	45,3	5,78	
Honshu	West	YAMA	Nara	Yama 1	6.37	38.6	0.32	Summer
				Yama 2	7.03	37.3	5.92	
				Yama 3	7.16	30.5	6.45	
				Yama 4	7.03	35.3	6.45	
				Yama 5	7.29	32.8	8.08	
				Yama 6	7.58	32.5	7.17	
				Yama 7	7.91	30.4	7.54	
				Yama 8	7.94	29.5	7.2	
		NIIMI	Okayama	Niimi 1	7.18	13.8	8.81	
				Niimi 2	7.99	14.7	9.18	
				Niimi 10	8.17	17.7	8.98	
				Niimi 12	8.21	18.0	8.63	
				Niimi 14	8.10	18.6	8.53	
		KIBE	Shimane	Kibe 1	6.20	22.1	1.69	
				Kibe 2	6.23	22.0	2.68	
				Kibe 3	7.21	27.3	6.52	
				Kibe 4	7.77	27.6	7.22	
				Kibe 5	7.92	27.2	7.42	
Aomori	North	FURU	Aomori	Furu 1	7.19	41.2	0.22	Summer
				Furu 2	7.54	40.7	0.23	
				Furu 3	7.87	35.1	0.25	
				Furu 4	8.12	33.6	0.23	
		OKU	Akita	Oku 1	6.07	44.7	0.03	
				Oku 2	7.78	36.9	0.19	
				Oku 3	7.71	35.0	0.22	
Hokkaido		OHF	Hokkaido	Ohf 1	6.82	62.4	0.03	
				Ohf 2	6.49	78.3	0.02	
				Ohf 3	6.72	61.5	0.04	
				Ohf 4	6.62	46.0	0.09	
		FUTA	Hokkaido	Futa 1	7.03	39.5	0.16	
				Futa 2	7.23	38.9	0.19	
				Futa 3	7.77	31.7	0.2	
				Futa 4	7.73	28.9	0.22	
				Futa 5	7.42	24.5	0.24	

APÊNDICE 2: Tabela de parâmetros físico químicos da água amostrada em todos os *hot springs*. Cinza claro representa a ilha de Kyushu (Sul), cinza médio representa a ilha de Honshu (Oeste) e cinza escuro representa a ilha de Hokkaido (Norte).

	pH	water temp.	DO (mM)	Alk (meq/L)	Na^+ (mM)	K^+ (mM)	Ca^{2+} (mM)	Mg^{2+} (mM)	Cl^- (mM)	NO_3^- (mM)	SO_4^{2-} (mM)	IB	Calcite	Aragonite	P_{CO2} (matm)	□□
NAG 1	7.94	34.6	0.28	35.8	20.7	1.9	2.4	12.7	11.5	n.d.	11.1	-0.02	28.2	20.4	22.9	3.4
NAG 2	7.87	37.7	0.25	36.5	20.6	2.0	3.1	12.5	11.5	n.d.	10.9	-0.02	34.7	25.7	28.8	3.9
NAG 3	7.93	37.4	0.26	38.8	20.4	2.0	3.5	12.6	11.0	n.d.	10.6	-0.02	46.8	34.7	26.3	4.6
NAG 4	8.13	13.8	0.36	36.4	20.4	2.0	2.1	12.5	11.2	n.d.	10.4	-0.02	21.4	15.1	11.2	3.1
MYO 1	6.85	55.6	0.13	19.0	8.7	1.0	3.9	3.6	8.3	n.d.	1.8	-0.01	6.2	4.6	234.4	0.3
MYO 2	6.85	54.8	0.18													
MYO 3	7.69	52.5	0.18													
MYO 4	7.05	54.0	0.18	18.9	8.7	1.0	3.8	3.7	8.3	n.d.	1.9	-0.01	9.1	6.8	141.3	0.7
MYO 5	7.39	52.3	0.19													
MYO 6	7.44	52.2	0.18	18.7	8.8	1.0	3.7	3.7	8.2	n.d.	1.9	-0.01	20.0	14.8	55.0	3.2
SHIO 1	6.17	50.2	0.08	16.0	7.8	1.0	2.8	3.2	8.4	n.d.	1.4	-0.01	0.7	0.6	1258.9	0.0
SHIO 2	6.27	49.2	0.04													
SHIO 3	6.86	48.5	0.16	15.8	7.9	0.9	2.8	3.3	9.2	n.d.	2.0	-0.01	3.3	2.5	169.8	0.2
SHIO 4	7.21	46.7	0.17													
SHIO 5	7.35	45.0	0.18													
SHIO 6	7.48	46.0	0.17													
SHIO 7	7.58	45.3	0.19	15.9	7.9	1.0	2.7	3.2	8.7	n.d.	1.8	-0.01	14.8	11.0	30.9	3.7
YAMA 1	6.37	38.6	0.32	34.1	29.1	2.7	9.8	1.6	22.0	n.d	n.d	0.00	4.7	3.5	891.3	0.0
YAMA 2	7.03	37.3	5.92	33.0	30.5	2.7	9.2	1.6	25.2	n.d	n.d	0.00	18.6	13.5	186.2	0.8
YAMA 3	7.16	30.5	6.45	21.7	19.8	1.5	5.9	1.0	15.1	n.d	n.d	0.00	10.7	7.8	85.1	0.9
YAMA 4	7.03	35.3	6.45	32.0	26.6	2.6	8.6	1.6	21.6	n.d	n.d	-0.01	16.6	12.0	177.8	0.7
YAMA 5	7.29	32.8	8.08	31.5	28.9	2.9	7.7	1.5	21.1	n.d	n.d	0.00	24.5	17.8	91.2	1.8
YAMA 6	7.58	32.5	7.17	27.3	28.5	2.5	6.6	1.5	20.9	n.d	n.d	0.00	36.3	26.3	40.7	5.1
YAMA 7	7.91	30.4	7.54	21.0	22.0	2.1	4.6	1.2	17.1	n.d	n.d	0.00	42.7	30.9	14.1	9.9
YAMA 8	7.94	29.5	7.2	19.6	21.2	1.8	4.5	1.3	17.0	n.d	n.d	0.00	40.7	29.5	12.3	10.4
NIIMI 1	7.18	13.8	8.81	2.8	0.1	n.d	2.0	0.1	0.1	0.1	0.1	0.00	0.5	0.4	9.5	0.4
NIIMI 2	7.99	14.7	9.18	3.2	0.1	n.d	2.0	0.1	0.1	0.1	0.1	0.00	3.9	2.8	1.7	14.6
NIIMI10	8.17	17.7	8.98	3.3	0.1	n.d	1.7	0.1	0.1	0.1	0.1	0.00	5.8	4.1	1.2	16.1
NIIMI12	8.21	18.0	8.63	3.8	0.2	n.d	1.7	0.1	0.1	0.1	0.1	0.00	7.1	5.0	1.2	16.0
NIIMI14	8.10	18.6	8.53	3.8	0.2	n.d	1.5	0.1	0.1	0.1	0.1	0.00	5.1	3.6	1.6	14.1
KIBE 1	6.20	22.1	1.69	33.6	54.8	0.6	9.0	1.3	47.7	n.d	n.d	-0.01	1.6	1.2	1000.0	0.0
KIBE 2	6.23	22.0	2.68	32.9	49.3	0.5	8.7	1.1	43.1	n.d	n.d	-0.01	1.7	1.2	933.3	0.0
KIBE 3	7.21	27.3	6.52	30.0	49.9	0.5	8.3	1.3	45.8	n.d	n.d	-0.01	16.6	11.7	95.5	1.1
KIBE 4	7.77	27.6	7.22	28.3	51.8	0.5	6.5	1.2	45.0	n.d	n.d	-0.01	43.7	31.6	24.5	7.2
KIBE 5	7.92	27.2	7.42	21.7	46.6	0.1	4.8	1.0	36.9	n.d	n.d	0.00	38.0	26.9	13.5	8.9
FURU 1	7.19	41.2	0.22	21.4	30.8	1.5	11.4	4.1	28.7	n.d.	7.0	0.00	20.9	15.1	85.1	2.0
FURU 2	7.54	40.7	0.23	20.3	27.4	1.4	9.9	3.3	28.3	n.d.	7.0	-0.02	31.6	22.9	37.2	6.5
FURU 3	7.87	35.1	0.25	17.8	27.1	1.4	9.8	3.6	25.1	n.d.	5.8	0.00	60.3	44.7	13.2	12.9
FURU 4	8.12	33.6	0.23	12.9	24.5	1.4	8.2	3.4	22.2	n.d.	5.1	0.00	64.6	46.8	5.1	16.0
OKU 1	6.07	44.7	0.03	24.6	17.6	0.9	15.9	5.4	25.1	n.d.	5.5	0.00	2.8	2.1	1380.4	0.0

OKU 2	7.78	36.9	0.19	16.2	17.8	0.9	12.7	5.5	26.1	n.d.	5.7	0.00	60.3	44.7	14.8	13.1
OKU 3	7.71	35.0	0.22	16.2	18.2	0.9	12.5	5.6	26.9	n.d.	6.3	0.00	49.0	35.5	17.0	11.2
OHF 1	6.82	62.4		0.03	6.2	3.5	0.2	0.4	n.d.	33.0	n.d.	1.3	-0.04	0.3	0.2	100.0
OHF 2	6.49	78.3		0.02	7.3	2.3	0.2	0.3	0.2	32.5	n.d.	1.4	-0.04	0.2	0.1	331.1
OHF 3	6.72	61.5		0.04	5.8	2.4	0.2	0.3	0.2	33.1	n.d.	1.7	-0.04	0.2	0.1	114.8
OHF 4	6.62	46.0		0.09	4.9	2.7	0.2	0.3	0.2	25.7	n.d.	1.3	-0.03	0.1	0.1	93.3
FUTA 1	7.03	39.5	0.16	25.3	82.8	14.2	16.1	6.2	98.5	n.d.	n.d.	0.02	19.5	14.5	131.8	1.2
FUTA 2	7.23	38.9	0.19	24.0	80.7	13.8	15.4	6.0	101.2	n.d.	n.d.	0.01	28.2	20.4	77.6	2.7
FUTA 3	7.77	31.7	0.2	16.8	79.3	13.6	11.3	5.9	101.1	n.d.	n.d.	0.01	41.7	30.2	13.8	10.0
FUTA 4	7.73	28.9	0.22	14.9	80.8	13.8	10.6	6.0	101.0	n.d.	n.d.	0.01	30.2	21.9	13.2	8.8
FUTA 5	7.42	24.5	0.24	13.4	81.9	13.8	9.1	5.2	102.4	n.d.	n.d.	0.01	10.5	7.6	23.4	7.4

APÊNDICE B

Tabelas de variações geoquímicas, faciológicos e de ambientes deposicionais de Fontes Hidrotermais do Japão.

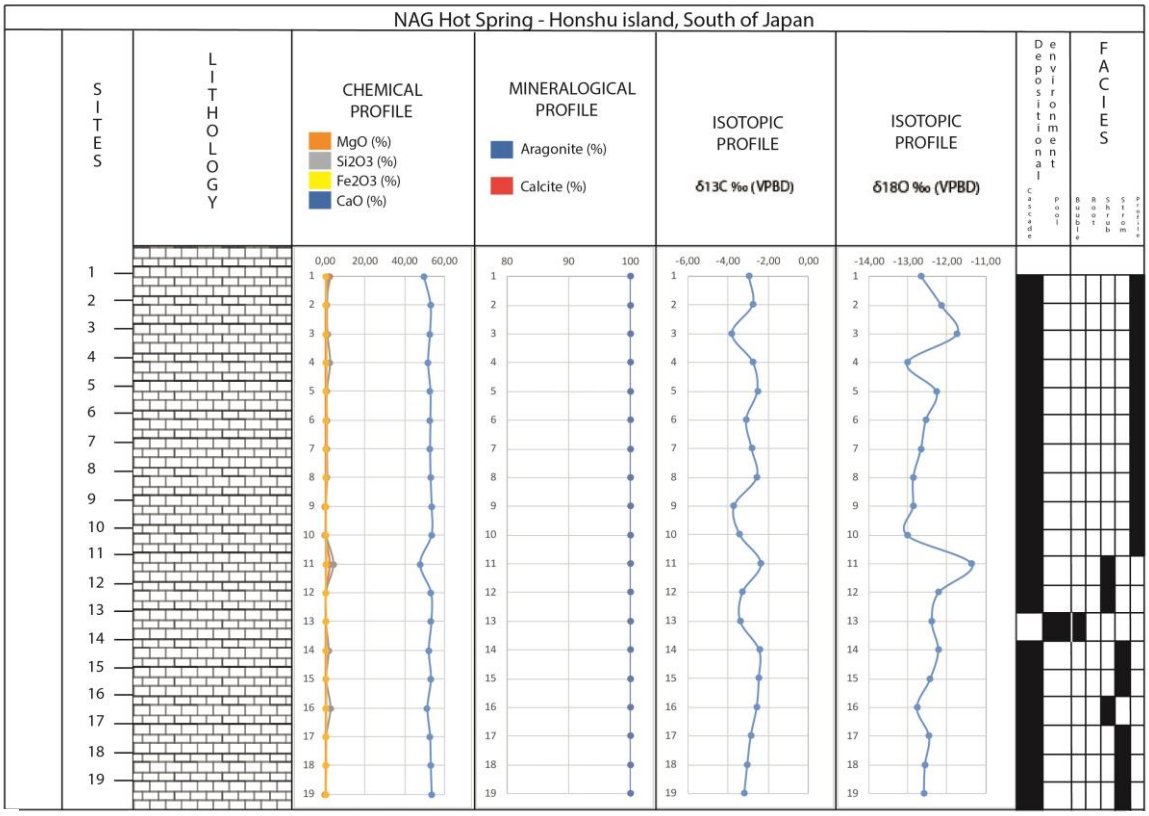

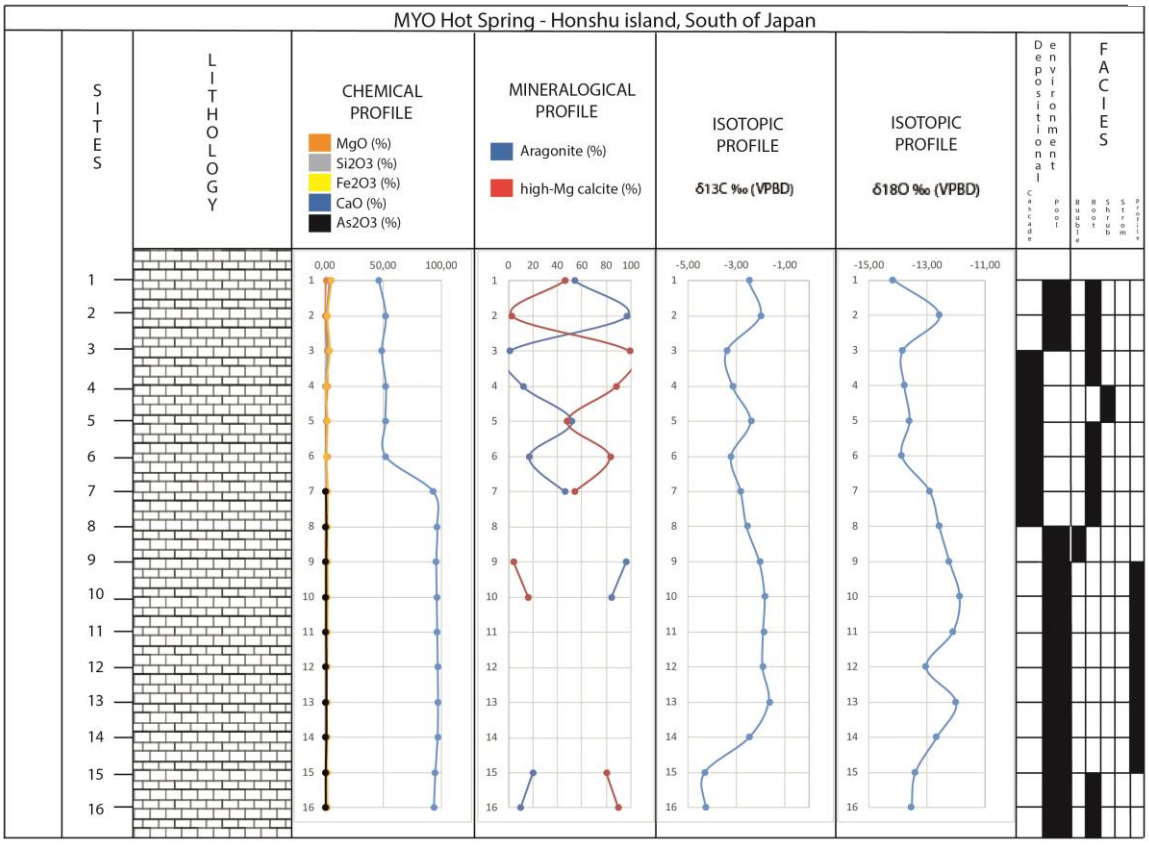

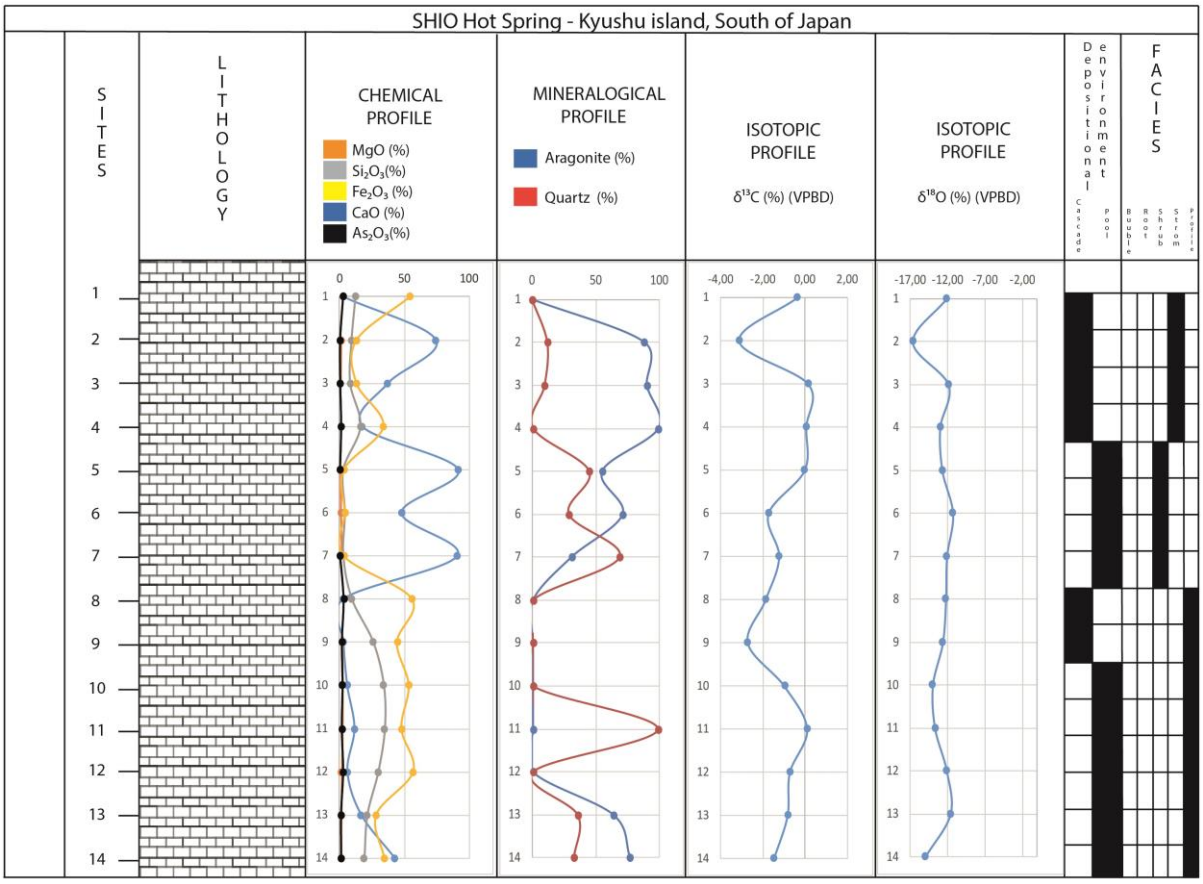
SHIO Hot Spring - Kyushu island, South of Japan
SITES
LITHOLOGY
CHEMICAL PROFILE
MgO (%)
Si2O3(%)
Fe2O3 (%)
CaO (%)
As2O3(%)
MINERALOGICAL PROFILE
Aragonite (%)
Quartz (%)
ISOTOPIC PROFILE
δ13C (%) (VPBD)
ISOTOPIC PROFILE
δ18O (%) (VPBD)
Depositional environment
Cascade
Pool
FACIES
Bubble
Root
Shrub
Strom
Protist

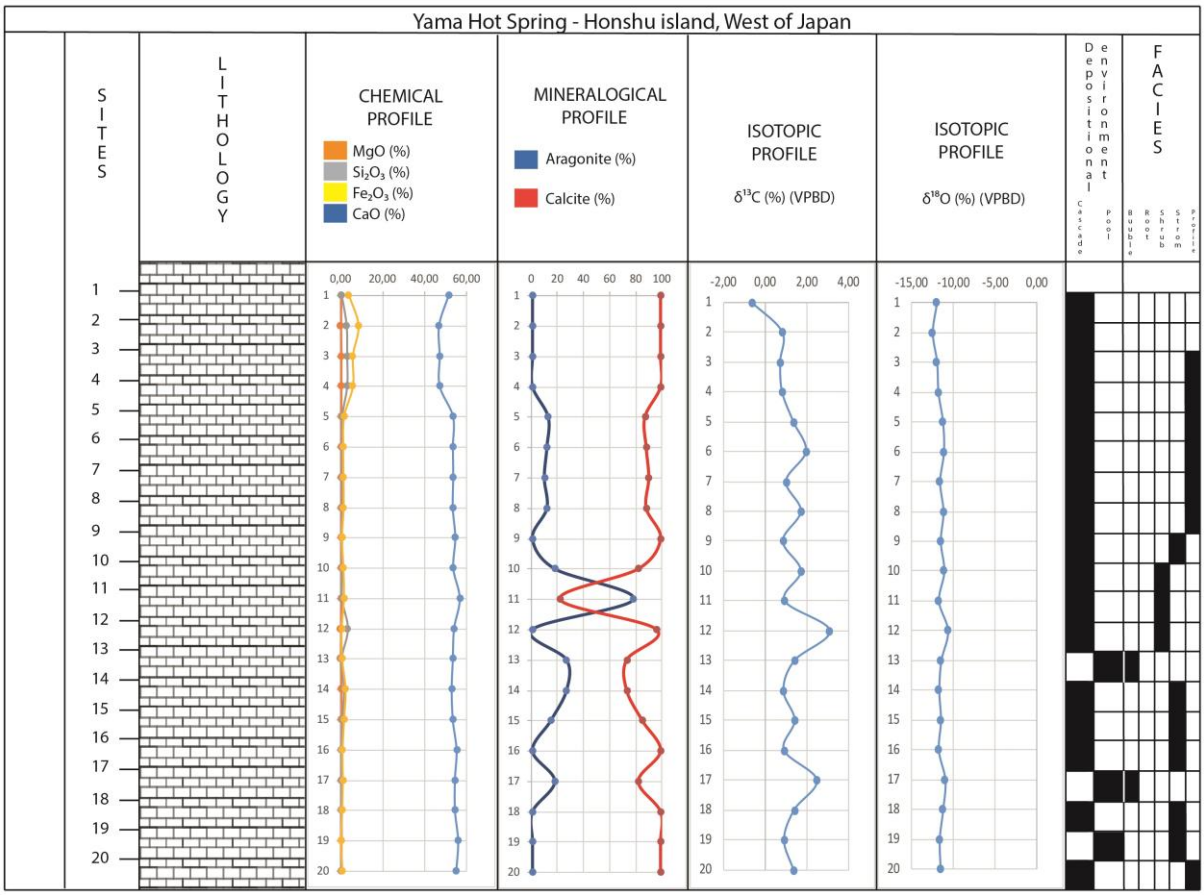
Yama Hot Spring - Honshu island, West of Japan
SITES
LITHOLOGY
CHEMICAL PROFILE
MgO (%)
Si2O3 (%)
Fe2O3 (%)
CaO (%)
MINERALOGICAL PROFILE
Aragonite (%)
Calcite (%)
ISOTOPIC PROFILE
δ13C (%) (VPBD)
ISOTOPIC PROFILE
δ18O (%) (VPBD)
Depositional environment
Cascade
Pool
FACIES
Bubble
Root
Shrub
Stroma
Protist

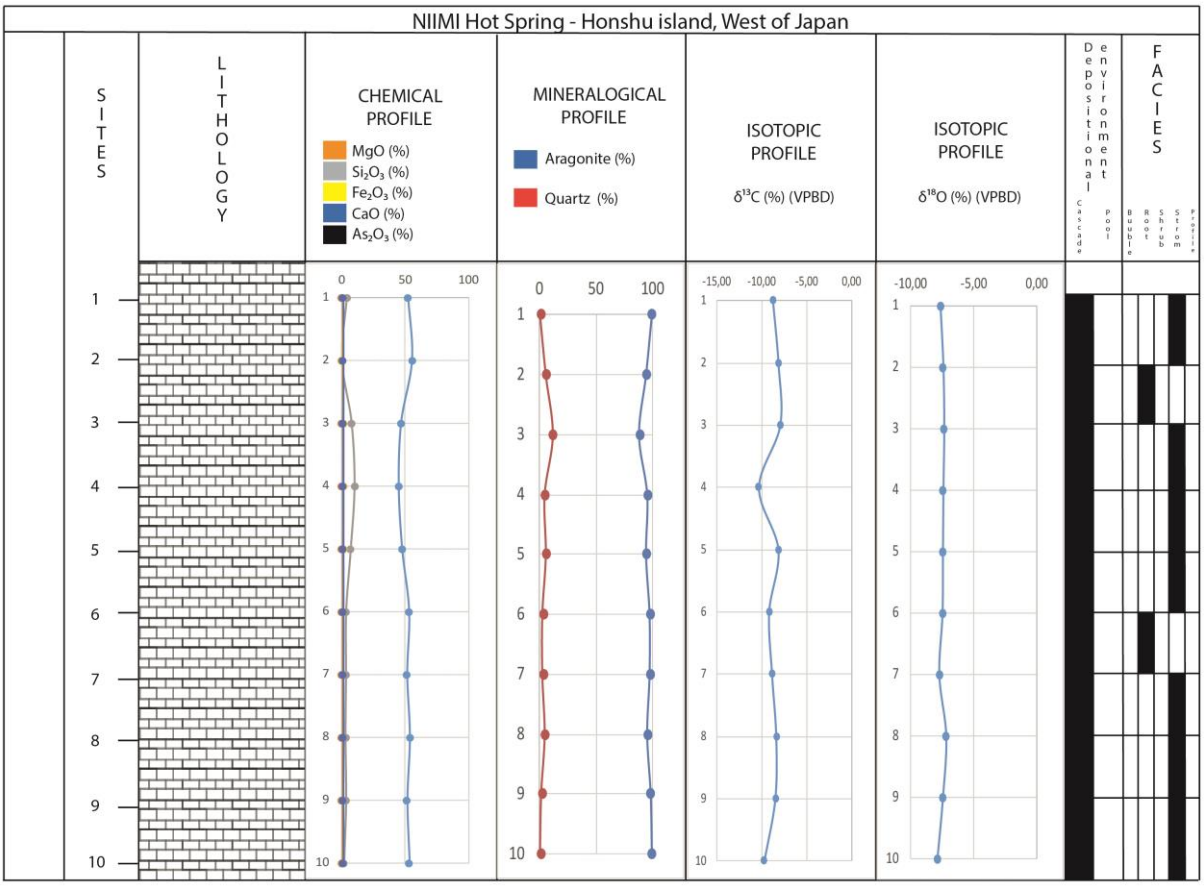
NIIMI Hot Spring - Honshu island, West of Japan
SITES
LITHOLOGY
CHEMICAL PROFILE
MgO (%)
Si2O3 (%)
Fe2O3 (%)
CaO (%)
As2O3 (%)
MINERALOGICAL PROFILE
Aragonite (%)
Quartz (%)
ISOTOPIC PROFILE
δ13C (%) (VPBD)
ISOTOPIC PROFILE
δ18O (%) (VPBD)
Depositional environment
Cascade
Pool
FACIES
Bubble
Root
Shrub
Stromatolite

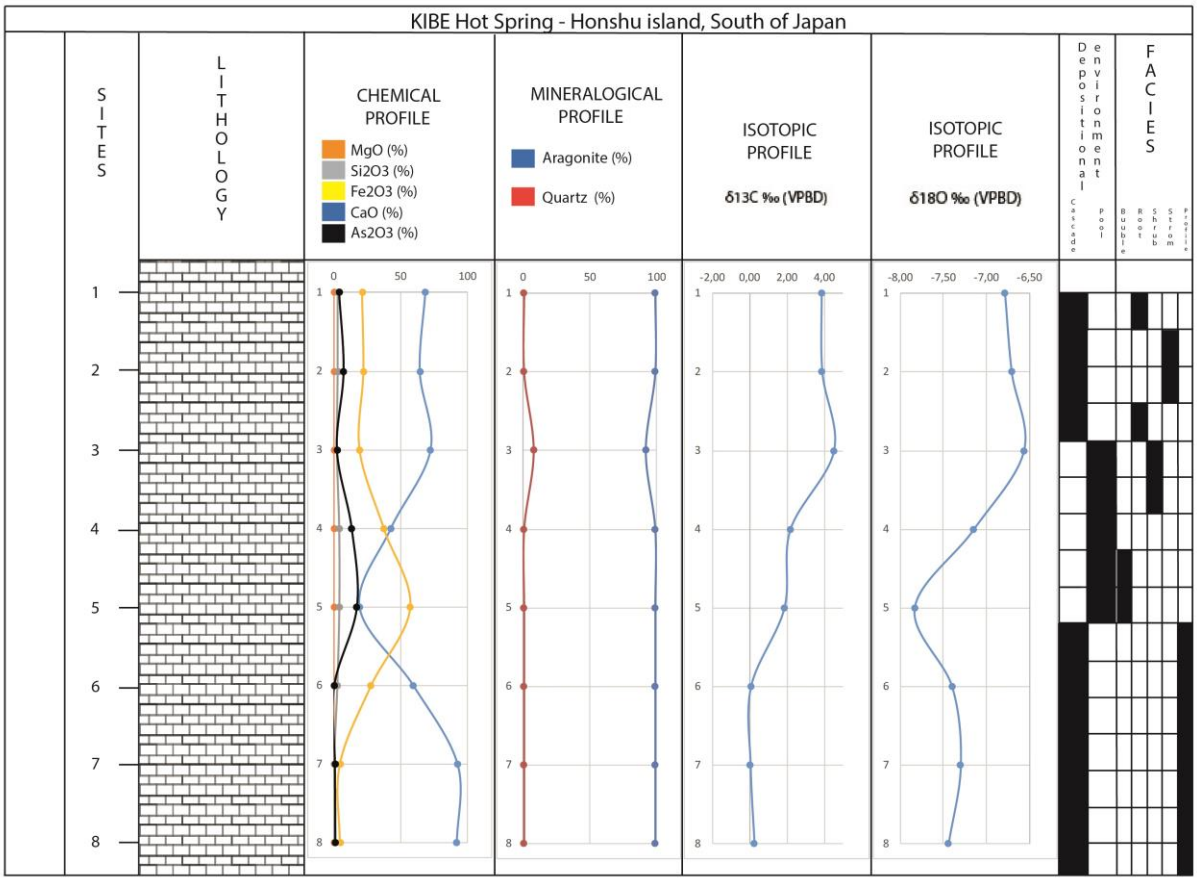
KIBE Hot Spring - Honshu island, South of Japan
SITES
LITHOLOGY
CHEMICAL PROFILE
MgO (%)
Si2O3 (%)
Fe2O3 (%)
CaO (%)
As2O3 (%)
MINERALOGICAL PROFILE
Aragonite (%)
Quartz (%)
ISOTOPIC PROFILE
δ13C ‰ (VPBD)
ISOTOPIC PROFILE
δ18O ‰ (VPBD)
Depositional environment
Cascade
Pool
FACIES
Bubble
Root
Shrub
Stromatolite

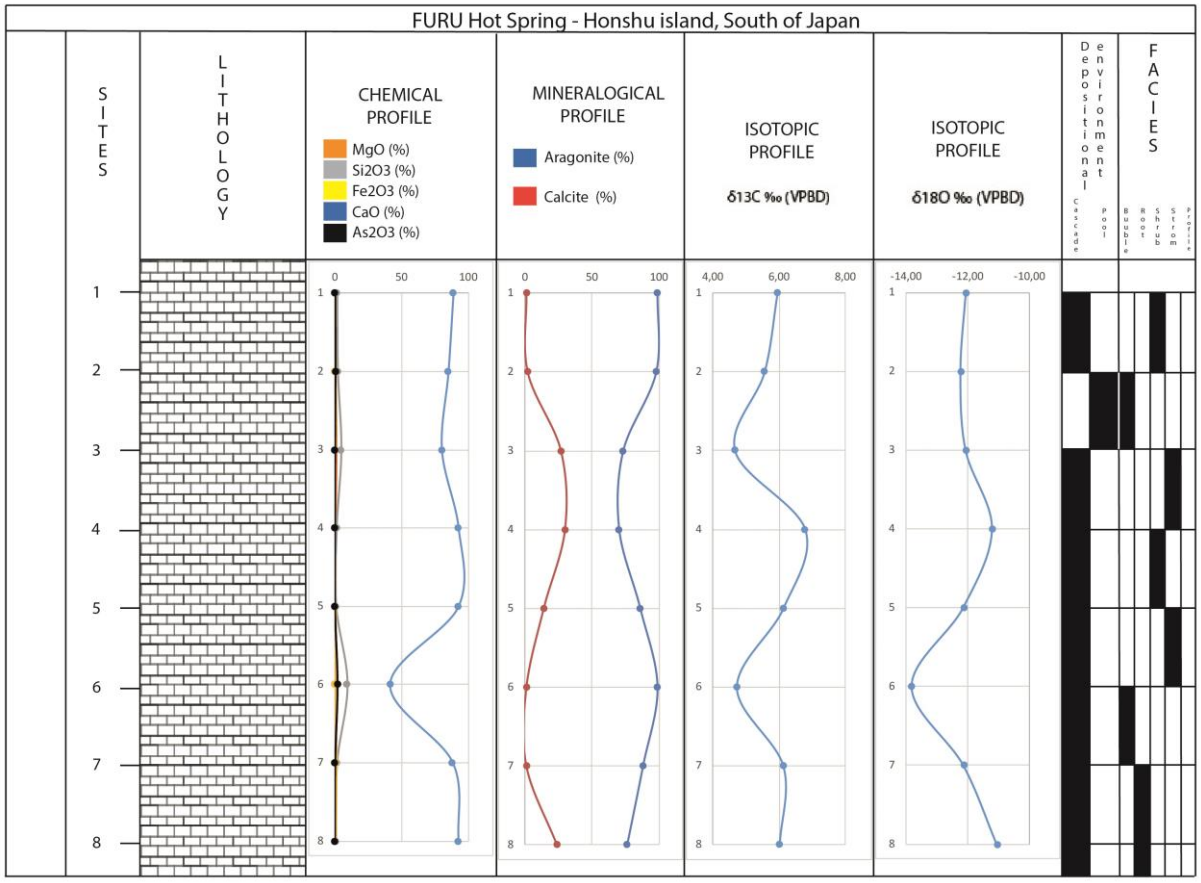
FURU Hot Spring - Honshu island, South of Japan
SITES
LITHOLOGY
CHEMICAL PROFILE
MgO (%)
Si2O3 (%)
Fe2O3 (%)
CaO (%)
As2O3 (%)
MINERALOGICAL PROFILE
Aragonite (%)
Calcite (%)
ISOTOPIC PROFILE
δ13C ‰ (VPBD)
ISOTOPIC PROFILE
δ18O ‰ (VPBD)
Depositional environment
Cascade
Pool
FACIES
Bubble
Root
Shrub
Stromatolite

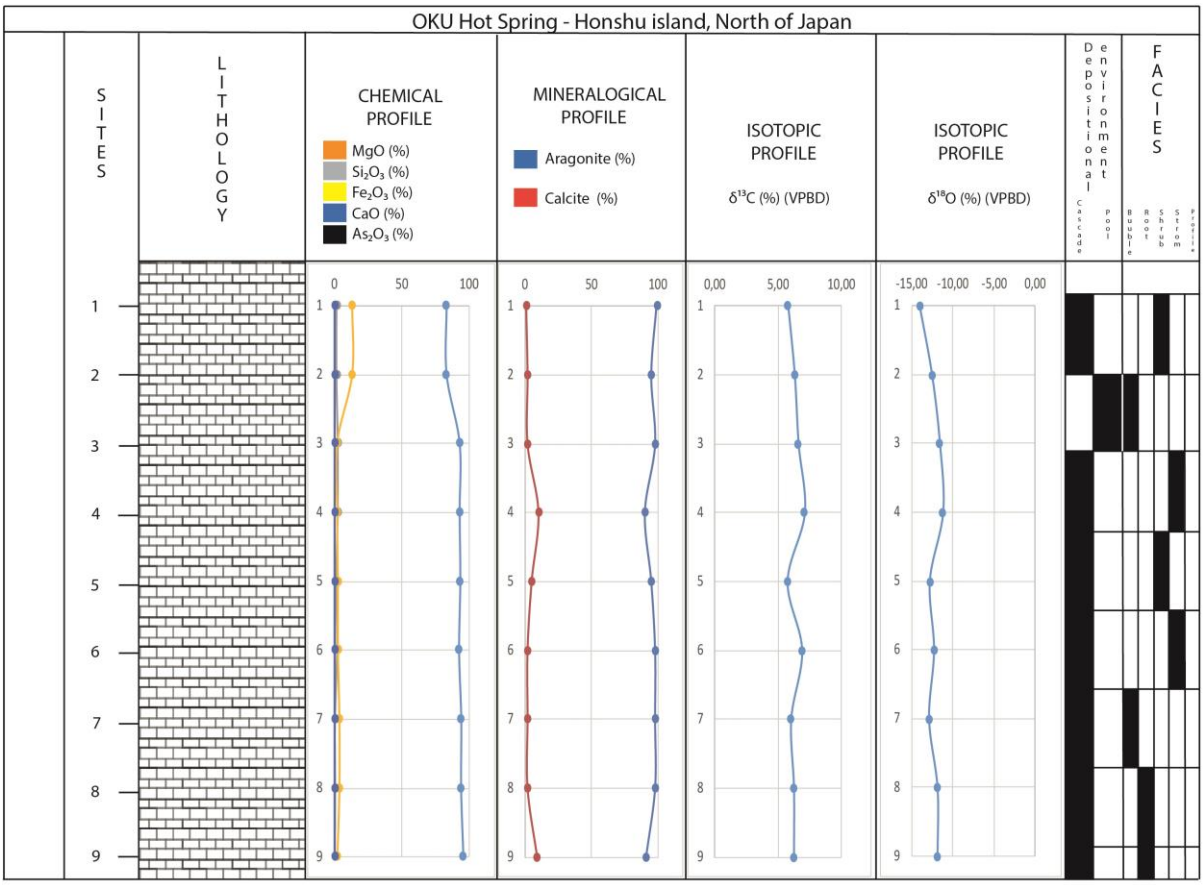
OKU Hot Spring - Honshu island, North of Japan
SITES
LITHOLOGY
CHEMICAL PROFILE
MgO (%)
Si2O3 (%)
Fe2O3 (%)
CaO (%)
As2O3 (%)
MINERALOGICAL PROFILE
Aragonite (%)
Calcite (%)
ISOTOPIC PROFILE
δ13C (%) (VPBD)
ISOTOPIC PROFILE
δ18O (%) (VPBD)
Depositional environment
Cascade
Pool
FACIES
Bubble
Root
Shrub
Stromatolite

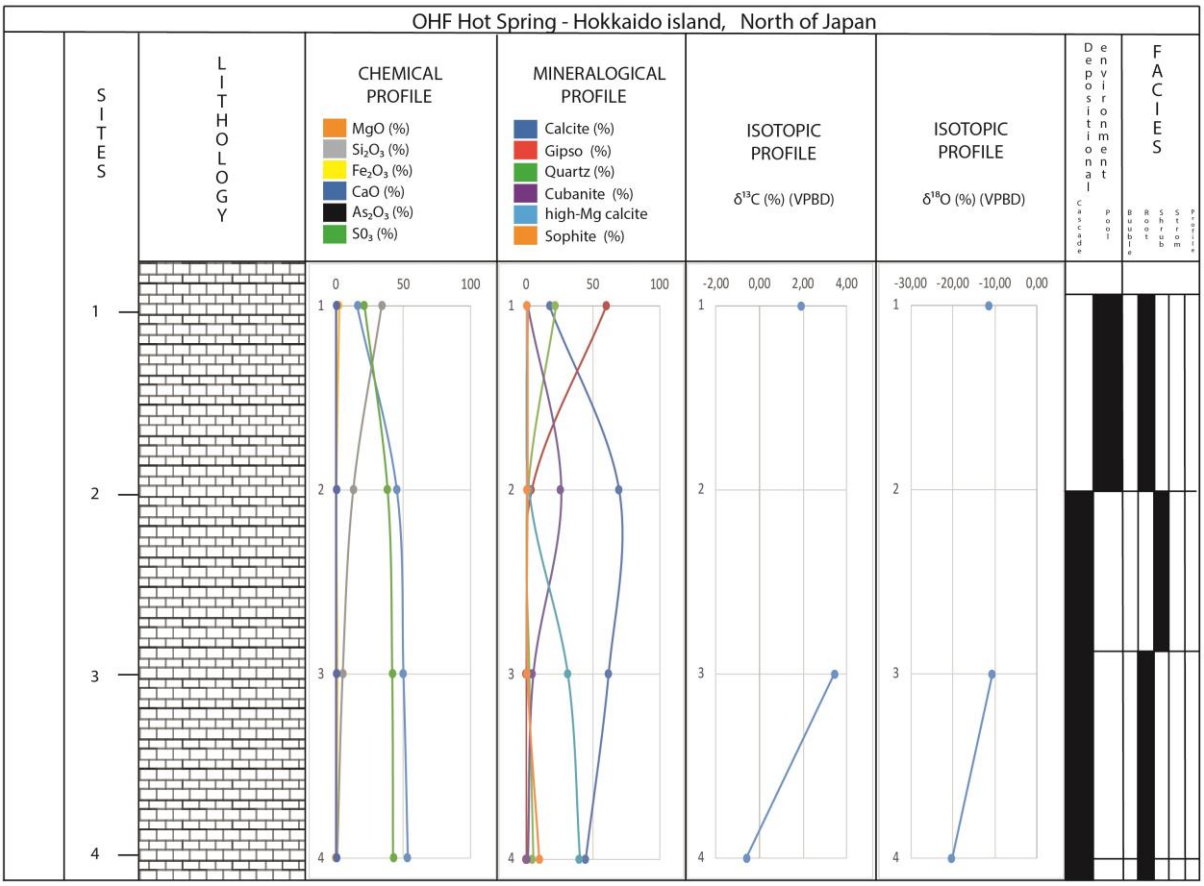
OHF Hot Spring - Hokkaido island, North of Japan
SITES
LITHOLOGY
CHEMICAL PROFILE
MgO (%)
Si2O3 (%)
Fe2O3 (%)
CaO (%)
As2O3 (%)
SO3 (%)
MINERALOGICAL PROFILE
Calcite (%)
Gipso (%)
Quartz (%)
Cubanite (%)
high-Mg calcite
Sophite (%)
ISOTOPIC PROFILE
δ13C (%) (VPBD)
ISOTOPIC PROFILE
δ18O (%) (VPBD)
Depositional environment
Cascade
Pool
FACIES
Bubble
Root
Shrub
Strom
Proto
0 50 100
-2,00 0,00 2,00 4,00
-30,00 -20,00 -10,00 0,00
1
2
3
4

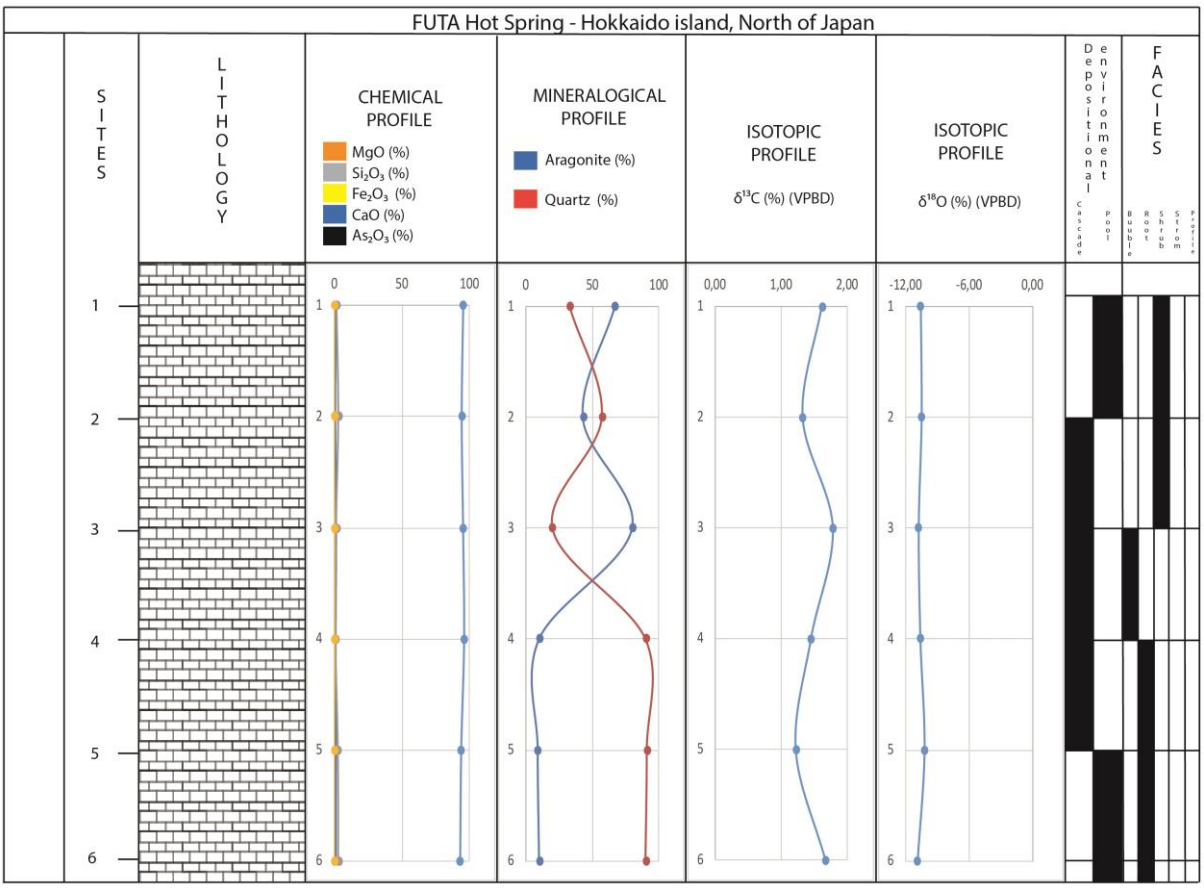
FUTA Hot Spring - Hokkaido island, North of Japan
SITES
LITHOLOGY
CHEMICAL PROFILE
MgO (%)
Si2O3 (%)
Fe2O3 (%)
CaO (%)
As2O3 (%)
MINERALOGICAL PROFILE
Aragonite (%)
Quartz (%)
ISOTOPIC PROFILE
δ13C (%) (VPBD)
ISOTOPIC PROFILE
δ18O (%) (VPBD)
Depositional environment
Cascade
Pool
FACIES
Bubble
Root
Shrub
Strom
Proto
0 50 100
0,00 1,00 2,00
-12,00 -6,00 0,00
1
2
3
4
5
6